Lys^{691}, a predicted phosphate coordination site, and Asp^{714}, a predicted water coordination site of the sodium pump **a** subunit are essential for enzyme activity

Inaugural-Dissertation
zur Erlangung des Grades eines Doktors der Medizin
des Fachbereichs Medizin
der Justus-Liebig-Universität Gießen

vorgelegt von Ping Su
aus Hubei, V.R. China
Gießen im April 2002

Aus dem Institut für Biochemie und Endokrinologie des Fachbereichs Veterinärmedizin, Justus-Liebig-Universität Gießen

Leiter: Prof. Dr. W. Schoner

Gutachter: Prof. Dr. G. Scheiner-Bobis

Gutachter: Prof. Dr. F. Dreyer

Tag der Disputation: 23. Juli 2002

Contents

1.	**Introduction**	1
1.1	The Na^+/K^+-ATPase	1
1.1.1	Physiologic function of the Na^+/K^+-ATPase	1
1.1.2	The reaction cycle of Na^+/K^+-ATPase	2
1.1.3	Subunit composition and topology of the Na^+/K^+-ATPase	3
1.1.4	Native inhibitors of the Na^+/K^+-ATPase	6
1.1.5	ATP interaction with the sodium pump	9
1.2	Haloacid dehalogenase	12
1.2.1	The reaction mechanism of haloacid dehalogenase and proposed reaction mechanism of the Na^+/K^+-ATPase	12
1.2.2	The crystal structure of L-2-haloacid dehalogenase	13
1.3	Question outcome	15
2.	**Materials and Methods**	18
2.1	Materials	18
2.1.1	Cells and plasmids	18
2.1.2	Oligonucleotides	19
2.1.3	Restriction endonucleases and other enzymes	20
2.1.4	Antibodies	21
2.1.5	Buffers and medium	21
2.1.6	Other enzymes, chemicals or biochemicals and kits	21
2.2	Equipment	22
2.3	Methods	23
2.3.1	Introduction of mutations into the plasmid pCGY1406αβ	23
2.3.1.1	Construction of the plasmid pKS^+-AS	23
2.3.1.2	Culture and storage of *E. coli*	23
2.3.1.3	Introduction of the plasmid DNA into *E. coli*	24
2.3.1.4	Isolation of plasmid DNA from *E. coli*	25
2.3.1.5	Quantification of the DNA	26
2.3.1.6	Endonuclease restriction analysis	26
2.3.1.7	Precipitation of the DNA	27
2.3.1.8	Separation of DNA fragments by agarose gel electrophoresis	27
2.3.1.9	Extraction of DNA fragments from the agarose gels	28

2.3.1.10	Inverse polymerase reaction — inverse-PCR	28
2.3.1.11	Blunt-ending of the 3´-end of PCR products	29
2.3.1.12	Phosphorylation of the DNA	30
2.3.1.13	Dephosphorylation of the DNA	30
2.3.1.14	Ligation of the DNA	30
2.3.1.15	DNA sequencing analysis	31
2.3.2	Heterologous expression of the native and mutant Na^+/K^+-ATPase in yeast *Saccharomyces cerevisiae*	31
2.3.2.1	Culture and storage of yeast cells	31
2.3.2.2	Introducing plasmid DNA into yeast cells	32
2.3.2.3	Palytoxin-induced K^+ efflux from yeast cells expressing the native or mutated sodium pump	32
2.3.2.4	Ouabain inhibition of PTX-induced K^+ efflux from yeast cells expressing the native or mutated sodium pump	33
2.3.2.5	Microsomal membrane protein preparation	33
2.3.2.6	Protein assay	34
2.3.2.7	SDS-extraction of Na^+/K^+-ATPase from a membrane preparation	34
2.3.3	Binding of [^{3}H]ouabain to yeast membranes containing native or mutant Na^+/K^+-ATPase	35
2.3.3.1	[^{3}H]ouabain binding in the presence of P_i	35
2.3.3.2	Inhibition of [^{3}H]ouabain binding by K^+	35
2.3.3.3	Binding of [^{3}H]ouabain as a function of Mg^{2+}	35
2.3.3.4	[^{3}H]ouabain binding to phosphoenzyme formed from ATP	36
2.3.4	Na^+/K^+-ATPase activity assay	36
2.3.5	SDS-polyacrylamide gel electrophoresis (SDS-PAGE)	37
2.3.6	Western blotting	37
2.3.7	Measurement of ^{18}O exchange between P_i and water	38
3.	**Results**	40
3.1	Sequence comparison	40
3.2	Introduction of the mutations into the vector pKS^+-AS	41
3.2.1	Plasmid construction	41
3.2.2	Mutagenesis by inverse PCR	42
3.2.3	Confirmation of the introduced mutations in the pKS^+-AS	44

3.3	Expression of the native or mutant Na^+/K^+-ATPase in yeast cell line30-4	47
3.3.1	Introduction of the mutations into the shuttle vector pCGYαβ1406	47
3.3.2	Confirmation of expression of the native or mutant Na^+/K^+-ATPase in yeast	49
3.4	Functional detection for mutated α1 subunit of the Na^+/K^+-ATPase expressed in yeast	50
3.4.1	PTX-induced K^+ efflux from yeast cells expressing either wild-type or mutant Na^+/K^+-ATPase	50
3.4.2	Ouabain inhibition of the PTX-induced K^+ efflux from yeast cells expressing either mutant or wild-type Na^+/K^+-ATPase	52
3.5	Measurement of [^{3}H]ouabain binding to yeast membranes containing native or mutant Na^+/K^+-ATPase	54
3.5.1	Binding of [^{3}H]ouabain to the phosphoenzyme formed from P_i	54
3.5.1.1	[^{3}H]ouabain binding in the presence of P_i	54
3.5.1.2	Inhibition of [^{3}H]ouabain binding by K^+	55
3.5.1.3	Binding of [^{3}H]ouabain as a function of Mg^{2+}	57
3.5.2	[^{3}H]ouabain binding to phosphorenzyme formed from ATP	58
3.6	Na^+/K^+-ATPase activity assay	59
3.7	Measurement of ^{18}O exchange between P_i and water	59
4.	**Discussion**	61
5.	**Summary**	69
6.	**Zusammenfassung**	70
7.	**References**	71
8.	**Acknowledgements**	79
9.	**Appendix (Lebenslauf)**	80

List of Abbreviations

Å	Angstrom (1 Å = $1 \cdot 10^{-10}$ m)
Ab	Antibody
ADK	Adenylate kinase (EC 2.7.4.3)
AP	Alkaline phosphatase
Ap_5A	P1,P5-bis-(5′-adenosine)-pentaphosphate
APS	Ammonium persulfate
ATP	Adenosine 5‘-triphosphate
bp	Base pair
BSA	Bovines serum albumin
Ca^{2+}-ATPase	Ca^{2+}-transporting ATP-phosphohydrolase (EC 3.6.1.38)
cDNA	Complementary DNA
CUP1	Copper-binding metallothionein
dATP	Deoxyadenosine triphosphate
dCTP	Deoxycytidine triphosphate
ddH_2O	Double-distilled water
dGTP	Deoxyguanosine triphosphate
DNA	Deoxyribonucleic acid
dNTPs	Mixture of dATP, dCTP, dGTP and dTTP
DTT	Dithiothreitol
DTTP	Deoxythymidine triphosphate
E.coli	*Escherichia coli*
E_1	Enzyme conformation which with a high affinity to Na^+ and TP
E_2	Enzyme conformation with a high affinity to K^+ and low affinity to ATP
EC	Enzyme classification
EC_{50}	Median effective concentration
EDTA	Ethylenediaminetetraacetic acid
HBC	Hepes/borate/calcium chlorid
H^+/K^+-ATPase	H^+/K^+-exchanging ATP-phosphohydrolase (EC3.6.1.3)
IC_{50}	Median inhibitory concentration
$K_{0.5}$	Concentration of median relative affinity
K_D	Dissociation constant

kb	Kilobase
kDa	Kilodalton
LB	Luria-Bertani (medium for bacteria)
LD_{50}	Median lethal dose
LiDS	Lithium dodecyl sulfate
IgG	Gamma immunoglobulin
mRNA	Messenger ribonucleic acid
NADH	Reduced form of nicotinamide adenine dinucleotide
Na^+/K^+-ATPase	Na^+/K^+-activated Mg^{2+}-dependent ATP phosphohydrolase (EC 3.6.1.37)
NMR	Nuclear magnetic resonance
8-N_3-ATP	8-Azidoadenosine 5´-triphosphate
3´-N_{3P}-ATP	3´-*O*-[3(4-azido-2-nitrophenyl)propionyl]adenosine 5´-triphosphate
OD_λ	Optical density at the wavelength λ
ori	Origin of replication
PAGE	Polyacrylamide gel electrophoresis
PBS	Phosphate-buffered saline
PCR	Polymerase chain reaction
PEG	Polyethylene glycol
PGK	Phosphoglycerate kinase
P_i	Inorganic phosphate
PMSF	Phenylmethylsulonyl fluoride
PTX	Palytoxin
PVDF	Polyvinylidene difluroide
RNA	Ribonucleic acid
RNase	Ribonuclease
rpm	Revolutions per minute
RT	Room temperature
RT-PCR	Reverse transcription–polymerase chain reaction
SD	Standard deviation
SDS	Sodium dodecyl sulfate
STET	Sodium chloride/Tris-EDTA/Triton® X 100
TAE	Tris-acetate/EDTA

TCA	Trichloroacetic acid
TE	Tris-EDTA
TEMED	N,N,N,N-Tetramethylethylendiamine
TM	Transmembrane
Tris	Tris(hydromethyl)aminomethane
Triton®	Polyethyleneglycol-mono-(p-(1,1,3,3-tetramethylbutyl)-phenyl) ether
TRP_1	Gene for tryptophan-biosynthesis
	[(N-(5‘-phosphoribosyl) anthranilatisomerase gene]
Tween®	Polyxyethylensorbitanmonolaurat (poly-sorbate)
U	Unit
UV	Ultraviolet
v/v	Volume/volume
w/v	Weight/volume
WT	Wild-type
YBB	Yeast breakage buffer
YNB	Yeast nitrogen base (Medium, nitrogen source to yeast culture)

For amino acids, the commonly used three- or one-letter codes were used as abbreviations.

1. Introduction

All cells possess an array of membrane-bound enzymatic systems that perform various processes essential for life. It is estimated that approximately 30% of genes may encode membrane proteins [1]. A major functional class of these membrane-bound enzymes includes those categorized as primary active transporters, called ATPases because they catalyze the transport of molecules against an electrochemical potential by reactions directly linked to ATP hydrolysis. The ATPases are categorized into three classes: F-type ATPases, V-type ATPases, and P-type ATPases [2]. The P-type ATPases are broadly distributed and are importance in maintaining cellular ionic homeostasis [3]. They are characteristically dependent on the autophosphorylation, using ATP, of a conserved aspartic acid residue, and the phosphoenzyme intermediate undergoes rapid turnover during the reaction cycle. The phospho- as well as dephosphoenzymes exist in at least two distinct conformational states, E_1 and E_2, which have kinetic variables, e.g. affinities for substrates [4-8]. For this reason, the P-type ATPases are also called E_1-E_2 ATPases. The P_2-type ATPases according to the classification proposed by Palmgren and Axelsen [9], including Na^+/K^+-ATPase, H^+/K^+-ATPase, and two main types of Ca^{2+}-ATPases, are nonheavy metal ion pumps and have been characterized in great detail [7, 10-13].

1.1 Na^+/K^+-ATPase

1.1.1 Physiological function of the Na^+/K^+-ATPase

Na^+/K^+-ATPase (sodium pump, EC 3.6.1.37), a member of the P_2-type ATPases, is an integral membrane protein and exists ubiquitously in all animal cells [3, 14]. The pump transports Na^+ ions out of the cell and K^+ ions into the cell utilizing ATP as a driving force at stoichiometries of 3:2:1 (Na^+:K^+:ATP), and produces both a chemical and an electrical gradient across cell membranes [8, 15]. In general, the Na^+ ion concentration is 10 mM inside and 140 mM outside the cells and K^+ ions exhibit an intracellular concentration of 140 mM and extracellular concentration of 5 mM. In addition, the transmembrane potential difference is about -50~-80 mV, the Na^+ transport is therefore against both a chemical and an electrical gradient, and the K^+ ions are transported down an electrical gradient but against their chemical gradient [15-17]. Because one positive charge per turnover is transported across the membrane, the Na^+/K^+-ATPase generates outward, hyperpolarizing electrical current; it is “electrogenic”. This electrogenic transport is very important for maintaining the resting

membrane potential of cells and for the excitable activity of muscle and nerve tissue. The gradient for Na^+ is also used as a free energy source for cotransport of other substances such as sugars, amino acids, Cl^-, and for countertransport of Ca^{2+} or H^+ against gradients across cell membranes. With the negative membrane potential, the intracellular concentration of diffusible anions is lower than the extracellular. This compensates for the osmotic effect of intracellular anions which cannot pass the membrane, and helps to regulate the cell volume. In addition, the Na^+/K^+-ATPase present in organs such as intestine and kidney regulates fluid reabsorption and electrolyte movement by establishing an ionic gradient across epithelial membranes. The high K^+ concentration inside cells is also of importance for a number of intracellular enzymatic reactions and cell growth and cell division in general [18, 19]. Approximately 23-28% of the ATP consumed in humans is utilized by the sodium pump [3, 20, 21].

1.1.2 The reaction cycle of Na^+/K^+-ATPase

As shown in Scheme1.1, the ion translocation is brought about by a series of conformational changes coupled to the formation and breakdown of a phosphorylated aspartyl intermediate, the hallmark of the P-type ATPase family [5, 22, 23]. The catalytic reaction begins with the binding of three cytoplasmic Na^+ ions at the transport sites of the E_1 form, which displays high affinity for Na^+ and ATP in the presence of Mg^{2+} ions. After phosphorylation of the enzyme at Asp^{369} by the γ-phosphate group of ATP, the Na^+ ions are occluded within the membrane as indicated by brackets in Scheme 1 [24-27]. Following conformational changes in the phosphoenzyme ($E_1P \rightarrow E_2P$), the occluded Na^+ ions are released on the extracytoplasmic side of the membrane. As shown in Scheme 1, it is proposed that one of the Na^+ ions is released before the others and that this release is associated with the electrogenic step [28, 29]. The E_2P form of the Na^+/K^+-ATPase exhibits a high affinity for ouabain, a specific inhibitor of the enzyme (E^*_2P·ouabain). The ensuing dephosphorylation of the E_2P form is triggered by the binding of two extracytoplasmic K^+ ions which are subsequently occluded within the membrane [30, 31]. Following ATP binding to the low affinity site, the occluded K^+ ions are transported to the inside of the membrane. At this point, the first cycle is finished and the enzyme can enter the next reaction cycle again by a conformational change from the E_2ATP to the E_1ATP form [32, 33]. The chemical energy released from hydrolysis of the terminal phosphate of ATP is transformed into electrical energy [15, 34-36]. The Na^+/K^+-ATPase turnover represents 10,000 cycles min^{-1} [37] and requires about 42 kJ/mol/ per turnover (i.e. per ATP utilized) [4]. In all, the pump characteristically exhibits at least two

phenomenologically and structurally distinct conformations, E_1 and E_2, which have distinct kinetic variables, e.g. affinities for substrates [5, 38].

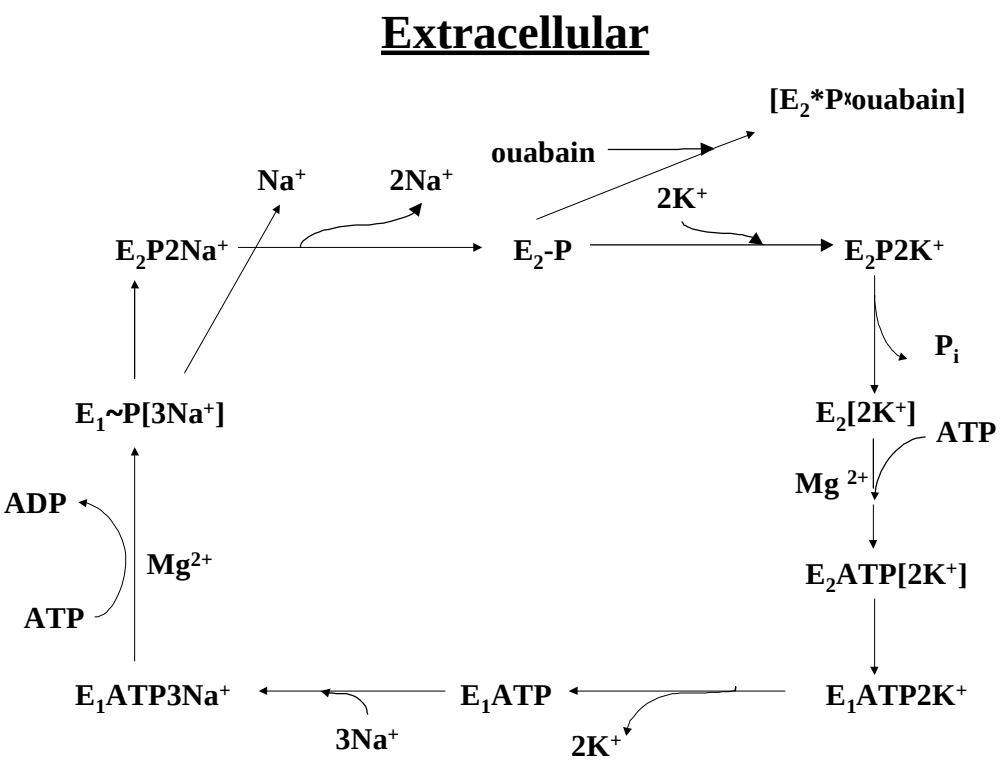

Scheme 1.1 Reaction scheme for Na^+/K^+-ATPase

A basic Albers-Post scheme describing the cycle of Na^+/K^+-ATPase is shown. Active Na^+ and K^+ ions transport involves (i) Na_{cyt}-dependent phosphorylation from ATP and Na^+ ions occlusion, E_1® $E_1P(Na)$; (ii) Na^+ ions transport outward across the membrane coupled to E_1P® E_2P; (iii) K_{exc}-activated dephosphorylation and K^+ ions occlusion, E_2P® $E_2(K)$; and (iv) K^+ ions transport inward across the membrane coupled to $E_2(K)$ ® E_1, accelerated by ATP acting with low affinity. Occluded ions are depicted in brackets (adapted from Glynn and Karlish, 1990).

1.1.3 Subunit composition and topology of the Na^+/K^+-ATPase

For most P-type ATPases, the exact topology of the membrane domain that permits specific substrate transport is not known. The entire primary structure of Na^+/K^+-ATPase and other P-type ATPases has been revealed using cDNA cloning and sequencing techniques [39-42]. Based on these primary sequences, hydropathy plots reveal that four strongly hydrophobic amino acid stretches in the NH_2-terminal third of the Na^+/K^+-ATPase are conserved throughout the family of ion-transporting ATPases and are predicted to cross the membrane as

α-helices (M_1-M_4). The middle third of Na^+/K^+-ATPase has no hydrophobic stretches long enough to span the membrane and is assumed to be folded as a globular domain on the cytoplasmic surface of the membrane [43-45], which has been identified as the ATP binding domain of the sodium pump. Hydropathy-based predictions vary greatly with respect to the COOH-terminal third of the Na^+/K^+-ATPase; the number of the transmembrane (TM) spans of the α subunit in this region varies from four to six in different models [46-50]. The total number of hydrophobic spans of the α subunit is assumed to be either 8 or 10. Furthermore, studies on this region using proteolytic analysis [48], β-galactosidase fusion proteins [51], epitope tag insertion [52], electron microscopy [53] and site-directed chemical labelling [54] supports a specific 10-TM segment model of the Na^+/K^+-ATPase and that both the NH_2-terminus and the COOH-terminus are in the cytosol. The β subunit has only a single TM domain (Hβ), a short cytoplasmic N-terminal domain and a large extracellular domain [11, 50, 55, 56]. Fig. 1.1 shows the predicted 10-TM model of the Na^+/K^+-ATPase α1 subunit derived from β-galactosidase fusion proteins [51].

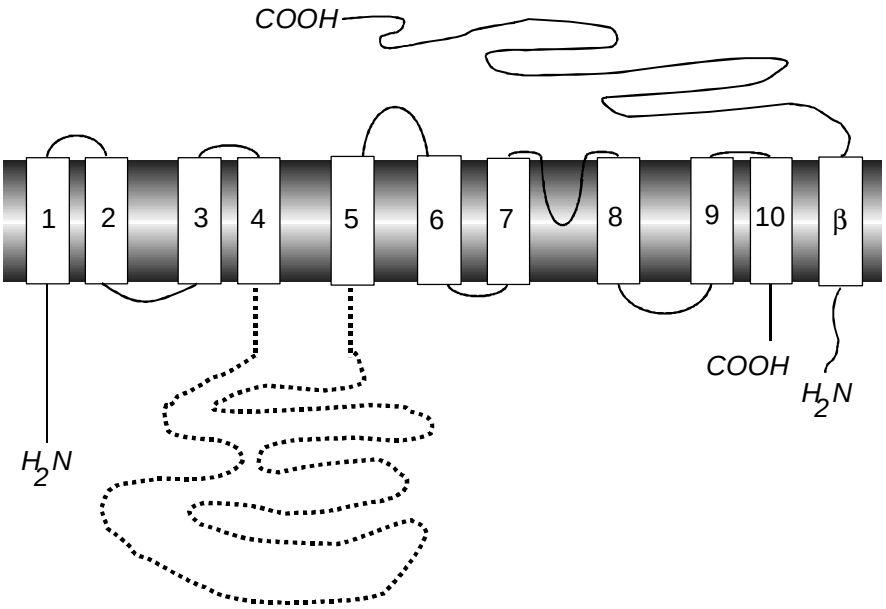

Fig. 1.1 Topological model of the Na^+/K^+-ATPase

The model shows the 10 TM spans of the a1 subunit of the Na^+/K^+-ATPase derived from studies using b-galactosidase fusion proteins (Fiedler and Scheiner-Bobis, 1996) **[51]**. *The cytoplasmic center between M_4 and M_5 transmembrane segments is shown with a dashed line. Both N- and C-termini are*

inside the cell. The b subunit displays only one TM span with a short N-terminus inside the cell and a large C-terminus outside (Lingrel 1994) [21,51].

Functional Na^+/K^+-ATPase is an oligomeric enzyme comprised of at least one α subunit of about 110 kDa and one 55-65 kDa glycoprotein β-subunit associated in an equimolar ratio. The apparent molecular mass of the β subunit on SDS-PAGE is highly variable, depending upon the degree of glycosylation, but the deglycosylated core protein is always the same size with approximately 35 kDa [14]. The α subunit, a polypeptide with 10 TM segments (H_1-H_{10}), contains the ATP-hydrolyzing center on the large cytoplasmic protrusion (L_4-L_5), cation binding and occlusion sites within the membrane, and a receptor site for cardiac glycosides on the extracellular surface [57]. The β subunit, with only a single TM domain, has the bulk of its mass in the extracellular space containing 6 extracellular cysteine residues. It plays a major role in the formation of the functionally mature and active αβ complex and in the targeting of the complex to the plasma membrane [58-60]. It also influences the holoenzyme's enzymatic and transport functions [61-64].

Although the Na^+/K^+-ATPase subunits are not linked by covalent bonds, the intersubunit interactions are strong enough that the complex remains stable upon solubilization in nonionic detergents, and subunits can be separated only using SDS [61, 65-67].

Another small, single-transmembrane protein, the so-called γ subunit with a molecular weight of 7.2 kDa, originally is believed to be a third subunit of the pump. The γ subunit was discovered by Forbush [68] and later cloned in rat, mouse, cow, sheep [69], human [70], and *Xenopus laevis* [71]. The γ subunit has a tissue-specific distribution and is detected only in kidney tubules by a specific monoclonal antibody [72, 73]. The γ subunit has sequence homology to a family of channel-inducing peptides including CHIF, mat 8, and phospholemman [74, 75]. Although the γ subunit does not appear to be necessary for normal Na^+/K^+-ATPase activity, it might play a modulatory role in pump function in a tissue-specific manner [72, 73, 76].

Isoforms exist for both the α (α1, α2, α3, α4) and the β (β1, β2, β3) subunit [77]. The different isoforms of the pump are expressed in a tissue- and development-specific fashion, and are to believed to be distinct in both function and modes of regulation [78-81]. The α1 isoform occurs in most tissues, while the α2 isoform is predominant in skeletal muscle and is also detected in brain and heart. The α3 isoform is limited essentially to neural and cardiac

tissue. The α4 isoform was recently identified in rat testes and has been expressed in mammalian cells [79, 80, 82]. The β2 isoform appears mostly on neural tissue while the β1 is ubiquitously expressed [42, 83]. The β3 isoform has been newly identified in mammals. The proportion of β3 isoform in the rat is highest in lung and testes and is also present in liver and skeletal muscle, whereas kidney, heart, and brain contain it only as a minor component of the Na^+/K^+-ATPase [81, 84]. Pestov *et al.* have identified recently a novel β subunit isoform of X,K-ATPase in human skeletal muscle designated β_m (β_{muscle}) which is different from other β subunits in the glycosylation and extension of its glutamic acid rich N-terminus. The β_m provides the only known example of the alternative splicing among the mammalian X,K-ATPase β-subunit mRNAs [85, 86].

1.1.4 Native inhibitors of the Na^+/K^+-ATPase

The Na^+/K^+-ATPase translocates Na^+ and K^+ ions across the membrane against their electrochemical gradient, resulting in the ionic homeostasis in animal cells. It ubiquitously exists in the cell plasma membrane and is of great importance for cell physiology [15, 21, 87]. Na^+/K^+-ATPase is also a molecular target for some toxins, such as palytoxin, cardiac glycosides, and sanguinarine. They bind to specific sites on Na^+/K^+-ATPase and strongly alter the pump character and its functional features [26, 64, 88, 89]. Toxins are thus useful tools for investigating the structure and properties of the ionophore of the Na^+/K^+-ATPase and its molecular mechanism. Palytoxin and ouabain are the two most used tools in Na^+/K^+-ATPase investigations.

Palytoxin (PTX) is synthesized by corals (palythoa species) and is the most potent animal toxin known. First isolated by Moore *et al.* in 1971 [90], this large hydrophilic molecule with a mass of 2680.17g/mol is about fifty times more toxic than the neurotoxin tetrodotoxin or saxitoxin with an LD_{50} for rodents in the range of 10-120 ng/kg of body weight [91]. As shown in Fig.1.2, PTX is a rather unique and large molecule with the molecular formula $C_{129}H_{223}N_3O_{54}$. It consists of three residues connected by peptide bonds, i.e., a large amino terminal polyhydroxy ω-amino acid followed by a dehydro-β-analine residue and an aminopropanol group. The number of free hydroxyl groups is 42 [90, 92]. A potent positive inotropic effect suggests that the Na^+/K^+-ATPase is a target of PTX [93, 94]. Ishida demonstrated an inhibitory effect of PTX on Na^+/K^+-ATPase from guinea-pig heart and brain [89]. The presence of PTX-induced channels is reported on frog red blood cells treated with PTX [95], in cultured aortic myocytes [96] and in excitable cells [97]. Furthermore, Scheiner-

Bobis [64, 76] demonstrated a PTX-induced K^+ efflux from yeast cells only when they expressed the mammalian Na^+/K^+-ATPase. A cysteine-scanning mutagenesis study suggests that the PTX-induced channel formation is largely mediated by the TM segments of Na^+/K^+-ATPase, and highlights the role of the 5th TM segment [98]. All this evidence points to the Na^+/K^+-ATPase as the target of the toxin.

In all, PTX interacts specifically with the sodium pump, inducing channel formation and resulting K^+ efflux and Na^+ influx down their electrochemical gradients. It is thus a useful tool in sodium pump investigation.

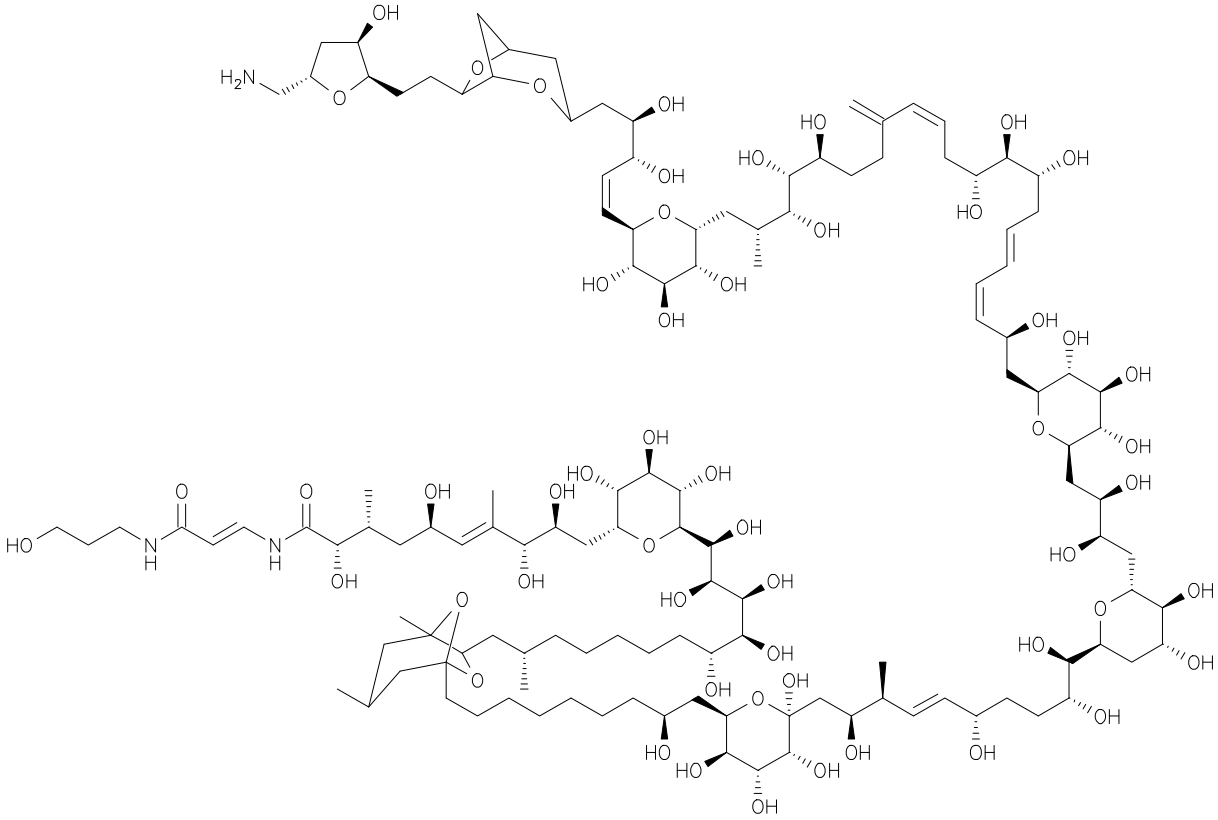

Fig. 1.2 Structure of the palytoxin

The structure of palytoxin was resolved by using NMR measurements [92].

Na^+/K^+-ATPase is specifically inhibited by cardiac glycosides, a class of steroids with an unsaturated lactone at the 17β position and a sugar moiety at the 3β position. Cardiac glycosides are frequently used in the treatment of congestive heart failure and some arrhythmia as their inhibition of Na^+/K^+-ATPase activity results in an increase in the force of myocardial contractility or positive inotropy [99].

Ouabain (Fig.1.3), a member of the cardiac glycosides, is highly polar and has been widely used in biomedical studies as a specific inhibitor of the sodium pump [57, 100-102]. Ouabain, which is an arrow poison of the African Ouabaio tree and of *Strophanthus gratus* plants, has been also identified in blood plasma, adrenal glands, and the hypothalamus of mammals and appears to function as an endogenous regulatory hormone [103].

Site-directed mutagenesis studies using ouabain-sensitive sheep or *Xenopus laevis* Na^+/K^+-ATPase α1 isoforms have revealed that multiple amino acid residues in the putative extracellular H_1-H_2, H_3-H_4, and H_7-H_8 loops and H_1 and H_5 TM regions of the α subunit are involved in determining the enzyme's ouabain sensitivity [104-109]. Studies of chimeras of the α subunit of Na^+/K^+-ATPase and H^+/K^+-ATPase [110] or Ca^{2+}-ATPase [111] establish that the large domains at both N- and C-terminal regions of the Na^+/K^+-ATPase are necessary for achieving high-affinity ouabain binding. Ouabain preferentially stabilizes a phosphorylated intermediate (E_2P) in the reaction cycle of the Na^+/K^+-ATPase and thereby stops ATP hydrolysis and active Na^+, K^+ transport across the plasma membrane [33]. PTX-induced K^+ efflux can be inhibited by ouabain [26, 64, 101].

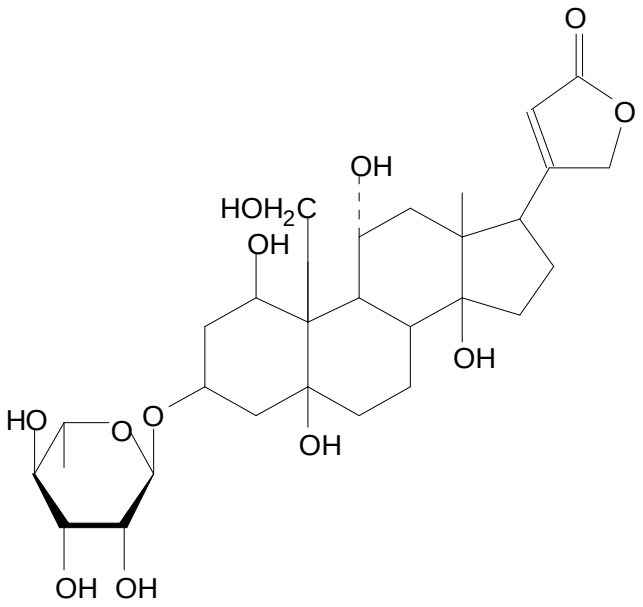

Fig. 1.3 Prototypical structure of the ouabain

Ouabain is composed of the basic steroid nucleus with a five-member lactone ring linked at C17 and is a glycoside due to the presence of a sugar linked via C3. Its systematic name is 3-[6-deoxy-α-L-mannopyranosyl)oxy]-1,5,11α,14,19-pentahydroxycard-20(22)-enolid with a molecular weight of 729 g/mol [99].

1.1.5 ATP interaction with the sodium pump

The sodium pump is a ubiquitous membrane complex that couples ATP hydrolysis and cation transport. The chemical energy is converted into the electrical energy during the turnover: the chemical energy released through ATP hydrolysis is the driving force of the cation transport by the Na^+/K^+-ATPase [15, 27, 83]. Understanding the ATP interaction with the enzyme has therefore been the focus of the studies on the sodium pump.

A three-dimensional microcrystal structure of the Na^+/K^+-ATPase with high resolution in the presence of its substrates is certainly the most powerful means for understanding the mechanism of its molecular function. Unfortunately, crystallography of integral membrane proteins still remains difficult [112]. The structure of the Na^+/K^+-ATPase at 20-25 Å resolution reveals the overall shape of the protein and the distribution of mass of α and β subunits [113]. The best microcrystal structure thus far available at 11-Å resolution [114] only clearly reveals cytoplasmic, transmembrane, and extracellular regions of the molecule with densities separately attributable to α and β subunits. Hence, most information about the functional mechanisms are from chemical modification and site-directed mutagenesis, i.e. biochemical or molecular biochemical studies.

Asp369 is the phosphorylation site of the Na^+/K^+-ATPase during catalytic turnover [116] and is located within the large cytoplasmic domain between the fourth and fifth TM segments (L_4-L_5 loop) of the catalytic α subunit [5]. The L_4-L_5 loop consists of 420-440 amino acid residues of around 45 kDa, including four of the most highly conserved P-type ATPase [21, 112]. It is therefore believed that ATP must originally bind to this globular domain during the enzymatic cycle.

Gatto *et al* have overexpressed this large cytosolic loop (a 6-histidine-tagged fusion protein called His_6-α-loop) of the rat sodium pump in *E. coli*. Their results suggest that this His_6-α-loop binds nucleoside triphosphate with the same specificity as the intact native protein [112]. In sequence studies, this large globular cytoplasmic domain has been truncated at a different C-terminal with a unique N-terminal and also successfully expressed in *E. coli*, and the expressed truncated cytoplasmic domain of the sodium pump was found to have a conformation that is similar to the homologous region in the native enzyme and the nucleotide binding site was retained in a fragment containing as few as ~250 amino acids (Ala345 to Thr610) [118]. This evidence lends further support to the notion that this large catalytic center supplies the ATP-binding site in the intact sodium pump.

Based on this structural model, some amino acids within this cytoplasmic domain that are thought to be important for ATP binding or hydrolysis have been also identified. For example, Glu472, Lys480, Lys501, Gly502, Asp710, Asp714, Lys719, and Lys767 are all modified by a variety of chemical agents in the absence of ATP but not in its presence, suggesting a role in ATP binding [21, 112, 119-121]. Furthermore, replacement of Glu472 and Lys480 via mutagenesis induces an inactivation of the enzymatic activity of the pump, probably by arresting the α- and β-phosphate groups of ATP in an unfavorable position prior to hydrolysis of the γ-phosphate group; these residues are thus perhaps essential for ATP-recognition [122]. The ^{709}GDGVND segment in the M_4-M_5 loop is highly conserved in P-type ATPases and is of great importance for Mg^{2+} binding, phosphorylation, and energy transduction in the Na^+/K^+-ATPase [123, 124]. Changing of the polar residues in this segment results in a reduction (D^{710}, N^{713}) or elimination (D^{714}) of the catalytic activity. The amino acids D^{710} and N^{713} contribute to coordination of Mg^{2+} during transfer of γ-phosphate of ATP to the phosphorylation site Asp369, in the high energy $Mg{\cdot}E_1P[3Na^+]$ intermediate but do not contribute to Mg^{2+} binding in the E_2P·ouabain complex [123]. Transition to E_2P thus involves a shift in Mg^{2+} coordination away from D^{710}, N^{713}, and the two residues become more important for hydrolysis of the acyl phosphate bond at Asp369. Another amino acid residue Cys577, is believe to be a conformationally mobile residue in the ATP binding domain due to its conformation-sensitive reactivity and its variable reactivity in different enzyme-cation bound states [119]. This work indicates that structural changes in the ATP-binding domain are transmitted through at least 100 of the amino acid residues in the primary structure and suggests that the sequential binding of each of the two transported K^+ ions produces changes in ATP-binding domain [119]. Stable oxygen isotope exchange studies suggest that Lys^{501} interacts with ATP, thought also to be an essential component of ATP interaction with the Na^+/K^+-ATPase [125].

The outcome of the crystal structure studies of Ca^{2+}-ATPase of sarcoplasmic reticulum at 2.6-Å resolution with two Ca^{2+} ions bound in the transmembrane helix provides a helpful tool for understanding the structure-function relationship of P-type ATPases, including the sodium pump, at the molecular level [126]. This crystal structure reveals the functional architecture of the cytosolic region of the Ca^{2+}-ATPase with its corresponding amino acids in the electron-density maps and the conformational changes in this region during ATP hydrolysis. In this crystal structure, the cytosolic region of the Ca^{2+}-ATPase includes a short N-terminal segment (Met1-Glu58) and the loop (Trp107-Ser261) between the M_2-M_3 TM segment, folded in the A

domain (adenosine binding site), and the large loop between the M_4 and M_5 TM segment (cytoplasmic center), folded in separate P (phosphorylation) and N (nucleotide binding) domains (Fig. 1.4) [126, 127]. The N-domain is mobile in the presence of Ca^{2+} but fixed in its absence, and it comes close to the P-domain in the phosphorylated states by thermal fluctuation and/or by conformational change induced by ATP-binding, thus transmitting the phosphorylation signal to the Ca^{2+} binding site. The A domain exists in another subunit separated from the P and N domains and acts as an actuator or an anchor for the movement of the N domain. The A domain is taken away from the cytosolic center induced by Ca^{2+}-binding. The large domain movements take place during the active transport [126]. Such conclusions help to confirm former hypotheses and studies on Na^+/K^+-ATPase.

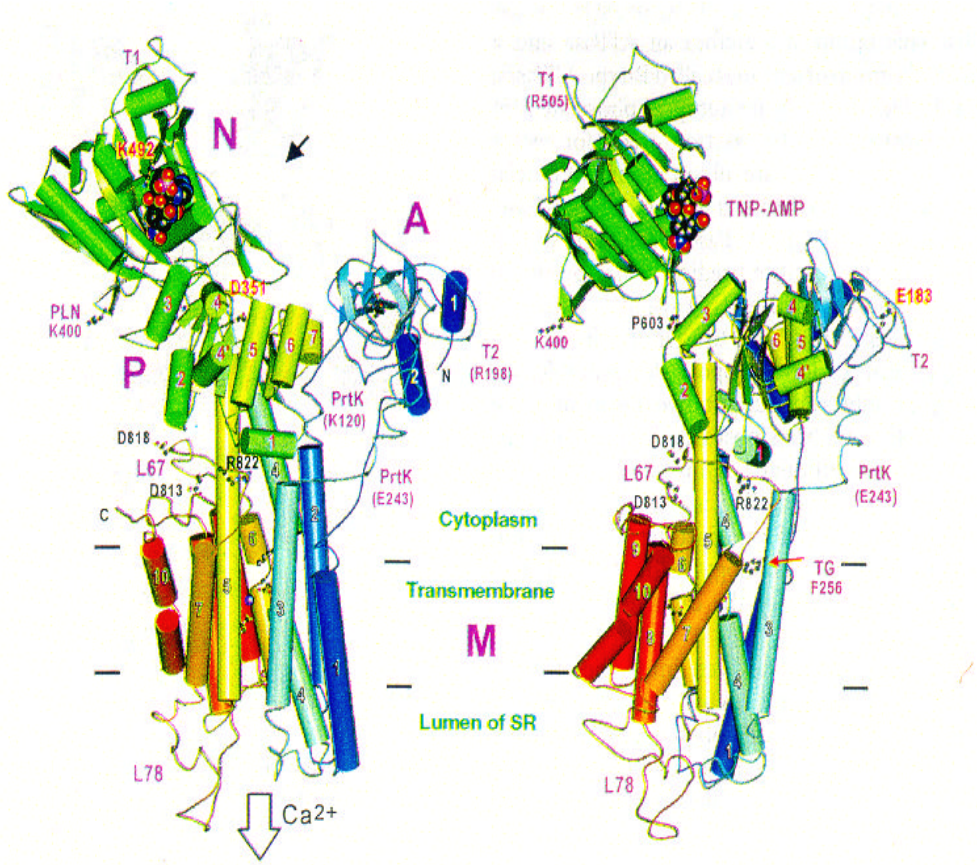

Fig. 1.4 Architecture of the sarcoplasmic reticulum Ca^{2+}-ATPase

a-Helices are represented by cylinders and b-strands by arrows. Color changes gradually from the N-terminus (blue) to the C-terminus (red). Three cytoplasmic domains are labeled (A, N, and P). TM helices (M_1-M_{10}) and those in domains A, N, and P are numbered. The model is oriented so that the TM helix M_5 is parallel to the plane of the paper. Several key residues are shown in ball-and-stick. Asp351 is the phosphorylation site for Ca^{2+}-ATPase (from Toyoshima et al, 2000) [126].

Although extensively studied, the structure-function relationship of the Na^+/K^+-ATPase and its evolutionary connections with other enzyme families remain unclear.

1.2 Haloacid dehalogenase

1.2.1 Reaction mechanism of the haloacid dehalogenase

A new work suggests that the P-type ATPases also belong to a large superfamily of hydrolases structurally typified by the L-2-haloacid dehalogenase [128]. The L-2-haloacid dehalogenase from *Pseudomonas sp*. YL (L-2-DEX YL; EC 3. 8. 1. 2), a member of the superfamily of HAD hydrolases which comprises phosphatases, epoxide hydrolases, and L-2-haloacid dehalogenases [129], catalyses the hydrolytic dehalogenation of L-2-haloalkanoates to produce corresponding D-2-hydroxyalkanoates [130, 131]. As shown in Scheme1.2, the

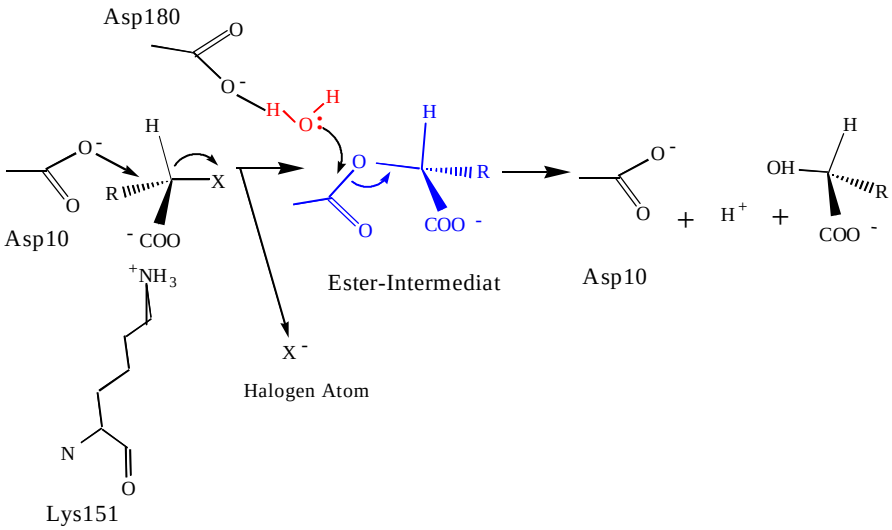

Scheme 1.2 Proposed reaction mechanism of L-2-DEX YL

In the first step of the enzyme reaction, the relative nucleophile Asp10 attacks the a-carbon of the substrate to form an ester intermediate and a halide ion. In this step, Lys151 serves to stabilize the excess negative charge in the substrate/reaction intermediates. In the second step, the ester intermediate is hydrolyzed by an activated water attacking on the g-carbon of the Asp10, and the Asp10 is regenerated while the product is formed. The water is proposed activated by the nucleophile Asp180.

reaction begins with a nucleophilic attack of Asp10 on the α-carbon atom of L-2-haloalkanoates, causing the release of a halide ion and the formation of an ester intermediate,

which is subsequently hydrolyzed by an activated water molecule restoring the side-chain carboxyl group of the Asp10 [132-134]. The putative reaction mechanism of the sodium pump shows in Scheme 1.3, just as in the case of L-2 DEX YL, the aspartate (Asp369) carboxyl oxygen can initiate a nucleophilic attack on the electron-rich γ-phosphate bond of ATP, resulting in phosphoester formation (phosphorylation). The phosphoenzyme is subsequently hydrolyzed (dephosphorylation) and the free energy of hydrolysis is utilized for ion transport.

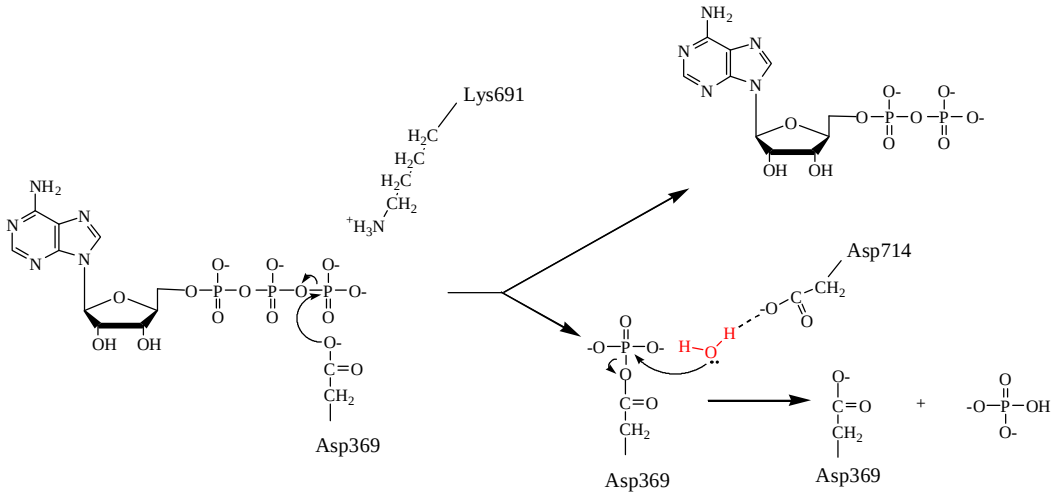

Scheme 1.3 Proposed reaction mechanism of the Na^+/K^+-ATPase

The Asp369, Lys691, and Aps714 residues of the sodium pump correspond to Asp10, Lys151, and Asp180 in L-2-EDX YL, respectively. As in the case of L-2 DEX YL, the reaction begins with a nucleophilic attack of the aspartate (Asp369) carboxyl oxygen on the electron-rich g-phosphate bond of ATP, resulting in phosphoester formation (phosphorylation). The phosphoenzyme is subsequently hydrolyzed (dephosphorylation) and the free energy of hydrolysis is utilized for ion transport. The Lys691 residue is believed to stabilize the excess negative charge in the substrate/reaction intermediates and Asp714 coordinate a water molecule (in red) that is directly involved in ester intermediate hydrolyze.

1.2.2 The crystal structure of L-2-haloacid dehalogenase

L-2-DEX YL is a homodimeric enzyme formed by two identical subunits. Each 26-kDa subunit consists of 232 amino acid residues whose sequence has been deduced from the gene sequence [135]. Its crystal structure at 2.5-Å resolution reveals the existence of two

structurally distinct domains in each subunit (Fig.1.5a). The core domain, comprising about 65% of all the residues, is an α/β sandwich formed by a six-stranded parallel β-sheet flanked by five α-helices with the topology of a Rossmann fold (β strand order 3-2-1-4-5-6) (Fig.1.5b). The subdomain, inserted into the core domain, has a four helix bundle structure providing the greater part of the interface for the dimer formation [135]. The identified nucleophilic residue Asp10 is located at the C-terminus of the β1-strand in the core domain [135, 136]. The other functional residues, Thr14, Arg41, Ser118, Lys151, Ser175, Asn177 and Asp180, detected by site-directed mutagenesis experiments, are arranged around the nucleophile in the active site [130, 135]. This typical haloacid dehalogenase fold, the so-called Rossmann fold, has been found in the crystal structure of Ca^{2+}-ATPase [126]. In the X-ray analysis of the L-2-DEX YL crystal structure, there is a water molecule close to Asp10, Ser175, Asn177 , and Asp180. The latter three residues are supposed to enhance the nucleophilicity of the water molecule for hydrolysis of the ester intermediate and Lys151 is involved in stabilizing the excess negative charge in the substrate/reaction intermediates [128, 130, 137].

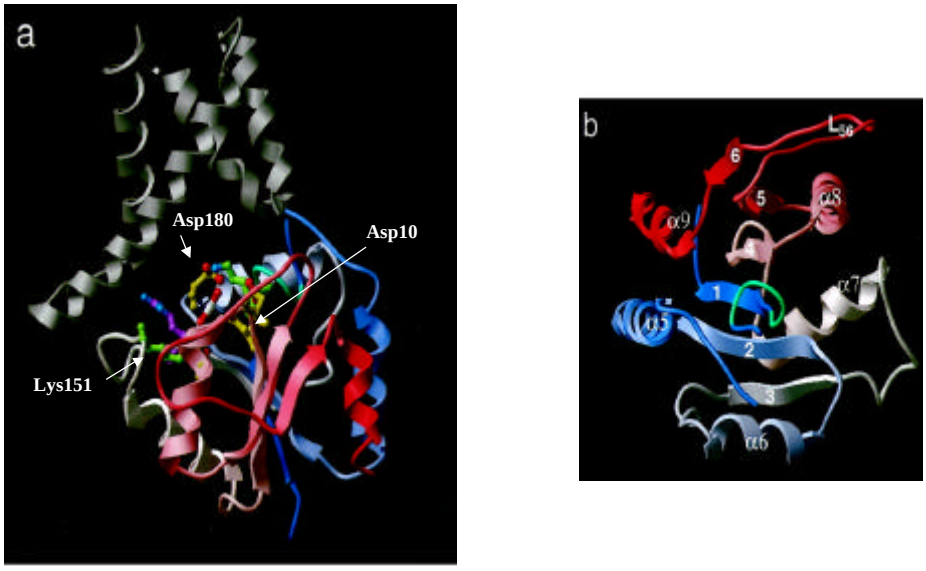

Fig. 1.5 Crystal structure of the L-2haloacid dehalogenase ps (L-2-DEX YL)

a*. The backbone of the Rossmann fold is coloured from blue at the N-terminus to red at the C-terminus. The inserted subdomain is gray. Catalytic residues are coloured as follows: Asp in yellow, Lys in green, Arg in purple.* ***b****. Rossmann fold from L-2-DEX YL. The active site Asp10 is located at the b1-loop (green).*

Protein sequence comparison shows a high sequence homology between these two enzymes. Sequences homologous to the dehalogenase core domain are referred to as the phosphorylation or P domain and the inserted domain (140-240 residues in the ATPase) as the adenosine-binding or A domain [128, 136].

1.3 Question outcome

L-2-DEX YL is a well studied member of the HAD hydrolases superfamily and has been characterized in great detail with regard to reaction kinetics utilizing chemical modification and site-directed mutagenesis [130, 131, 133, 134]. Structural studies using electron microscopy and X-ray analysis has provided considerable additional information [132, 135, 137]. As already described, the Na^+/K^+-ATPase has a significant sequence similarity between its P domain and the core domain of the L-2-DEX YL. Furthermore, they also have in common the use of an aspartyl ester intermediate during their reaction cycle, the dynamics of which, in the pumps, are closely linked to the occlusion and transport of cations across the membrane. Structure comparison suggests the phosphorylation domain of the P-type ATPase adopts a Rossman fold of L-2-DEX YL (Fig.1.4) [126, 136]. Such events support the evolutionary connection between the haloacid dehalogenases and P-type ATPases [129, 134, 138, 139].

It is thus proposed that the P-type ATPase evolved by fusion of a HAD superfamily phosphatase domain with a transmembrane protein, for example, that of a permease [128].
If this hypothesis is tenable, what role do the residues, which correspond to those of the critical amino acids for the activity of the haloacid dehalogenase, play in the function of the sodium pump? Is the functional mechanism similar to or the same as that of haloacid dehalogenase?

By protein sequence comparison, we have found that amino acid residues Lys691 and Asp714, located in the phosphorylation domain of the sodium pump α subunit, correspond to the Lys151 and Asp180 in L-2-EDX YL, which are absolutely conserved in the HAD superfamily and P-type ATPases **(**Fig. 1.6).

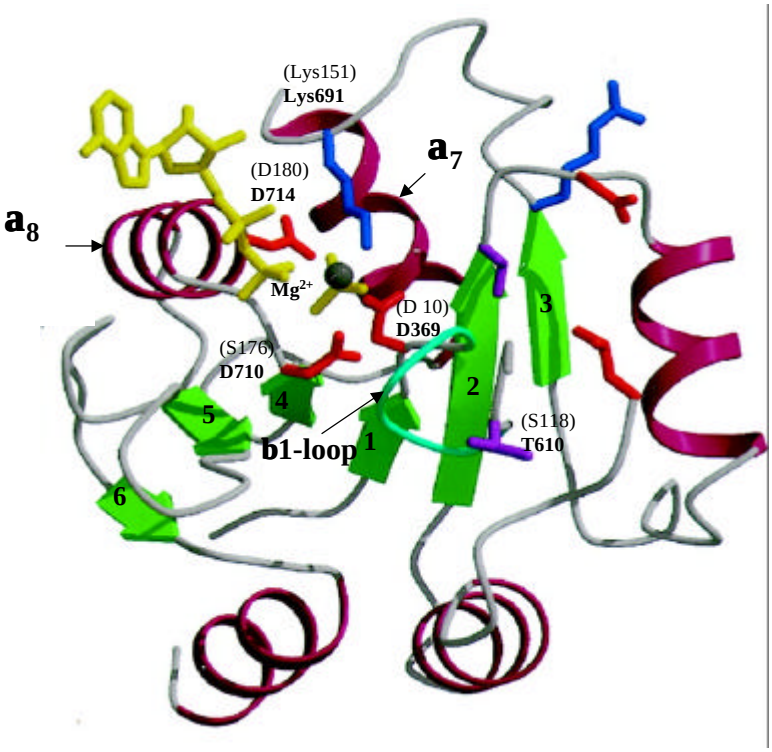

Fig. 1.6 Structure of the catalytic site of a haloacid dehalogenase from *Pseudomonas ps*

The important amino acid residues in haloacid dehalogenase are signed in brackets and the corresponding amino acid residues in Na^+/K^+*-ATPase a1 subunit are marked in bold. The crystal region of sodium pump was adapted from Stockes&Green* [136] *and Aravind et al* [128].

In the crystal structure, Lys151 and Asp180 are located around the phosphorylation site Asp10, which is located at the end of β1. Lys151 is located approximately at the beginning of the α_7-helix, and Asp180 in the α_8-helix. Nine water molecules in this region form a complicated hydrogen bond network with important functional residues such as Ser118, Thr44, and Asn176. The crystal structure of the intermediate of L-2-DEX YL demonstrates that the orientation of the carbonyl group $C^{\gamma}=O^{\delta 1}$ (side chain) in the ester intermediates varies according to the substrate used, and the carbonyl oxygen is oriented toward N^{ζ} (N atom in the side chain) of Lys151. The Lys151 is tightly hydrogen-bonded to the unesterified oxygen $O^{\delta 1}$ of Asp10, and thus acts as a component residue of the oxyanion hole for stabilizing the negative charge accumulated on the $O^{\delta 1}$, resulting in a nucleophilic attack on the C^{γ} atom of the Asp10 by an activated water [137, 140].

Asp180, however, activates the water molecule utilized for ester bond hydrolysis together with Asn177, and these residues are hydrogen-bonded with the side chain of Asp10. The formation of proper hydrogen bonds between the water molecule and the side chains of Ser175, Asn177, and Asp180 is essential for the hydrolysis of the ester. Lys151 makes a salt bridge to the active-site aspartate residue and activates the water molecule that hydrolyses the acyl intermediate; thereby, Lys151 probably also plays a role at this step [137, 141].
Side-directed mutagenesis studies suggest that Lys151 and Asp180 are essential for the enzymatic activity of the L-2-DEX YL [130, 133].

We therefore selected these two amino acid residues as targets for our experiments, exchanging them via site-directed mutagenesis for other residues. All mutant α subunits were coexpressed with respective β subunits in *Saccharomyces cerevisiae*, which does not contain endogenous Na^+/K^+-ATPase [62, 64, 76]. To determine the yeast transformation efficiency and characterize the mutant Na^+/K^+-ATPase, PTX-induced K^+ efflux from intact yeast cells expressing either native or mutant Na^+/K^+-ATPase and the related inhibitory effect by ouabain were assessed. Furthermore, ATPase activity and ouabain binding characteristics under various conditions were determined.

Our findings support that Aravind's proposal is most likely correct: Lys691 is essential for the phosphorylation process and Asp714 for the dephosphorylation process of the sodium pump. Nonconservative mutants of both amino acids are completely inactive and do not display any partial reactions typical for the sodium pump. On the other hand, conservative mutants of Lys691 remain most likely unphosphorylated while conservative mutants of Asp714 are probably phosphorylated but remain arrested in this state by not being able to hydrolyze the phosphoric ester bond formed between Asp369 and the terminal ATP phosphate. Thus, Lys691 and Asp714 residues on the sodium pump α subunit are critical for its enzymatic activity.

2. Materials and Methods

2.1 Materials

2.1.1 Cell strains and Plasmids

2.1.1.1. Cell strains

E. coli (*Escherichia coli*) strain DH5αF′ with the genotype F′ ϕ80d lacZΔM15 recA1 endA1 gyrA96 thi-1 hsdR17(r_K^-,m_K^+) supE44 relA1 deoR Δ(lacZYA-argF)U169, which was used as replication system for plasmid with native or mutated cDNA of Na^+/K^+-ATPase, were purchased from Gibco (Eggenstein/Germany).

The *Saccharomyces cerevisiae* yeast cell line 30-4 with genotype Mat-α trp1 ura3 Vn2 GAL^+ was used as heteroexpression system for either native or mutant Na^+/K^+-ATPase.

2.1.1.2 Plasmids

Plasmid pBluescript®™ KS II + (pKS^+) containing ampicillin selectivity (Stratagene, La Jolla/CA) was used as the cloning vector for mutagenesis of the Lys691 and Asp714 in the α1 subunit of Na^+/K^+-ATPase and subcloning the substitution into *E. coli*. DH5αF'. Its structure is shown in Fig.2.1.

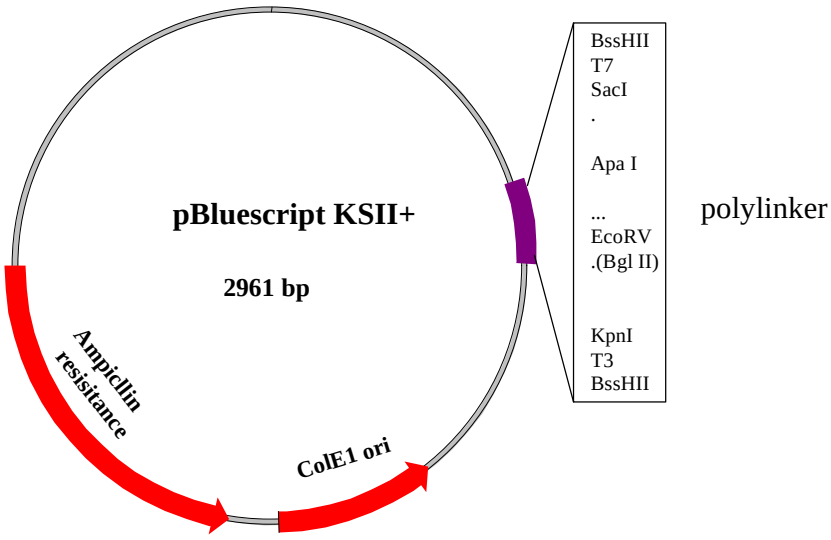

Fig.2.1 Map of the plasmid pBluescript KS II +

*The plasmid represents a high copy number ColE1-based phagemid and a large versatile polylinker with T_3 and T_7 promoters and ampicillin resistance to E. coli. * The restriction site EcoRV has been modified into a BglII site..*

Plasmid pCGY1406αβ containing cDNA encoding both the sheep kidney α1 subunit and the dog kidney β1 subunit of $Na^+/^+$-ATPase [62] was used as the yeast expression vector. As shown in Fig.2.2, this plasmid presented the 2μm replication origin from yeast and the pBR322 replication origin from *E. coli*, and provided ampicillin resistance to bacteria and tryptophan auxotrophy to yeast cells. The mRNA-synthesis of the α1 subunit and the β1 subunit were driven by copper metallothioini promotor (CUP1) and phosphoglycerate kinase promotor (PGK), respectively. The PGK-terminator served as the terminator of transcription for both molecules [64].

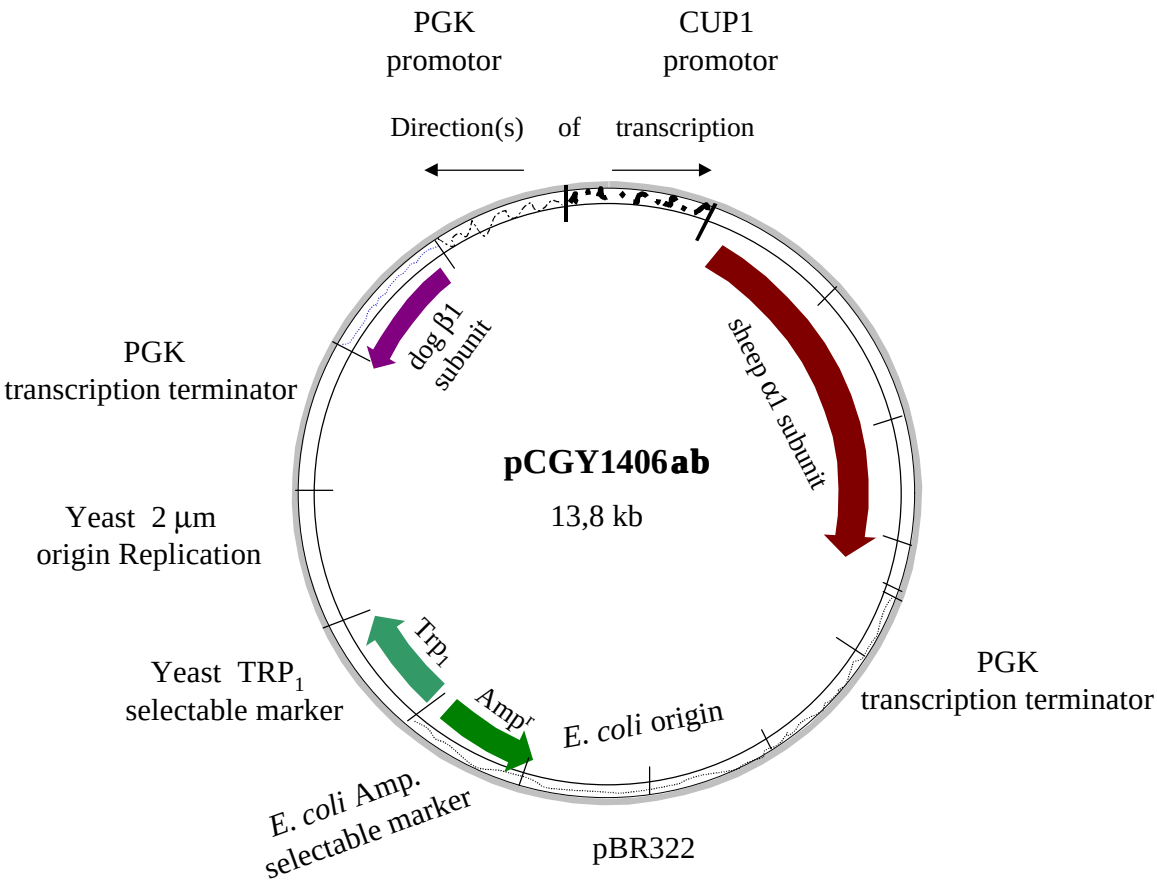

Fig.2.2 Map of the plasmid of pCGY1406ab

This figure shows the gene-card of the shuttle vector pCGY1406ab (adapted from Horowitz et al.) [62].

2.1.2 Oligonucleotides

All of the oligonucleotides, which served either as linkers of the plasmid construction or as primers for the PCR, were obtained from Roth (Karlsruhe/Germany).

Table 2.1 Oligonucleotides for pKS$^+$ construction

1	5´CCTTAAGGGTGACCA3´
2	5´GATCTGGTCACCCTTAAGGGGCC3´

Table 2.2 Primers for introduction of Lys691 mutations in α1 subunit by inverse-PCR

Mutation	oligonucleotide sequence
Native Lys691	5´TCTCCGCAGCAG**GAA**CTCATCATTGTG3´
Lys691Ala	5´TCTCCGCAGCAG**GCG**CTCATCATTGTG3´
Lys691Arg	5´TCTCCGCAGCAG**AGG**CTCATCATTGTG3´
Las691Asp	5´TCTCCGCAGCAG**GAT**CTCATCATTGTG3´
	5´GGTCCT*CGC*GAACACAATCTCCGTGTG3´
	Reverse primer with a new restriction site ***Nru*I** as the diagnostic signal.

Table 2.3 Primers for introduction of Asp714 mutations in α1 subunit by inverse-PCR

Mutation	oligonucleotide sequence
Native Asp714	5´GACGGTGTCAAT**GAC**TCCCCGGCTTTG3´
Asp714Ala	5´GACGGTGTCAAT**GCA**TCCCCGGCTTTG3´
	with a new restriction site ***Nsi*I**
Asp714Arg	5´GACGGTGTCAAT**CGA**TCCCCGGCTTTG3´
	with a new restriction site ***Cla*I**
Asp714Glu	5´GACGGTGTCAAT**GAA**TCCCCGGCTTTG3´
	with an increased restriction site ***Cfr*10I**
	5´TCCAGTTACAGCCACAATGGCACCCTG3´
	Reverse primer

2.1.3 Restriction endonucleases and other modifying enzymes

The restriction endonucleases, T_4 DNA ligase, T_4 DNA polymerase, T_4 polynucleotide kinase and Taq Polymerase used for PCR with their corresponding buffers were purchased by MBI Fermentas (Vilnius/Litauen) and Biolab (New England); the shrimp Alkaline Phosphatase was obtained from United State Biochemical Corporation (Cleveland/OH), the lysozyme , and RNase were purchased from Boehringer (Mannheim/Germany)

2.1.4 Antibodies

Both monoclonal antibodies against the β_1 subunit (anti-β) and α_1 subunit (anti-α) of the Na^+/K^+-ATPase used for detection of the subunits of the sodium pump are immunoglobulin G (IgG) derived from mouse (Alexis Corporation, Darmstadt/Germany). The antibody against mouse IgG coupled to HRP (horse radish peroxidase) served as the secondary antibody in Western blotting (Amersham Pharmacia Biotech, Freiburg/Germany).

2.1.5 Buffers and Medium

All solutions and glassware used in molecular cloning were sterilized by autoclaving at 120°C (glucose contained solutions at 110°C) for 1 h with an overpressure of 1.2 bar or by filtration through a 0.2-µm sterile filter (Sigma, Deisenhofen/Germany).

All aqueous solutions and buffers were prepared with double-distilled, deionized water (ddH_2O) obtained from Milli-Q® water system from Millipore.

The content of individual solutions is listed at the end of the corresponding method section.

2.1.6 Other enzymes, chemicals, biochemicals and kits

Nitrocellulose membrane (NC Membrane) and Whatman 3MM Chromatography paper used in Western blotting were from Schleicher & Schuell (Dassel/Germany) and Biometra® (Göttingen/Germany), respectively. Bovine serum albumin (BSA) was purchased from Boehringer Ingelheim (Heidelberg/Germany).

Palytoxin, which was isolated from *Palythoa caribaeorum*, was obtained from Dr. L. Bèress from Christian-Albrechts-University (Kiel/Germany) and ouabain was from Sigma (Deisenhofen/Germany).

The Netzmittel and K^+-Standard solution used in K^+ efflux measurement were the products from Eppendorf (Hamburg/Germany). Pyruvate kinase (PK) and lactate dehydrogenase (LDH), used in Na^+/K^+-ATPase activity assay, and the protease inhibitors such as leupeptin, pepstatin, and phenylmethylsulfonylfluoride (PMSF), used in membrane preparation were obtained from Boeringer Mannheim GmbH (Mannheim/Germany). Coomasie blue R-350 for SDS-polyacrylamide gel staining was from Serva (Heidelberg/Germany). The prestained protein marker with the protein mass spectrum of 122, 79, 47, 33, 24, and 20 kDa was from PeQ Lab (Erlangen/Germany). The DNA Marker of GeneRuler™ 1-kb DNA ladder and λ-DNA / *Eco47*III/*Eco*91I were from IBM Fermentas (Vilnius/Lithuania). The Na^+/K^+-ATPase from the pig kidney was a gift from Prof. Dr. Schoner (Institute of Biochemistry, Justus-

Liebig University, Germany). Agarose for agarose gel electrophoresis was from AGS GmbH (Heidelberg/Germany). The polyacrylamide Gel 40 used for SDS-PAGE and the scintillation solution of Rotiszint®2200, used for scintillation counting, were from Roth (Karlsruhe/Germany).

[^{3}H]Ouabain (22.5 Ci/mmol) was from Alexis Corporation (Darmstadt/Germany). The Kodak X-ray film used in chemiluminescence photography was obtained from INTEGRA Biosciences (Fernwald/Germany).

The JETsorb kit used in DNA extraction from agarose gels was ordered from Genomed (Bad Oeynhausen/Germany); the GFX micro plasmid preparation kit, used for plasmid isolation from *E. coli*, and the ECL™ Western blotting system RPN 2108 kit for protein detection, were obtained from Amersham Pharmacia Biotech (Freiburg/Germany).

All other chemicals and biochemicals were purchased by Sigma (Deisenhofen/Germany), Roth (Karlsruhe/Germany), or Merck (Darmstadt/Germany)

2.2 Equipment

The flame photometer, which was used for determination of the K^+ efflux from the yeast cells, and the thermocycler used in PCR were from Eppendorf (Hamburg/Germany). The electroporator used for plasmid transformation was obtained from PeQ Lab (Erlangen/Germany). The scintillation counter wallac 1409 used to determine radioactivity was from Wallac (Turku/Finland). The Semi-dry blot for the electrophoretic transfer of the protein from SDS-polyacrylamide gel into the NC membrane was from BioRad (Frankfurt/Germany). The gel documentation system for the detection of DNA bands in agarose gels after electrophoresis was from Biostep (Erzg./Germany). The Bead Beat used for breakage of the yeast cells was from Ebel (Hamburg/Germany), and the glass bead with a diameter of 0.25 to 0.3 mm was from Braun Melsungen GmbH (Melsungen/Germany). The L-70 ultracentrifuge was a product of Beckman (USA).

All other equipment such as centrifuges, incubators, electrophoresis sets, and photometers were the general facilities of a biochemical and molecular biological laboratory.

2.3 Methods

2.3.1 Introduction of mutations into shuttle vector pCGY1406ab

2.3.1.1 Construction of the plasmid pKS$^+$-AS

The pKS$^+$ was constituted by inserting an *Apa*I-*Bgl*II linker to generate a *BstE*II site between *Apa*I and *Bgl*II sites.

The oligonucleotides (Table 2.1) were dissolved in sterile H_2O to reach a final concentration of 20 pmol/µl at RT. Both oligonucleotides were mixed in equimolar amounts and heated to 90°C for 1 min, and the DNA allowed to anneal by natural cooling down at RT forming an oligolinker with the new restriction site of *BstE*II and the cohesive site of *Apa*I and *Bgl*II at both end, respectively (Fig. 2.3). This linker applied in a 100-fold molar excess over the plasmid was ligated into the commercially available bacterial pKS$^+$ digested with restriction enzyme of *Apa*I and *Bgl*II, and this pKS$^+$ plasmid with *BstE*II site was called pKS$^+$-*BstE*II. The pKS$^+$-*BstE*II plasmid was then digested with *Bgl*II and *BstE*II to obtain a 2937 bp long *BstE*II-*Bgl*II fragment as a vector which was purified from a 1% agarose gel after electrophoresis. An other *BstE*II-*Bgl*II fragment with 1010 bp from the sheep sodium pump α1 subunit cDNA served as an insert was then placed into the same restriction site of the pKS$^+$-*BstE*II plasmid using T_4 DNA ligase, this plasmid with 3947 bp was denoted as pKS$^+$-AS and served as the vector for site-direct mutagenesis.

5´**C**CTTAAGG<u>GTGACC</u>**A**3´
3´**CCGGG**GAATTCC<u>CACTGG</u>**TCTAG**5´
*Apa*I *BstE*II *Bgl*II

Fig.2.3 Oligonucleotide linker with *BstE*II restriction site

The new restriction site of BstEII was indicated with underline and the cohesive site of ApaI and BglII at both end were in bold.

2.3.1.2 Culture and storage of the *E. coli*

The rate of the growth is dependent on the medium, the genotype of the strain, the temperature and the degree of the aeration. The rate of the growth can be monitored by withdrawing aliquots and measuring the optical density at a wavelength of 600 nm (OD_{600}) [142]. For *E. coli* strain DH5αF′, 1 $OD_{600} = 1 \times 10^{11}$ cells/ml.

A single clone of *E. coli* strain DH5αF′ transformed with plasmid DNA was inoculated in 5 ml LB-medium with 0.1 mg/ml ampicillin (ampicillin must be omitted for untransformed *E. coli*) and was incubated at 37°C with 156 rpm shaking overnight. 500 µl of the culture was centrifuged by 3,000 rpm at 4°C for 5 min and the supernatant was discarded. The bacteria pellet was dissolved in 15% glycerol and could be kept for long-term storage at –70°C.

For daily use, the short-term storage was performed using. 1 µl of the overnight culture diluted in 1 ml LB-medium. This was well mixed and ca. 50-100 µl of the dilution was spotted in the center of a LB-agar/ampicillin plate. The cells was spread over the entire surface of the agar and incubated at 37°C overnight. The bacterial clone on the plate tightly wrapped in parafilm could be maintained for several months at 4°C. The rest of the culture was used for isolation of the plasmid DNA (see Methods 2.3.1.4).

LB-Medium: 10 g/L Bacto-trptone, 5 g/L Bacto-yeast extract; 10 g/L NaCl; pH 7.5
LB-Agar/Ampicillin-Plate: LB-medium with 15 g/L Bacto^{TM} agar-agar, and 0.1 mg/ml ampicillin
15% (w/v) Glycerol: 15 g Glycerol in 100 ml dest. H_2O

2.3.1.3 Introduction of the plasmid DNA into *E. coli*

A rapid and simple method of transforming *E. coli* by cDNA is electroporation [143, 144]. High-voltage electric pulses can induce the cell plasma membrane to fuse and the cells can take up exogenous DNA from the surrounding solution, apparently through the holes momentarily created in the plasma membrane.

To prepare the fresh electrocompetent cells of *E. coli* DH5αF′, a single clone of the *E. coli* DH5αF′ was incubated in 5 ml LB medium at 37°C under continuos shaking at 140 rpm overnight. Then, 2 ml of the overnight culture were transferred into 200 ml of LB medium and incubated continuos to reach a OD_{600} value of 0.5 corresponding to a cell density of 1×10^{11} cells/ml. All following steps were performed on ice. The culture was centrifuged at 4°C for 20 min at 5,000 rpm and cooled on ice for 15 min. The cell sediments were carefully washed twice with 200 ml ice-cold ddH_2O, centrifuged as above. The cell pellet was suspended in 20 ml ice-cold ddH_2O and split into 100 µl aliquots for use. For storage of the electrocompetent cells, ice-cold glycerol was added into the washed cell suspension with an final concentration of 10%. At this point, the electrocompetent cells could be kept in aliquots at –70°C for a long term.

The ligated plasmid DNA was precipitated (see Methods 2.3.1.7) to decrease the ionic strength in the DNA sample. A total of 0.1 µg plasmid DNA was then mixed with 100 µl fresh prepared electrocompetent cells and transferred into the electroporation cuvette which

was placed on ice. The electroporation was performed using the following electroporation program: High Voltage (volt) 2300, Capacity (µF): 0025, Shunt (ohm): 0156, Pulse (msec): 5
One ml SOC solution was then immediately added into the electroporated cell suspension and the mix was transferred into a 1.5 ml Eppendorf tube and incubated at 37°C for 1 h. Alternatively, 50 µl of the culture were spread on the surface of a LB-agar plate with 0.1 mg/ml ampicillin, and incubated at 37°C overnight. Transformed *E. coli* cells containing the plasmid grew overnight. The formed colonies were picked for minipreparation.

SOC-solution: 20 mM Glucose, 2% Bacto-tryptone, 0.5% Bacto-yeast-extract, 0.05% NaCl

2.3.1.4 Isolation of the plasmid DNA from *E. coli*

The mini-boiling plasmid preparation method is one of the widely used methods of plasmid DNA isolation from small culture volumes and gives high yields of plasmid DNA [199].
An overnight culture of 4.5 ml was centrifuged at 4°C for 10 min under 3,000 rpm, the supernatant was removed by aspiration. The bacterial pellet was resuspended in 0.35 ml STET solution, 25 µl of a freshly prepared lysozyme solution (10 mg/ml in 10 mM Tris/HCl, pH8.0) was added and mixed by vortexing for 3 sec. The reaction mix was then placed in a boiling water bath for 40 sec and centrifuged immediately after for 10 min at RT in an Eppendorf centrifuge. The pellet was removed with a platinum loop, 42 µl ice-cold 10 M ammonium acetate and 420 µl ice cold isopropanol were added to the supernatant. Following incubating at –20°C for 15 min, the supernatant was centrifuged at 4°C for 15 min at 13,000 rpm, the plasmid pellet was washed twice with ice-cold 70% ethanol and then dried by treatment in a vacuum desiccator for 1-2 min. The plasmid DNA was dissolved at the desired concentration with TE buffer or sterile H_2O for following experiments or stored at –20°C.

The plasmid, which was used for DNA sequencing and transformation into *S. cerevisiae* 30-4 or was served as template of PCR, was isolated from *E. coli* with the GFX micro plasmid prep kit performed according to the manufactures instructions.
Briefly, 4.5 ml overnight culture was centrifuged at 4°C for 5 min at 3,500 rpm, the supernatant was discarded. The cell pellet was suspended in 300 µl solution I (100 mM Tris/HCl, pH7.5, 10 mM EDTA, 400 µg/ml RNase I) and was then carefully mixed with 300 µl solution II [188 mM NaOH, 1% (w/v) SDS] and 600 µl solution III (acetate and chaotropic buffer) sequentially by head to head shaking for 10-15 times, respectively. The reaction mix was centrifuged at 13,000 rpm for 10 min at RT. The supernatant was transferred

into the column incubated for 1 min at RT, and centrifuged as above. 300 µl solution III was added into the column, after 1 min at RT, the column was centrifuged again. The column was then washed using 400 µl wash buffer (Tris-EDTA in 80% ethanol). The plasmid DNA held in the column was eluted in an appropriate volume of sterile ddH_2O.

STET-solution: 8% (w/v) Saccharose, 0.5% (w/v) Triton X-100®, 50 mM EDTA, and 10 mM Tris/HCl, pH 8.0
TE-buffer: 10 mM Tris/HCl, 1 mM Na_2EDTA, pH 8.0

2.3.1.5.Quantification of DNA

Spectrophotometric determination, based on the measuring of the amounts of UV irradiation absorbed, is widely used to measure the amounts of DNA or RNA in a preparation. Readings are taken at wavelengths of 260 nm and 280 nm. The reading at 260 nm allows calculation of the concentration of nucleic acids in the sample. An OD of 1 corresponds to approximately 50 µg/ml for the double-stranded DNA. The ratio between the readings at 260 nm and 280 nm provides an estimate for the purity of the nucleic acid. Pure preparation of DNA has an OD_{260}/OD_{280} value of 1.8 [199].

We used this spectrophotometric method for determination of DNA concentration in a sample with the Spec™ Smart 3000 photometer (PeQLab/Germany).

2.3.1.6 Endonuclease restriction analysis

Each restriction enzyme has a set of optimal reaction conditions, which are given on the information sheet supplied by the manufacturer. When DNA is to be cleaved with two restriction enzymes, the digestion can be carried out simultaneously, if both enzymes work in the same buffer. If not, the enzyme that works in the buffer of lower ionic strength is used first. After inactivation of the first enzyme at 65°C for 20 min, the appropriate amount of salt and the second enzyme can be added and the incubation continued. Alternatively, the DNA that has been digested by the with first enzyme can be precipitated (see Methods 2.3.1.7) and prepared for digestion with another enzyme [199].

Reactions typically contain 0.2-1.0 µg DNA in a final volume of 10 or 20 µl as the example followed:

. 8 µl DNA (0.8 µg in sterile H_2O)
1 µl restriction endonuclease
1 µl 10× appropriated digestion buffer

The reaction mix was prepared and incubated at the recommended temperature for 2 h. To stop the reaction the mix was placed at 65°C for 20 min.

2.3.1.7 Precipitation of DNA

The most widely used method for concentrating DNA is precipitation with ethanol. The DNA precipitate which is allowed to form at low temperature (-20°C or less) in the presence of moderate concentrations of monovalent cations is recovered by centrifugation and dissolved in an appropriate buffer at the desired concentration ([145]).

A total of 2–3 volumes of ice-cold ethanol can be used in the presence of 0.1–0.5 M monovalent cations at low temperature. In this work ammonium acetate was generally used, because it was more easily removed by washing with 70% ice-cold ethanol than the other salts (e.g. NaCl or Na-acetate). Glycogen was used for precipitation of very short DNA molecules (< 400 bp) or very small amounts (< 0.1 µg/µl) improving the precipitation efficiency [146]. The following was a typical DNA precipitation reaction set:

17 µl	DNA sample
3 µl	NH_4OAc (3 M, pH 4.6)
60 µl	ethanol (ice-cold)
0.5µl	glycogen (20 µg/µl)

The reaction mixture was mixed well and stored at –20°C for 30 min to allow the DNA to precipitate. The mix was then centrifuged at 4°C for 30 min at 13,000 rpm (Eppendorf/Germany). Then, the supernatant was discarded. The DNA pellet was carefully washed twice with ice-cold 70% ethanol to remove any solute that could be trapped in the precipitate. The DNA precipitate was dried and redissolved to the desired concentration with TE buffer or sterile ddH_2O depending upon the further applications.

2.3.1.8 Separation of the DNA fragment using agarose gel electrophoresis

The standard method used to separate, identify, and purify DNA fragments is electrophoresis in agarose gels. The electrophoretic migration rate of DNA through agarose gels is dependent upon the molecular size of the DNA, the agarose gel concentration, the conformation of the DNA, and the current applied [147]. The location of DNA within the gel can be determined directly using low concentration, the fluorescent or intercalating dye ethidium bromide [148].

In this work 0.8-1% agarose gels were used in the absence of ethidium bromide for separation, identification, and purification of the DNA. Typically, 10 µl of the DNA sample

from restriction analysis or PCR was mixed with 2.5 µl of 6× DNA loading buffer and were loaded into the slots of the submerged gel. GeneRuler^{TM} 1 kb DNA Ladder (0.5 mg DNA/ml) and λ-DNA/Eco47III/Eco91I (0.5 mg DNA/ml) were used to control the DNA size. The electrophoresis was performed in TAE running buffer at 5 V/cm for an appropriate time. The gel was stained in 0.5 µg/ml ethidium bromide at RT for 15 min with agitation. The DNA fragments were photographed directly under UV-illumination of Biostep.

TAE: 40 mM Tris/acetate, 1 mM Na_2EDTA, pH 8.0;
6´ DNA loading buffer: 30% glycerin (w/v), 0.25% bromphenolblau (w/v), 0.25% xylenolcyanol

2.3.1.9 Extraction of the DNA fragment from the agarose gels

The DNA fragments can be separated using gel electrophoresis. To recover the DNA fragments from the agarose gel we used the JETsorb-DNA extraction kit.
The slice of the gel with the target DNA band was cut out under UV light (λ of 300-360nm to minimize damage to the DNA) and weighted. then, 100 mg of gel slice were mixed with 300 µl of buffer A1 and 10 µl of JETSORB suspension and incubated at 50°C for 15 min. The suspension was mixed every 3 min during the incubation to avoid the sedimentation of the JETSOB beads. The culture was then centrifuged at 13,000 rpm for 1 min at room temperature. The pellet was washed again with 300 µl buffer A1 to recover JETSORB minibreads, and then was washed with 300 µl buffer A2. The pellet was dried completely (not overdried) in a speedvaccum for 1-2 min to be free of ethanol. After this, the pellet was resuspended with 20 µl TE or sterile H_2O and was incubated at 50°C for 5 min to elute the DNA. After centrifugation as above, the DNA supernatant was transferred into a new tube and was stored ready for use.

JETSORB suspension: With a DNA capacity of 7.5 µg / 10 µl JETSORB suspension
Buffer A1: contains concentrated $NaClO_4$, TBE-Solublizer, sodium acetate
Buffer A2: contains ethanol, NaCl, EDTA and Tris/HCl

2.3.1.10 Inverse polymerase chain reaction ¾ inverse-PCR

The PCR is based on the DNA polymerase-catalyzed doubling of target DNA with each cycle, and leads to an exponential amplification of specific DNA sequences by using repeated cycles involving heat denaturation, primer hybridization, and primer-extension (polymerization) [199].

The introduction of mutations was performed using inverse-PCR corresponding to the protocol by Sakai *et al* [149] and Hemsley *et al* [150]. The constructed plasmid pKS^+-AS served as the template. The annealing temperature, which influences the specificity of the PCR reaction, was calculated based the "2+4 (G/C) rule" using the computer program Vect NT 1 [151, 152], and the time of the strand extension was adapted to the length of the target strand to be reproduced.

Typically, 20 ng of pKS^+-AS plasmid DNA were added into the appropriate buffer with 2 mM $MgCl_2$, 0.12 mM dNTPs, 1 µM each of forward and reverse primer, 2 U Taq polymerase to a final volume of 100 µl. The reaction was cycled 28 times in a thermocycler with the following temperature program:

	Temp.	Rouning	Time
Denaturation	94°C,	2S/°C	1 min
Primer annealing	53.7°C	2S/°C	1 min
Extension	72°C	2S/°C	4.5 min

This was done 28 times and followed once a end step at 72°C for 10 min.

The PCR-products were separated by 1% agarose gel electrophoresis, and were purified by using the Kit of JETsorb (see Methods 2.3.1.9) from the agarose gels.

2.3.1.11 Blunt-ending of the 3´-end of PCR-products

The PCR-products are not blunt-ended, because Taq polymerase lacks 3´ to 5´ exonuclease activity and has a tendency to add an extra dA residue to the 3´-end of each strand, giving rise to a single-nucleotide 3´-extension (A-overhang) at each end of the fragment . This 3´-extra added dA can be removed in a combined exonuclease/repair reaction with T_4 DNA polymerase in the presence of all four deoxynucleoside triphosphate. T_4 DNA polymerase possesses a 5´→3´ polymerase activity and a 3´→5´ exonuclease activity, and it is more active upon single-stranded DNA than double-stranded DNA. In addition, the activity on double-stranded DNA is blocked by the 5´→3´ polymerase activity, therefore, a blunt end can be formed by using this enzyme[153, 154].

Routinely, 2 µg PCR product were incubated with 2 U T_4 DNA polymerase in the presence of 50 µM ATP, 100 µM dNTPs in the T_4 DNA polymerase buffer at 4°C for 20 min. Afterwards the reaction was stopped by heating at 65°C for 20 min.

2.3.1.12 Phosphorylation of the DNA

The DNA used for phosphorylation was purified by agarose gel electrophoresis or density gradient centrifugation to remove low molecular-weight nucleic acid, which would have provided a much larger proportion of the 5´ ends. Ammonium ion is a strong inhibitor of polynucleotide kinase, thereby DNA should be free from ammonium salts [155].

A total of 1 µg of blunted PCR-product was incubated with 2 U T_4 DNA polynucleotide kinase and 50 µM ATP at 37°C for 1 h in the buffer provided by the T_4 DNA polynucleotide kinase supplier. Then, the reaction mix was heated to 65°c for 20 min to inactivate the enzyme.

2.3.1.13 Dephosphorylation of the DNA

To avoid self-ligation of the vector DNA fragment in intended ligations alkaline phosphatase was used to removing 5´-phosphate residues from the DNA fragment.

This reaction was carried out by incubating 1 µg DNA with 2 UT_4 DNA alkaline phosphatase in corresponding buffer at 37°C for 1 h. The enzyme was inactivated by heating to 65°C for 20 min.

2.3.1.14 Ligation of the DNA

T_4 DNA ligase, a single polypeptide, catalyzes the formation of a phosphodiester bond between adjacent 3´-OH and 5´-phosphate termini in DNA.

The molar ratio of the insert:vector is also an important parameter to consider. The larger the size difference, the bigger the ratio of insert to vector required [156].

Mixture for self-ligation:

11.4 µl	phosphorylated PCR-DNA (0.054 µg/µl)
1,5 µl	10 × T_4 DNA ligase buffer
0.6 µl	T_4 ligase (1U /µl)

As an example, for the ligation between a linker and a vector DNA

10 µl	dephosphorylated vector DNA (2914 bp, 0.06 pmol/µl)
6 µl	DNA-linker (23 bp, 10 pmol/µl)
1 µl	T_4 DNA ligase
2 µl	10 × T_4 DNA ligase buffer
1 µl	sterile H_2O

are incubated 4°C overnight (12-16 h). The ligated DNA can then be used to transform *E. coli*, in order to verify the efficiency of the ligation.

2.3.1.15 DNA sequencing analysis

Sequencing is often used to map and identify mutations (e. g. point mutations and deletions) and to verify the orientation and structure of recombinant DNA constructs. In this work the DNA sequencing was performed to confirm mutations generated by oligonucleotide-mediated mutagenesis. As shown in Fig.2.1, the universal T_3 promotor could be used anneal an appropriate sequencing primer. The plasmid containing either original or mutated DNA sequence were prepared according to the method of GFX micro plasmid prep kit (see Methods 2.3.1.4) and were dissolved in sterile H_2O at a concentration of 50 ng/µl. The sequencing reaction was performed in an automated DNA sequencer coupled with the computer software of Sequence Editor 2. The DNA sequence could be read using Chromas curve (Chromas 1.45) [157].

2.3.2 Heterologous Expression of the native and mutated Na^+/K^+-ATPase in *S. cerevisiae* cells

Yeast cells do not contain endogenous sodium pump. They are therefore very suitable for the heterologous expression of the sodium pump and its mutants, because this allows to address their properties without the interference of endogenous Na^+/K^+-ATPase [64, 76].

2.3.2.1 Culture and storage of yeast cells

A single clone of yeast cells 30-4 expressing native or mutant Na^+/K^+-ATPase was incubated in 10 ml YNBU medium at 30°C overnight. The culture was continuously shaken at 180 rpm on a orbital shaker. Then, 5 ml of the culture were centrifuged at 4°C for 5 min at 3,500 rpm, the cell pellet was then resuspended in 150 µl of 15% glycerol and stored at –70°C. In this way stocks remain viable for several years.

The remaining 5 ml of the culture was transferred to 200 ml of YNBU and incubated till reaching the desired OD_{600} value.

For large scale cultures, the 5 ml culture was transferred to 1.3 l YNBU medium with 13 ml 100 fold supplement mix, and further incubated before use.

YNBU medium: 1.7 g/l yeast nitrogen base without amino acids, 5 g/l ammonium sulfate, 20 g/l glucose, 20mg/l uracil

100´ supplement mix: 2g/l adenine, L-histidine/HCl, L-arginine/HCl, and L-methionine, respectively; 3g/l L-tyrosine, L-leucine, L-isoleucine, L-lysine/HCl, individual; 5g/l L-phenylalanine; 10g/l L-glutamate acid, and L-aspartate acid, respectively; 15g/l L-valine; 20g/l L-threonine; 40g/l L-serine (45)

2.3.2.2 Introducing plasmid DNA into yeast cells

The plasmid pCGY1406αβ containing cDNA of the Na^+/K^+-ATPase was introduced into yeast cells 30-4 according to the protocol of Gietz e*t al* [158, 159].

A single yeast cell clone of 30-4 cells was inoculated into 5 ml YPD medium and was incubated at 30°C and continuos shaking at 180 rpm for 12-16 h till an OD_{600} value of 0.6-0.8 was reached. The cells were then centrifuged at 3,500 rpm at a temperature of 4°C. The sediment was washed with 0.1 M LiOAc in TE buffer pH 7.5 and was suspended again in 100 µl of the same solution. After incubation at 30°C for 1 h, ca. 1 µg of plasmid DNA and 5 µl of RNA carrier were added into the reaction sample and the incubation continued for an additional 30 min. The reaction sample was mixed carefully with 700 µl solution containing 40% (w/v) of polyethylenglycol and 0.1 M LiOAc, pH 7.5 and was incubated at 30°C for another 1 h. The mixture was then heated to 42°C for 2h, and centrifuged under the conditions described above to sediment the cells. The sediment was suspended in 100 µl TE, pH 7.5 and spread on a YNBU-plate, before 72 h incubation at 30°C.

YPD medium: 10 g/L Bacto-yeast extract; 20 g/L Bacto-peptone; 20 g/L D(+)-glucose monohydrate
YNBU-plate: YNBU medium with 20 g/l Bacto-agar-agar

2.3.2.3 Palytoxin-induced K^+ efflux from the yeast cells expressing the native or mutated sodium pump

Palytoxin (PTX), the mostly potent animal toxin known, acts through the Na^+/K^+-ATPase, causing Na^+ ion influx and K^+ ion efflux from vertebrate cells with both ions following their electrochemical gradients [95, 160-162]. *S. cerevisiae* becomes PTX-sensitive and lose intracellular K^+ ions only when they express both α and β subunits of the mammalian Na^+/K^+-ATPase [26, 64, 163]. The determination of the PTX-induced K^+ efflux was performed by the method of Scheiner-Bobis *et al* [64].

Single yeast clone expressing either wild-type or various mutant Na^+/K^+-ATPases were grown overnight at 30°C in 5 ml YNBU. The cell suspensions were transferred into 200 ml YNBU medium and grown for an additional 24 h. Cells were then sedimented at 4°C by centrifugation for 5 min at 3,500 rpm and washed twice using 50 ml HBC buffer. The cells

were diluted in HBC buffer with 200 mM NaCl to reach a cell density of 5×10^6 cells/ml and incubated at 30°C for 2 h with various concentrations of palytoxin. The total reaction volume was 1 ml. Thereafter, cells were centrifuged for 2 min at 13,000 rpm, the supernatant was collected, and the concentration of K^+ ion was determined by flame photometry. The total K^+ concentration of the cells was measured after cell membranes were dissolved by incubation in 0.01% LiDS at 65°C for 30 min.

HBC buffer: 10 mM Hepes, 0.5 mM borate, 1 mM $CaCl_2$, pH 7.5
Palytoxin was diluted in HBC buffer with 0.1% BSA

2.3.2.4 Ouabain inhibition of palytoxin-induced K^+ efflux from yeast cells expressing the native or mutated sodium pump

Ouabain, a cardioactive steroid, inhibits the PTX-induced K^+ efflux from yeast cells expressing the Na^+/K^+-ATPase, which is the unique known receptor of ouabain [164-166].
A suspension of 5×10^6 yeast cells/ml expressing either wild-type or mutant Na^+/K^+-ATPase was incubated in the same buffer as in the palytoxin experiment described above at 30°C for 2 h with a defined concentration of palytoxin and various concentrations of ouabain. The cells were then sedimented and the concentration of K^+ in the supernatant was determined by flame photometry.

2.3.2.5 Microsomal membrane protein preparation

The membrane preparation was performed as described formerly [62]. Thus, the large scale yeast culture was grown to reach an OD_{600} value of 2-3. The yeast cells were collected by centrifugation at 9,500 rpm in an RC-5B centrifuge using the GSA rotor at 4°C for 10 min. The cells were suspended in ice-cold ddH_2O and centrifuged at 4,000 rpm at 4°C for 10 min, and this wash step was repeated once. The wet weight of the cells was estimated, and the cell pellets at this point could be frozen at –70°C.
The cells were thawed in 2 ml Yeast Breakage Buffer (YBB) per gram wet-weight of cells at 37°C. The cell supernatant and 10 ml beads were then added into the Bead Beater's inner chamber, and a little more YBB was added to fill the chamber up to 3 mm from the rim. The cells were beaten 8 times for 15 sec with 105-sec intervals. After the eighth beating, the suspension was separated from the beads and transferred into a cold tube on ice. The beads were washed twice in YBB, each time including six repetitions of 10-sec beating followed by a 30-sec rest. The broken cells were centrifuged at 4°C for 20 min at 4,000 rpm, and the supernatant was centrifuged again at 4°C for 10 min at 9,500 rpm, in an RC-5B centrifuge

with an AS 2.8 rotor to remove the cell debris. To pellet the cell membrane fragment, the suspension was centrifuged at 4°C for 1 h at 48,000 rpm, in a Beckman ultracentrifuge with a Ti70 rotor. The membrane fragments were homogenized in 26 ml imidazole buffer, ultracentrifuged again, as above, for 30 min, and rehomogenized in the appropriate volume of imidazole buffer. The membrane preparation was divided in to aliquots, frozen in liquid nitrogen, and then stored at –70°C until the SDS extraction.

YBB: 200 mM Tris/HCl, pH 7.5, 10 mM $MgCl_2$, 10% (w/v) glycerin, 1 mM EDTA, 2 mM DTT, 0.2 mM PMSF, 0.5 mg/ml leupeptin, 0,7 mg/ml pepstatin

Imidazole buffer: 25 mM imidazole, 1 mM disodium EDTA, pH 7.5

2.3.2.6 Protein assay

The protein assay was performed according to the method of Lowry [167, 168]. Protein sample (10 to 40 µl) were incubated with 0.5 ml ddH_2O, 3.5 ml 10% Na_2CO_3, and 0.5 ml 0.1% $CuSO_4$ for 15 min at room temperature. During the incubation, the Folin–Ciocalteus-phenol reagent was diluted 1:3 with steril H_2O. The reaction was mixed with 0.5 ml diluted Folin-Ciocalteus phenol reagent and incubated for another 15 min. The protein concentration was determined from the absorbency at 578 nM using a spectrophotometer. BSA (0.7%) served as a standard.

2.3.2.7 SDS extraction of Na^+/K^+-ATPase from a membrane preparation

Microsomal membrane protein (3.6 mg/ml) was mixed with 50 mM imidazole, 2 mM disodium EDTA, pH 7.4, and 3 mM freshly prepared disodium ATP. SDS (4 mg/ml) was then added dropwise into the mix with continuous stirring to a final concentration of 1 mg/ml. The extraction was continued for 30 min at RT, starting with the first drop of SDS. The mixture was then carefully placed on the top of a prepared discontinuous sucrose gradient consisting of 9 ml of 50% and 8 ml of 20% sucrose in imidazole buffer and centrifuged at 4°C for 2 h at 48,000 rpm in a Beckman ultracentrifuge. The protein band at the sucrose gradient interface was collected using a Pasteur pipette, diluted with at least a 3-fold volume of imidazole buffer, and ultracentrifuged as above for 1 h. The protein pellet was homogenized in an appropriate imidazole buffer using a glass homogenizer. The protein homogenate was aliquoted and immediately frozen in liquid nitrogen. This extracted microsomal protein was stored at –70°C.

Imidazole buffer: 25 mM imidazole, 1 mM Na_2EDTA, pH 7.4

2.3.3 Binding of [^{3}H]ouabain to yeast membranes containing wild-type or mutant Na^+/K^+-ATPase

The inhibition of the Na^+/K^+-ATPase by ouabain is stoichiometric and relatively stable, and is at least partially competitive with K^+ [165, 166, 169, 170]. Ouabain inhibits the Na^+/K^+-ATPase by binding to the E_2-P phosphoenzyme form of the enzyme, which has a high affinity for ouabain, and forms the [E2*P·ouabain] complex [5]. This complex can be measured using [^{3}H]ouabain.

2.3.3.1 [^{3}H]ouabain binding in the presence of P_i

To determine whether the mutations had an effect on P_i/enzyme interaction, 250 µg microsomal membrane protein from yeast cells expressing either the wild-type or the mutant Na^+/K^+-ATPase was incubated at 30°C for 30 min with various concentrations of [^{3}H]ouabain in the presence of 10 mM Tris/HCl, pH 7.5, and 5 mM Tris/PO_4, pH 7.5 with or without 5 mM $MgCl_2$ in a final volume of 500 µl. Thereafter, the protein was pelleted by centrifugation at 13,000 rpm for 2 min in a bench-top centrifuge and washed twice with 500 µl ice-cold ddH_2O. The protein was dissolved in 250 µl of 1 N NaOH at 75°C for 15 min. After neutralization with 250 µl of 1 N HCl, 450 ml of scintillate fluid were added and the amount of bound [^{3}H]ouabain was determined by scintillation counting. The nonspecifically bound [^{3}H]ouabain was estimated in the presence of 1 mM nonradioactive ouabain. Maximum ouabain binding (B_{max}) and dissociation constants (K_D) were calculated from a Scatchard analysis [171, 172].

2.3.3.2 Inhibition of [^{3}H]ouabain binding by K^+

The binding of ouabain to Na^+/K^+-ATPase is at least partially competitive with K^+ ions [101, 173]. To determine whether this property was retained by mutant Na^+/K^+-ATPase, a total of 250 µg yeast membrane containing either wild type or mutant Na^+/K^+-ATPase was incubated at 30°C for 30 min with various concentrations of KCl in the presence of 10 mM Tris/HCl, pH 7.5, 5 mM Tris/PO_4, pH 7.5, and 100 nM [^{3}H]ouabain with or without 5 mM $MgCl_2$ in a final volume of 500 µl. The amount of bound [^{3}H]ouabain was measured as described above.

2.3.3.3 Binding of [^{3}H]ouabain as a function of Mg^{2+}

The binding of [^{3}H]ouabain to Na^+/K^+-ATPase requires Mg^{2+} ion [101, 174]. To examining whether the mutations of Na^+/K^+-ATPase have an effect on the Mg^{2+}/enzyme interaction, a total of 250 µg microsomal protein containing either wild-type or mutant Na^+/K^+-ATPase was

incubated at 30°C for 30 min with various concentrations of $MgCl_2$ in the presence of 10 mM Tris/HCl, pH 7.5, 50 nM [^{3}H]ouabain, and 5 mM Tris/PO_4, pH 7.5 in a final volume of 500 µl. Ionic strength was kept constant by adding choline chloride. The amount of bound [^{3}H]ouabain was determined as described above.

2.3.3.4 [^{3}H]ouabain binding to the phosphoenzyme formed from ATP

In the presence of ATP, Mg^{2+}, and Na^+, Na^+/K^+-ATPase is phosphorylated with a conformational change from the nonphosphorylated form (E_1) to the phosphoenzyme form (E_2-P). Ouabain binds with high affinity to this E_2-P phosphoenzyme [5].

A total of 250 µg of mocrosomal protein containing either wild-type or mutant Na^+/K^+-ATPase was incubated at 30°C for 30 min with 10 mM Tris/HCl, pH 7.5, 100 mM NaCl, and 100 µM Tris/ATP with or without 5 mM $MgCl_2$. The final volume of the sample was 500 µl. The amounts of bound [^{3}H]ouabain and the nonspecific binding were determined as described above.

2.3.4 Na^+/K^+-ATPase activity assay

The overall activity of Na^+/K^+-ATPase was determined with aliquots microsomal protein in the presence or absence of ouabain using the coupled spectrophotometric assay [176]. The formation of ADP by Na^+/K^+-ATPase was linked via phosphoenolpyruvate (PEP), pyruvate kinase (PK), lactate dehydrogenase (LDH), and NAD^+ to the formation of NADH plus H^+ as shown in Scheme 2.1. The formation of NADH plus H^+ could be measured at 366 nm as a function of time in a spectrophotometer ($\in$ = 3400 liters/mol/cm).

SDS-extracted microsomal protein (100 µg) was incubated in the presence or absence of 200 µM ouabain in a mixture containing 100 mM NaCl, 60 mM NH_4Cl, 3 mM $MgCl_2$, 3 mM Na_2-ATP, 0.4 mM phosphoenolpyruvate, 0.7 mM NADH, 60 mM imidazole/HCl, pH 7.5, 1.25 U/ml pyruvate kinase, and 1.5 U/ml lactate dehydrogenase at 37°C in a final volume of 1 ml. The decline of the absorption at 366 nm was followed during the incubation. The ouabain-inhibited fraction of the overall ATPase activity of the sample was used to distinguish the sodium pump activity from other ATPases contained in the microsomal protein.

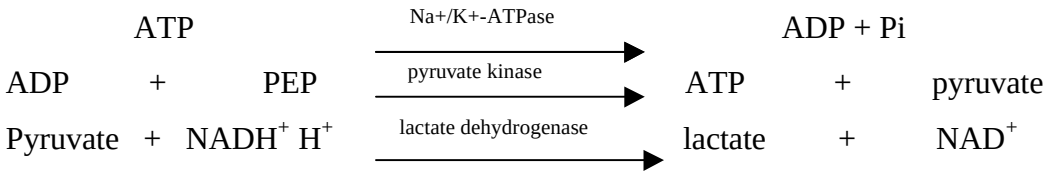

Scheme 2.1 Principle of the PK/LDH linked Na^+/K^+-ATPase activity assay

2.3.5 SDS-polyacrylamide gel electrophoresis (SDS-PAGE)

SDS-PAGE is a general method to separate DNA or protein. In this work, it was used to separate the α1 and β1 subunits of Na^+/K^+-ATPase according to the method of Laemmli and Weber [87, 177]. Prestained protein markers with molecular weights of 122, 79, 47, 33, 24, and 20 kDa were used.

A total of 15 µg of microsomal protein containing either native or mutant Na^+/K^+-ATPase was suspended in 10 µl of loading buffer. After incubation for 3 min at 94°C, proteins were separated by SDS-PAGE on 7.5% gels (for the α1 subunit) or 6.5% gels (for the β1 subunit) in 0.376 M Tris/HCl, pH 8.8, 0.1% SDS, 0.08% APS, and 0.08% TEMED. A 5% stacking gel in 0.120 M Tris/HCl, pH 6.8, 0.1% SDS, 0.1% APS, and 0.05% TEMED was used. Na^+/K^+-ATPase (50 ng) from pig kidney was used as the positive control, and 15 µg of microsomal protein from untransformed yeast served as the negative control. Prestained protein markers (0.1 µg) were run in parallel with the protein sample at 100 V for 2-2.5 h. After briefly washing with H_2O, the gel to be stained was fixed in 20% trichloreacetate (TCA) for 20 min and stained thereafter with Coomassie broil blue R350 in 10% acetic acid (HOAc) at 50°C for 15 min. The gel was destained by washing 3 times with 10% HOAc for 10 min. The gel was air-dried wrapped in foil after 20 min in conservation solution.

SDS-PAGE running buffer: 20 mM Tris, 100 mM glycine, 0.1% SDS

conservation solution: 10% glycerine, 25% ethanol

Loading buffer: 5% (v/v) β-mercataptoethanol, 5% SDS, 4 M urea, 125 mM Tris/HCl, pH 6.8, 12.5% (v/v) glycerol, and 0.05% bromophenol blue

2.3.6 Western blotting

Western blotting is a method of protein detection involving the transfer of proteins from a polyacrylamide gel onto a membrane of nitrocellulose or nylon, which bind protein strongly [178, 179]. These bound proteins are then available for analysis by a variety of specific protein-ligands interactions, most commonly using antibodies [180, 181].

After SDS-PAGE, the protein was transferred onto nitrocellulose (NC) membrane following the instructions provided by the commercially available ECL Western blotting system PRN 2180 kit. The polyacrylamide gel was equilibrated in the transfer buffer for 30 min, with the Whatman 3MM filter paper and NC membrane also being wetted in this buffer. The protein was transferred to the NC membrane by 15 V for 1 h using the semi-dry (BioRad) method with a transfer stack in this order (bottom to top): 3 layers of Whatman paper, the NC

membrane, then the SDS-polyacrylamide gel, and finally 3 layers of Whatman paper. After washing 1 × for 15 min and 2 × 5 for min in PBS-T under continuosly shaking, the NC membrane was blocked at 4°C overnight using 5% blocking reagent in PBS-T. After washing again as above, the membrane was incubated with the primary antibody (Ab) against the α1 subunit or β1 subunit of the Na^+/K^+-ATPase at RT for 2 h. Both antibodies were IgG from mouse and were diluted in blocking reagent by 1:2500. As the secondary Ab, an HRP (horseradish peroxidase)-coupled Ab against mouse IgG was used with a dilution of 1:2500 in blocking reagent. The membrane was washed again as above and was incubated with diluted secondary Ab at RT for 1 h. It was then washed with PBS-T as described above. For the detection of the protein bands, the membrane was incubated with an 1:1 mix of reagents 1 and 2 (provided by the kit) at RT for 1 min, and wrapped in plastic foil. At this point, the membrane could be exposed onto a Kodak X-ray film, which was then developed as a permanent record. The membrane, wrapped in foil, could be stored at 4°C for several months.

Transfer buffer: 12.5 mM Tris base, 96 mM glycine, 0.1% SDS, 20% (v/v) methanol, pH 9.2 to 9.4
PBS-T: 20 mM NaH_2PO_4, 80 mM Na_2HPO_4, 100 mM NaCl, 0.1% (v/v) Tween 20, pH 7.5

2.3.7 Measurement of ^{18}O exchange between P_i and H_2O **

The method developed by Stempel and Boyer [183] was used with the adaptions made by Faller [202] to measure the distribution of ^{18}O isotopomers [$P^{18}O_j{}^{16}O_{4-j}$] formed as a function of time when Na^+/K^+-ATPase catalyzes oxygen exchange between P_i and H_2O. The exchange reaction was started by the addition of enzyme to 0.5 ml of a solution containing 2 mM [^{18}O]P_i, 20 mM KCl, 2 mM $MgCl_2$, 0.1 mM DTT, 5 mM NaN_3 in 0.1 M Tris-HCl, pH 7.4 with or without 0.1 mM ouabain, and adjusted to a 200 mM ionic strength with choline chloride. The enzyme concentration and incubation time at 30°C were chosen to give a final average ^{18}O enrichment ($AE = \Sigma_j P^{18}O_j{}^{16}O_{4-j}/4\Sigma P^{18}O_j{}^{16}O_{4-j}$, $0 \le j \le 4$) ranging from 40% to 80% so that significant amounts of all five isotopomers were formed. The reaction was quenched, and P_i was isolated by applying the reaction mixture to a column (0.5 × 4 cm) of Dowex AG 1-X4 (100-200 mesh, Cl^- form). After successive washes with 10 ml of H_2O (18 MΩ), the column was acidified with 3.5 ml of 30 mM HCl, and the phosphate was eluted with an additional 5 ml of 30 mM HCl [182]. Approximately 95% of the phosphate was recovered, lyophilized, and converted into volatile triethyl phosphate by reacting with diazoethane [183]. The product was analyzed on a polar capillary column with a Hewlett-Packard 5972A GCMS operated in the SIM mode. Masses 155-163 were measured and corrected for spillover from

unprotonated diethyl phosphate. The calculation of the fraction of Pi containing from zero to four ^{18}O atoms as a function of time from the starting distribution of phosphate isotopomers was based on the equations derived by Hackney' [184].

** *This experiment was performed by departments of Med CURE, University of California, Los Angeles, Vaglahs.*

3. Results

3.1 Sequence comparison

The Na^+/K^+-ATPase and the L-2-DEX YL share a similar reaction mechanism by forming a aspartyl ester intermediate that is subsequently hydrolyzed during the catalytic cycle [134]. Protein sequence comparison provides further evolutionary information about these two divergent enzymes [128, 136]. Using a standard gap BLAST program, the sodium pump did not show any similarity to the haloacid dehalogenase, but iterated sequence comparison and position-specific iterated BLAST (PSI-BLAST) [185, 186] starting from haloacid dehalogenase have shown that these enzymes share three statistically significant motifs (Fig. 3.1) with P-type ATPase [138]. The first of these motifs (DLYGT in L-2-DEX YL, and DKTGT in Na^+/K^+-ATPase) contains an absolutely conserved aspartate (Asp10 in L-2-DEX YL, Asp369 in Na^+/K^+-ATPase), which covalently binds an α-hydroxy acid in L-2-DEX YL and a phosphate in Na^+/K^+-ATPase [133, 187]. The second motif contains a strictly conserved hydroxyl residue of serine or threonine; these two motifs are separated by large inserts of variable size as shown in Fig. 3.1. The third motif contains a strictly conserved lysine residue (Lys151 in L-2-DEX YL, Lys691 in Na^+/K^+-ATPase) and an absolutely conserved aspartate (Asp180 in L-2-DEX YL and Asp714 in Na^+/K^+-ATPase). If these residues are replaced via mutagenesis, the haloacid dehalogenase loses or strongly reduces its enzymatic activity [129, 130, 133].

		Motif I			Motif II			Motif III	
		10		118		151		180	
L-DEX_PS	9	FDLYGTL	(101)	LSNGS	(26)	VYKPD	(19)	VSSNAWDA	181
DHIB_Xa	7	FDAYGTL	(99)	LSNGA	(26)	VFKPH	(19)	VSSNGFDV	177
PSP_MJ	10	FDVDSTV	(82)	ISGGF	(44)	KGKVI	(14)	IGDGATDM	174
PMA1_sp	368	SDKTGTL	(234)	VTGDH	(75)	QQKLI	(14)	TGDGVNDA	715
1EUL	350	SDKTGTL	(264)	ITGDN	(53)	SHKSK	(14)	TGDGVNDA	708

Fig.3.1 Sequences surrounding the three motifs of the haloacid dehalogenase superfamily in rat Na^+/K^+-ATPase. *L-DEX_ps: haloacid dehalogenase from Pseudomonas; DHIB_Xa: haloacid dehalogenase from Xantho; PSP_MJ: phosphoserine phosphatase from Methanococcus jannaschii; PMA1_sp: Na^+/K^+-ATPase α1 chain from sheep kidney; 1EUL: Ca^{2+}-ATPase from human sarcoplasmic reticulum. The absolutely conserved Asp residue in motif I and III is marked in red, the highly conserved Lys residue in motif III is labeled in*

blau, and the highly conserved residue Ser/Thr is shown in green. The alignment is based on those of Koonin [201] *and Aravind et al.* [126], *which were obtained with iterative approaches using haloacid dehalogenase as the starting sequence.*

3.2 Introduction of the mutations into the vector pKS$^+$-AS

3.2.1 Plasmid construction

As shown in Fig. 2.3, the annealed linker presented a new restriction site of *BstE*II and two cohesive ends of *Apa*I and *Bgl*II site, respectively. This linker was inserted into the pKS$^+$ to generate a new *BstE*II site near the *Bgl*II site (pKS$^+$-*BstE*II). A *Bgl*II-*BstE*II fragment consisting of 1010 bp cDNA of the Na^+/K^+-ATPase α1 subunit from sheep kidney was cut from the plasmid pCGY1406αβ using *Bgl*II and *BstE*II restriction endonucleases and subsequently ligated into the same site of the newly linked pKS$^+$-*BstE*II. At this point, the pKS$^+$-AS with 3947 bp was constructed and could be used as template for site-directed mutagenesis by inverse-PCR.

The plasmid construction was controlled by restriction analysis. The pKS$^+$ was cleaved once by the *Hin*I endonuclease but not by *BstE*II, and it showed only one band of 2944 bp after digestion with these two enzymes in comparison to the linked pKS$^+$-*BstE*II plasmid, which demonstrated two bands with 1848 bp and 1096 bp shown in Fig. 3.2.1.

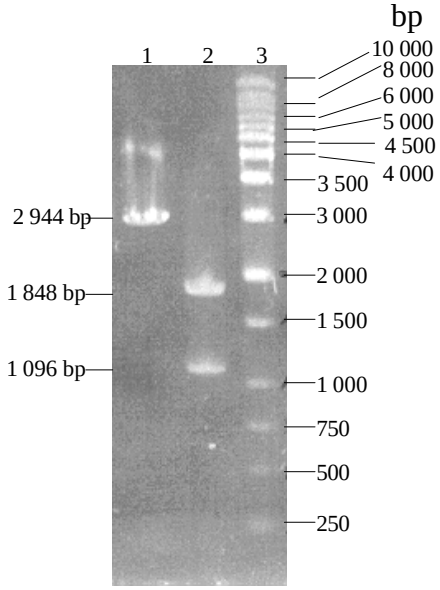

Fig. 3.2.1 Restriction analysis of the pKS$^+$ plasmid with *BstE*II site on 1% agarose gel. *Plasmid DNA (0.3 µg) was digested with HinI and BstEII at 37°C for 2 h . lane 1: pKS$^+$ with a band of 2944 bp; lane 2: pKS$^+$-BstEII with two bands of 1848 bp and 1096 bp; lane 3: 1 kb DNA ladder*

The newly constructed plasmid pKS$^+$-AS was confirmed using so-called linearization and insert-releasing. For linearization, the pKS$^+$-AS was digested with *Bgl*II to check the size of the enzyme, and for insert-releasing, cleaved with the enzymes *Bgl*II and *BstE*II to release the 1010-bp length cDNA fragment from the α1 subunit of the Na^+/K^+-ATPase. The plasmid pKS$^+$-*BstE*II consisting of 2944 bp was used as the control. As shown in Fig.3.2.2, the pKS$^+$-AS showed upon linearization one band with 3947 bp (total length) and upon double cleavage two bands with 2937 bp and 1010 bp (insert) in comparison with the control, which showed only one band of 2944 bp upon single digestion and 2937 bp (a 7-bp band was run out) upon double digestion.

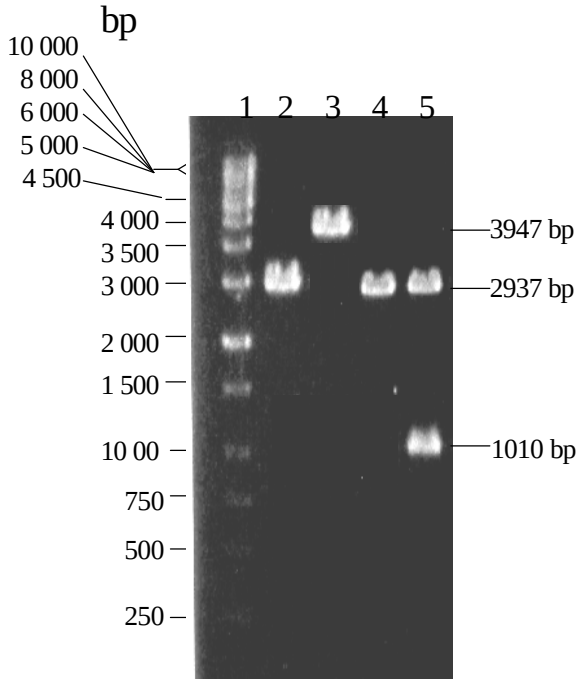

Fig. 3.2.2 Restriction analysis of the pKS$^+$-AS plasmid on 1% agarose gel.

Plasmid DNA (0.6 µg) was digested with BglII or BglII and BstEII at 37°C for 2 h.

lane 1: 1 kb DNA ladder;

lane 2: pKS$^+$-BstEII digested with BglII showed a band of 2944 bp;

lane 3: pKS$^+$-AS digested with BglII presented a band with 3947 bp;

lane 4: pKS$^+$-BstEII digested with BglII and BstEII showed a band of 2937 bp

lane 5: pKS$^+$-AS digested with BglII and BstEII showed two bands of 2937 bp and 1010 bp

3.2.2 Mutagenesis by inverse-PCR

PCR was performed as described in point 2.3.2.10 of the methods chapter. The constructed 3947 bp-length pKS$^+$-AS, which contained 1010-bp cDNA fragment of the α1 subunit of the

Na^+/K^+-ATPase from sheep kidney, was used as a template for the PCR. The primer pairs for each mutation are listed in Table 2.2 and Table 2.3. The annealing temperature was generally calculated based on the lower melting temperature of the two primers. In the case of bad yield or low specificity of the PCR-product, the annealing temperature of the reaction cycle was empirically modulated to adapt the reaction. Table 3.1 shows the individual annealing temperature used for the various mutations.

Table 3.1 Annealing temperature in PCR for individual mutations

Mutation of the α1 subunit	K691A	K691R	K691D	D714A	D714R	D714E
Annealing Temperature (°C)	51	53	53	54	54	52

The PCR products were separated on a 1% agarose gel and extracted using a JETsorb Kit (see Methods 2.3.1.9) from the gel. The PCR yield was in the range of 2 to 4 µg per 100 µl reaction mixture. After a series of treatments, including removal of the 3´ A-overhang, 5´ termini phosphorylation, and self-ligation, the PCR products were transformed into competent *E. coli* DH5αF´. The target PCR products showed a band with ~3947 bp as the template on the 1% agarose gel (Fig. 3.2.3).

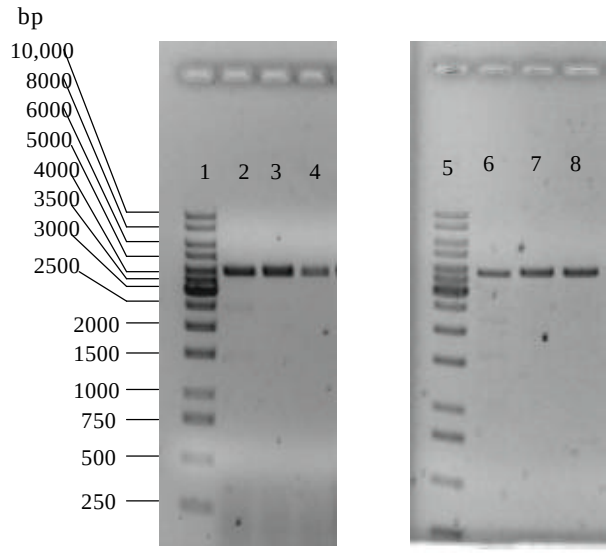

Fig. 3.2.3 The PCR products on a 1% agarose gel

PCR products of each mutant (8µl) were loaded and the gel was run at 100 V for 1 h. Lanes 1,5: GeneRuler™ 1 kb DNA Ladder: lane2: Lys691Ala; lane 3:Lys691Arg; lane 4: Lys691Asp: lane 6: Asp714Ala; lane 7: Asp714Arg; lane 8: Asp714Glu in pKS⁺-AS;

3.2.3 Confirmation of the introduced mutations in the plasmid pKS$^+$-AS

The wild-type or mutant plasmid pKS$^+$-AS was isolated from *E. coli*, and the mutations were verified using restriction analysis and DNA sequencing analysis.

For the three Lys691 mutants Lys691Ala, Lys691Arg, and Lys691Asp, the restriction endonuclease *Nru*I was used as a diagnostic tool whose restriction site was generated by a silent mutation in the reverse primer. Therefore, after digestion with *Nru*I, they showed a band with 3947 bp as shown in Fig. 3.2.4.

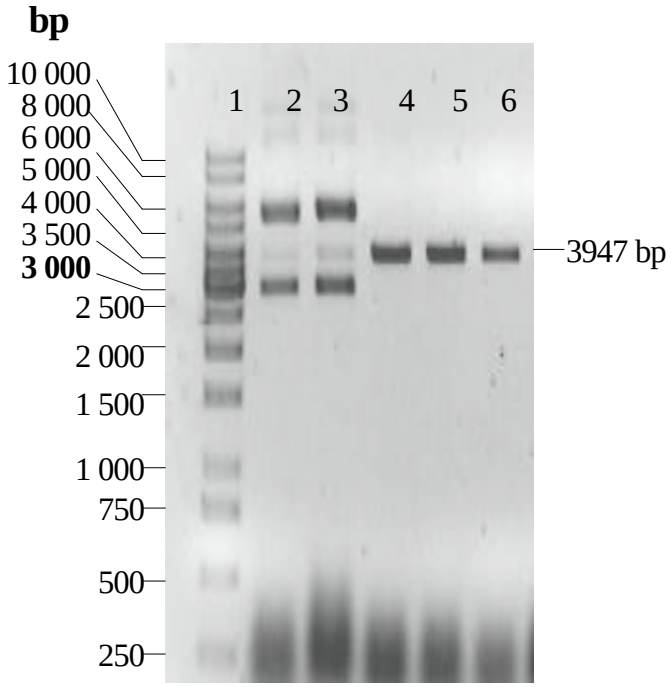

Fig. 3.2.4 Restriction analysis of pKS$^+$-AS including Lys691 mutants on 1% agarose gel

0.2 µg DNA was digested with NruI in corresponding buffer at 37°C for 2h. Lane 1: GeneRuler^{TM} 1 kb DNA ladder; pKS$^+$-AS (lane 2,3) showed only the non-digested DNA bands (relaxed and supercoiled forms) ; Lys691Ala, Lys691Arg, and Lys691Asp mutation in pKS$^+$-AS (lane 4,5,6) showed a band with 3947 bp

In the Asp714 mutants, a diagnostic restriction site for *Nsi*I was generated by the Asp714Ala mutation and a *Cla*I site by the Asp714Arg mutation. For the Asp714Glu mutant generation, however, the number of *Cfr*10I sites increased from 2 to 3. Hence, the diagnostic digestions were performed in different combinations for each mutation of the Asp714, each with its individual native plasmid control. As shown in Table 3.2, Asp714Ala digested with *Nsi*I and *Bgl*II demonstrated two bands of 700 bp and 3247 bp compared to one 3947 bp band for the

control. Asp714Arg digested with *Cla*I and *Bgl*II also showed two bands of 697 bp and 3250 bp with one control band of 3947 bp. Asp714Glu was digested only with *Crf*10I and presented three bands of 1074 bp, 1710 bp, and 1163 bp in comparison with the control exhibiting two bands with 1163 bp and 2784 bp (Fig. 3.2.5).

Table 3.2 Restriction analysis of the Asp714 mutations in pKS$^+$-AS

Mutation	restriction enzyme	number of cleavage	imaging on 1% agarose gel
Asp714Ala	*Nsi*I + *Bgl*II	1 + 1	700 bp, 3247 bp
wild-type		0 + 1	**3947 bp**
Asp714Arg	*Cla*I + *Bgl*II	1 + 1	697, 3250 bp
Wild-type		0 + 1	**3947 bp**
Asp714Glu	*Cfr*10I	3	**1075, 1710**, and 1162 bp
Wild-type		2	**2785 bp,** 1162 bp

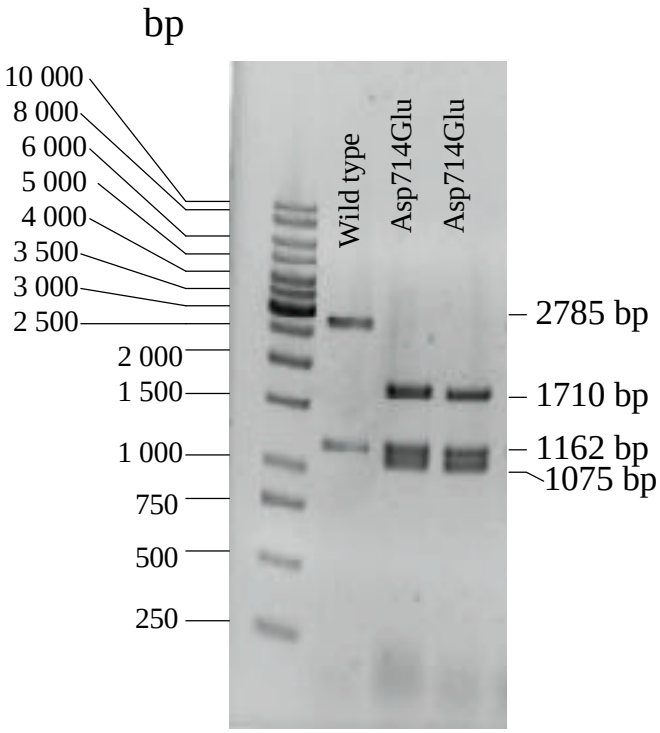

Fig. 3.2.5 Restriction analysis of pKS$^+$-AS including Asp714Glu mutant on 1% agarose gel. *0.2 µg DNA of wild-type or Asp714Glu in plasmid pKS$^+$-AS was digested with Cfr10I at 37°C for 2 h. The plasmid pKS$^+$-AS (wild-type) showed two bands of 2785 bp and 1162 bp and Asp714Glu in pKS$^+$-AS showed 3 bands of 1075 bp, 1710 bp, and 1162 bp*

The ligation site of the PCR product was determined with the restriction nucleases *Ppu*MI (Lys691 mutants) or *Esp*3I (Asp714 mutants), which recognize only one restriction site just across the ligation site of the desired cDNA fragment in the native and the mutant pKS$^+$-AS, to screen the plasmids without a deletion mutation that would be generated by using the T_4 DNA polymerase. As shown in Fig. 3.2.6, each mutation showed a bands of 3947 bp as the native pKS$^+$-AS.

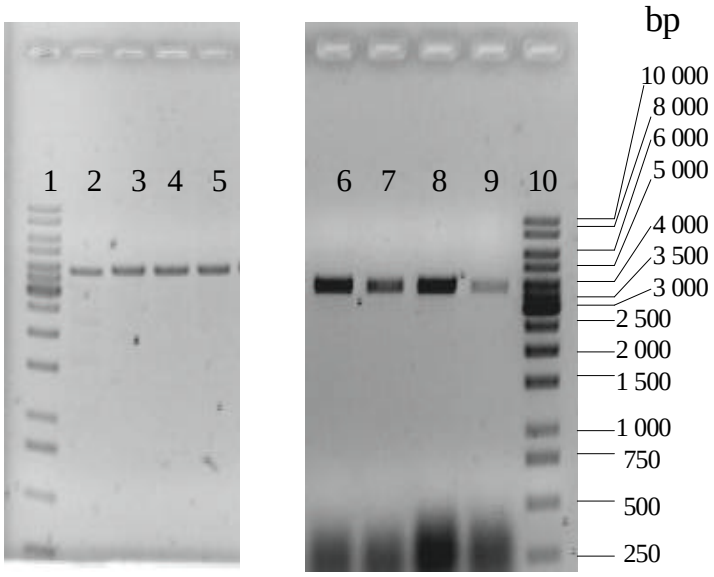

Fig. 3.2.6 The restriction analysis by *Ppu*MI or *Esp*3I endonucleases

0.2 µg of native (lane 2, 9), Lys691Ala (lane3), Lys691Arg (lane 4), Lys691Asp (lane5), Asp714Ala (lane6), Asp714Arg (lane 7), and Asp714Glu (lane8) in pKS$^+$-AS were incubated with PpuMI or Esp3I at 37°C for 2 h, respectively. Each mutant showed a band of 3947 bp as the wild-type. Lane 1 and 10: GeneRuler^{TM} 1 kb DNA ladder

The verified mutant clones were confirmed using DNA sequencing as described at point 2.3.1.15 of the methods chapter to determine that the mutation was generated in the desired site, that no random mutations occurred during the inverse-PCR, or that no deletion mutations were generated by T_4 polymerase during the blunt-ending of the PCR products. For each mutant, a *BstE*II-*Nco*I fragment with 353 bp that contained the target mutation was sequenced. This 353 bp-length cDNA fragment was then replaced into the pKS$^+$-AS to replicate in *E. coli*. The Chromas curve of the sequencing analysis was not shown.

3.3 Expression of the native or mutant Na^+/K^+-ATPase in yeast cell line 30-4

3.3.1 Introduction of the mutations into the shuttle vector pCGY1406αβ

To express the mutant Na^+/K^+-ATPase in *S. cerevisiae*, the plasmid pCGY1406αβ was digested with restriction endonucleases *Bgl*II and *BstE*II to remove the 1010 bp original cDNA fragment of the α1 subunit of the Na^+/K^+-ATPase and replaced with the corresponding mutated 1010 bp cDNA fragment from the plasmid pKS^+-AS. After replacement, the plasmid pCGY1406αβ containing wild-type or mutant Na^+/K^+-ATPase was transformed into *E. coli* cell strain DH5αF' as described in point 2.3.1.3 of methods chapter. The 12833 bp-length *Bgl*II-*BstE*II fragments were dephosphorylated to avoid self-ligation of the incompletely cleaved linear pCGY1406αβ fragments.

In order to confirm successful introduction of the mutated sequences into the pCGY1406αβ shuttle vector, restriction analysis was carried out.

For Lys691 mutations, *Nru*I endonuclease cleaved the plasmid pCGY1406αβ twice, showing two bands of 2578 bp and 11265 bp on the agarose gel, while the wild type plasmid showed only one band with the whole length of 13843 bp (Fig. 3.3.1).

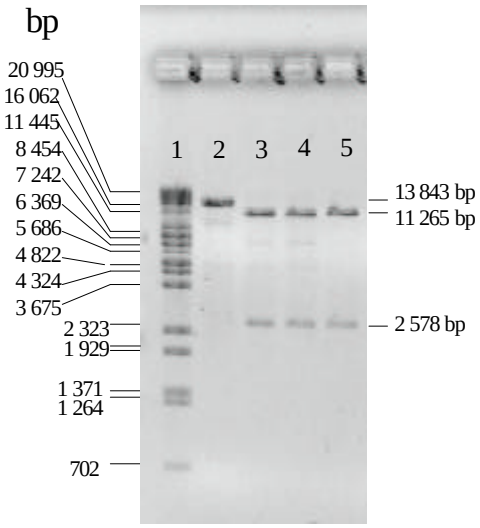

Fig. 3.3.1 Restriction analysis of Lys691 mutants on α1 cDNA of the Na^+/K^+-ATPase in plasmid pCGY1406αβ

0.2 µg DNA was digested with desired restriction endonucleases at 37°C for 2 h.

lane 1: lambda DNA/Eco47III/Eco91I (BstEII) marker;

lane 2: pCGY1406αβ digested with NruI with a band of 13843 bp;

lane 3-5: Lys691Ala, Lys691Arg, Lys691Asp digested with NruI with two bands of 11265 and 2578 bp

The restriction analysis and its results for Asp714 mutations are shown in Tab. 3.3. Fig. 3.3.2 is a representative restriction analysis of Asp714Ala mutant digested with NsiI.

Table 3.3 Restriction analysis of the Asp714 mutations in pCGY1406ab

mutation	restriction enzyme	number of cleavage	distinct on 1% agarose gel
Wild-type	*Nsi*I	3	**8105 bp**
Asp714Ala		4	7300 + 805 bp
Wild-type	*Cla*I	3	**3855 bp**
Asp714Arg		4	2299 + 1556 bp
Wild-type	*Cfr*10I	8	**4404 bp**
Asp714Glu		9	4404 bp disappeared

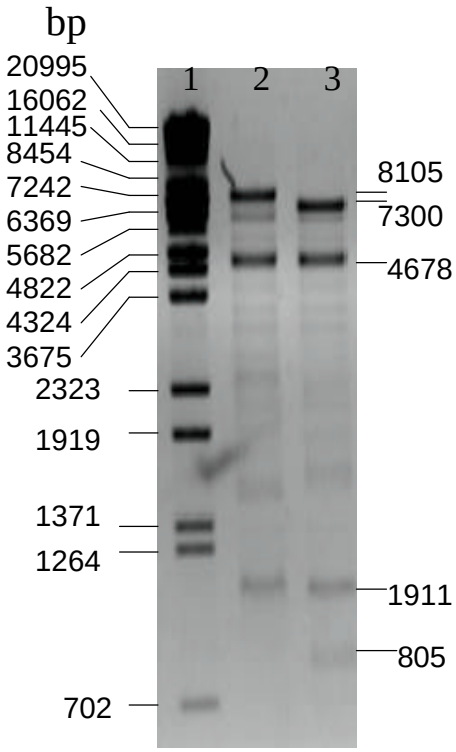

Fig. 3.3.2 Restriction analysis of Asp714Ala mutant on a1 cDNA of the Na^+/K^+-ATPase in the plasmid pCGY1406ab

0.2 µg DNA was digested with desired restriction endonucleases at 37°C for 2 h.

lane 1: lambda DNA/Eco47III/Eco91I (BstEII) marker

lane 2: pCGY1406ab digested with NsiI with 3 bands of 8105, 4678 and 1911 bp

lane 3-5: Asp714Ala digested with NsiI with 4 bands of 7300, 4678, 1911 and 805 bp

3.3.2 Confirmation of the expression of the native or mutant Na^+/K^+-ATPase in yeast

The identified shuttle plasmid pCGY1406αβ containing either native or mutated Na^+/K^+-ATPase was transformed into the yeast cell line 30-4. To ensure that either native or mutant Na^+/K^+-ATPases were adequately expressed in yeast cells, the microsomal protein isolated from yeast cells (see Methods 2.3.2.7) were probed in a Western blot with a monoclonal antibody raised against the Na^+/K^+-ATPase α1 or β1 subunit. As shown in Fig. 3.3.3, the wild type and each of the mutated Na^+/K^+-ATPase demonstrated approximately 110 kDa of α1 subunit as the positive control of kidney Na^+/K^+-ATPase from pig. The antibody did not recognize any protein of ~110 kDa corresponding to the wild type or mutant Na^+/K^+-ATPase α1 subunits in microsomal protein from nontransformed 30-4 yeast cell. Fig. 3.3.4 shows the β1 subunit of the wild-type and all of the mutants of Na^+/K^+-ATPase expressed in yeast cells with a molecular weight of ~39 kDa in SDS-polyacrylamide gels. In the case of α1 subunit detection, nontransformed yeast cells were used as the negative control.

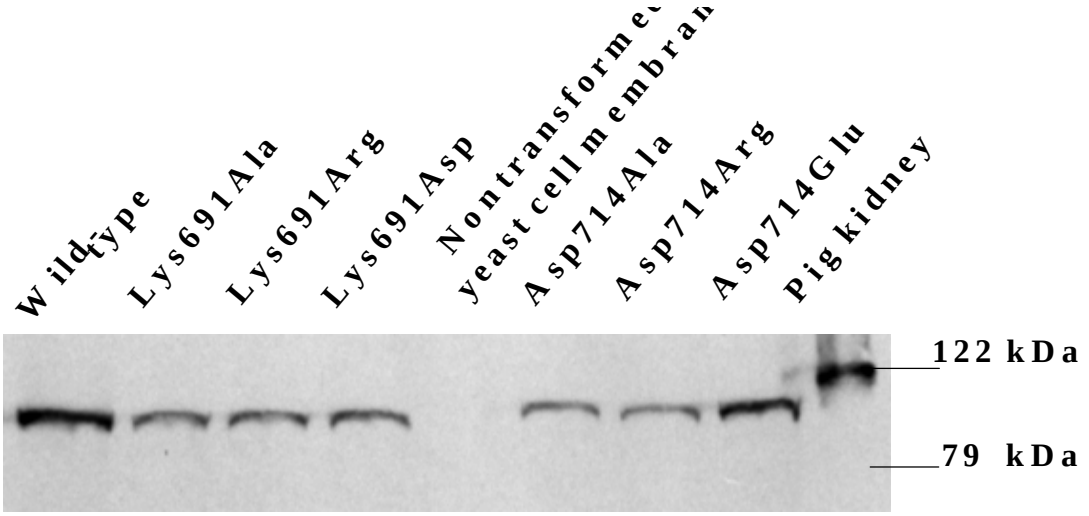

Fig. 3.3.3 Expression of each mutated Na^+/K^+-ATPase α1 subunit in yeast cells

15 mg of the yeast cell membranes containing either wild-type or mutant Na^+/K^+-ATPase were separated by 7.5% SDS-PAGE and then transferred to a nitrocellulose membrane (NC membrane). The blots were subsequently probed with monoclonal antibody against α1 subunit of the Na^+/K^+-ATPase as primary antibody and horseradish peroxidase-coupled anti-mouse IgG as secondary antibody. The Na^+/K^+-ATPase purified from pig kidney was used as the positive control. The nontransformed yeast cell membrane was used with the same procedure as the negative control.

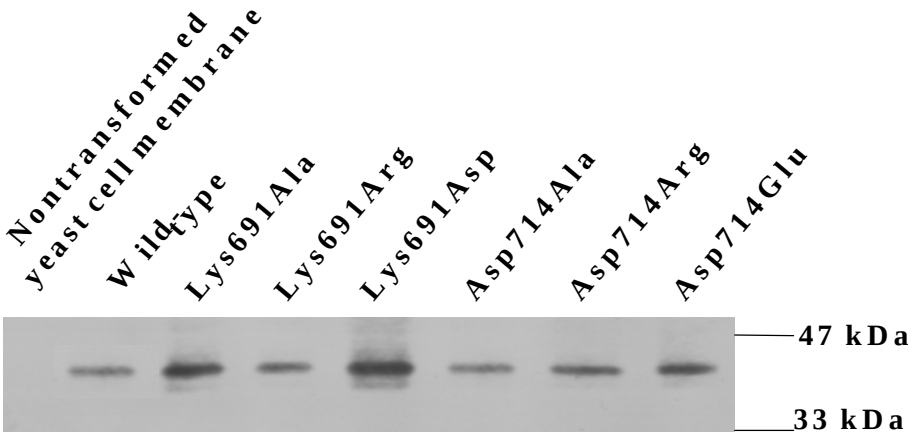

Fig. 3.3.4 Expression of each mutated Na^+/K^+-ATPase β1 subunit in yeast cells

15mg of the yeast cell membranes containing either wild-type or mutant Na^+/K^+-ATPase were separated by 6.5% SDS-PAGE and then transferred to a nitrocellulose membrane (NC membrane). The blots were subsequently probed with monoclonal antibody against b1 subunit of the Na^+/K^+-ATPase as primary antibody and horseradish peroxidase-coupled anti-mouse IgG as secondary antibody. The nontransformed yeast cell membrane was used with the same procedure as a negative control.

The Western blot demonstrated that both the wild-type and mutated Na^+/K^+-ATPases were successfully co-expressed with sheep α1 and dog β1 subunit of the sodium pump.

3.4 Functional detection for mutated α1 subunit of the Na^+/K^+-ATPase expressed in yeast

3.4.1 PTX-induced K^+ efflux from yeast cells expressing either wild-type or mutant Na^+/K^+-ATPase

PTX acts on Na^+/K^+-ATPase, causing formation of a channel within the enzyme [64, 91] that allows ions to flow down their electrochemical gradient. As expected, yeast cells expressing wild type Na^+/K^+-ATPase displayed a significant PTX-induced K^+ efflux with an EC_{50} value of 17.8 ± 2.7 nM where the nontransformed yeast cells did not show any PTX-induced K^+ efflux effect (Fig.3.4.1 and 3.4.2). The interactions of PTX with each of the Lys691 or Asp714 mutated Na^+/K^+-ATPases were affected: the EC_{50} values obtained with cells expressing the Lys691Arg or Asp714Glu mutation in Na^+/K^+-ATPase were about 7-fold (117.6 ± 23.8 nM) or 4-fold (76.5 ± 3.6 nM) higher than that of the wild-type, respectively,

and the maximal K^+ efflux from the cells was 68.1 ± 17.5% and 70.9 ± 28.7% compared with the wild-type with a corresponding value of 72.2 ± 8.4%.

The other 4 mutations, Lys691Ala, Lys691Asp, Asp714Ala, and Asp714Arg, however, were very insensitive to PTX. The PTX-induced K^+ efflux was strongly reduced with a normalized K^+ efflux percentage value of 21.1% and 14.4 for Lys691Ala and Lys691Arg, respectively, and 3.8% and 5.4% for Asp714Ala and Asp714Arg in the presence of 2 µM PTX, respectively (Fig.3.4.1 and 3.4.2).

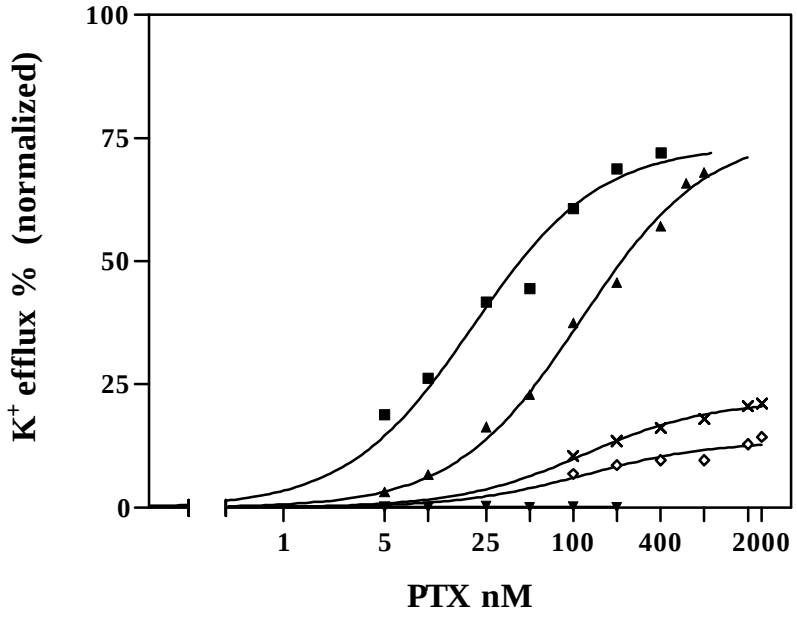

Fig 3.4.1. PTX concentration dependence of the K^+ efflux from the yeast cells expressing wild-type or Lys691 mutant of Na^+/K^+-ATPase. *Yeast cells (5´10^6 cells / ml) expressing either wild type (■), or Lys691Arg (▲), Lys691Ala(´)and Lys691Asp (à) mutants of Na^+/K^+-ATPase, or nontransformed yeast cells (▼) were incubated with various concentrations of PTX at 30°C for 2 h as described in Methods 2.3.2.3. Cells were then centrifuged, and the K^+ concentration in the supernatant determined by flame photometry. The percentage of K^+ efflux was normalized based on the total [K^+] measured in the presence of LiDS and the so-called 0-value obtained from the sample in the absence of PTX.*

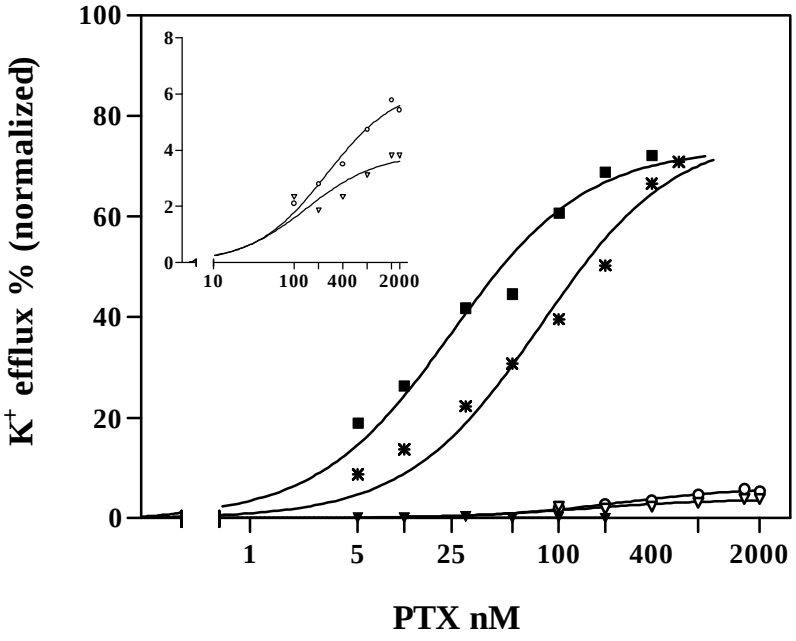

Fig 3.4.2. PTX concentration dependence of the K^+ efflux from the yeast cells expressing wild-type or the Asp714 mutants of Na^+/K^+-ATPase. *Yeast cells (5´10^6 cells / ml) expressing either wild-type (■), or mutants Asp714Ala (Ñ), Asp714Arg (O) and Asp714Glu (✳) of Na^+/K^+-ATPase, or nontransformed yeast cells (▼) were incubated with various concentrations of PTX at 30°C for 2 h as described in "Methods" 2.3.2.3. Cells were then centrifuged, and the K^+ concentration in the supernatant determined by flame photometry. The percentage of K^+ efflux was normalized based on the total [K^+] measured in the presence of LiDs and the so-called 0-value obtained from the sample in the absence of PTX. The inset shows the PTX-induced K^+ efflux by Asp714Ala (Ñ) and Asp714Arg (O) mutants of Na^+/K^+-ATPase.*

3.4.2 Ouabain inhibition of the PTX-induced K^+ efflux from yeast cells expressing either mutant or wild-type Na^+/K^+-ATPase

Ouabain, a potent and specific inhibitor of the Na^+/K^+-ATPase, inhibits the K^+ efflux induced by PTX [26, 64, 101]. Hence, determination of the EC_{50} value for ouabain inhibition of the PTX-induced K^+ efflux allows one to obtain a measure of the relative affinity of the yeast-expressed Na^+/K^+-ATPase for ouabain.

PTX-induced K^+ efflux from yeast cells expressing wild type Na^+/K^+-ATPase was completely inhibited by ouabain (Fig.3.4.3) with an EC_{50} value of 5.13 ± 0.71 µM in the presence of 50

nM PTX. The corresponding values obtained from cells expressing the Lys691Arg or Asp714Glu mutant of Na^+/K^+-ATPase were 131 ± 13 µM by 200 nM PTX and 2520 ± 342 µM by 100 nM PTX. For the other four mutations, Lys691Ala, Lys691Asp, Asp714Ala, and Asp714Arg, the ouabain inhibition was determined in the presence of 800 nM PTX and showed also a concentration-dependent ouabain inhibition (data not shown). The EC_{50} values under these conditions were 144 µM and 210 µM for Lys691Ala and Lys691Asp, respectively, and 221 µM and 225 µM for Asp714Ala and Asp714Arg, respectively (Table 3.5).

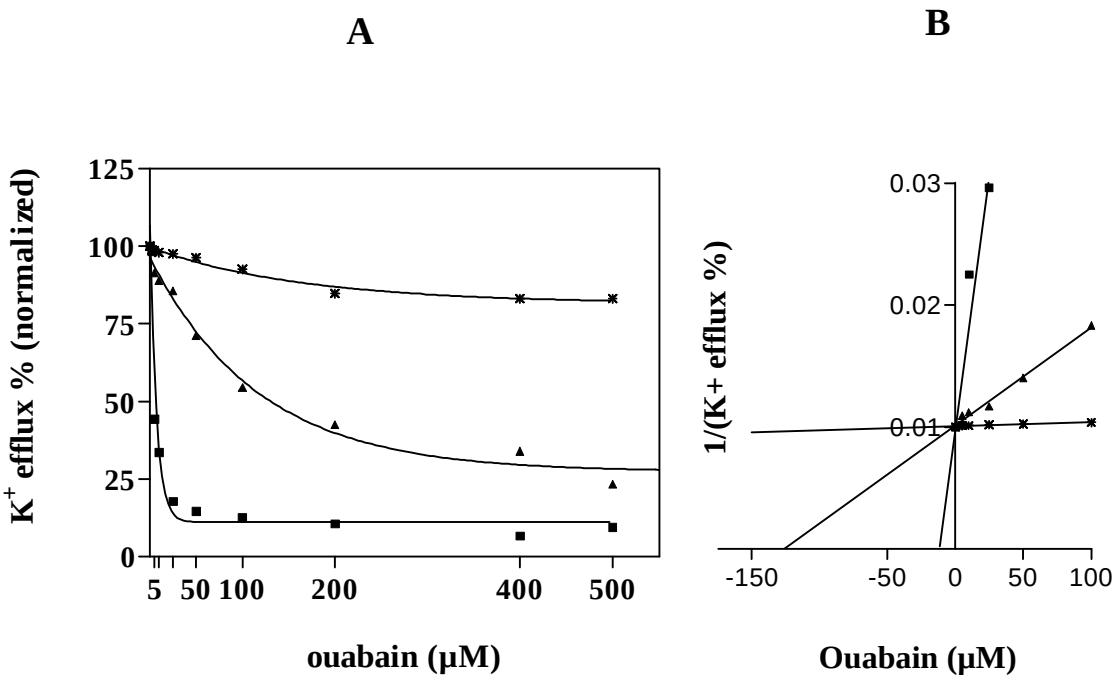

Fig.3.4.3 Ouabain-inhibition of the palytoxin-induced K^+ efflux from yeast cells expressing either wild-type or Lys691Arg and Asp714Glu mutants of Na^+/K^+-ATPase

Yeast cells containing wild-type (■) or Lys691Arg (▲) and Asp714Glu (✳) mutants of Na^+/K^+-ATPase were incubated with defined concentrations of PTX and various concentrations of ouabain at 30°C for 2 h, as described above. ***A****: Determination of K^+ concentration in the supernatant.* ***B****: Determination of EC_{50} values for inhibition of the PTX-induced K^+ efflux by ouabain. The EC_{50} value is the negative of the intercept with the abscissa.*

Table.3.5 Measurement of the palytoxin and ouabain effect (± SD)

sodium pump	EC_{50} for PTX (nM)	EC_{50} for ouabain (μM)	ouabain binding with ATP (pmol/mg protein)
Wild-type	17.8 ± 2.7	5.13 ± 0.71	0.715 ± 0.026
Lys691Ala	n. d.	114*	0.051 ± 0.024
Lys691Arg	118 ± 24	131 ± 13	0.084 ± 0.018
Lys691Asp	n. d.	210*	
Asp714Ala	n. d.	221*	0.042 ± 0.021
Asp714Arg	n. d.	225*	0.034 ± 0.020
Asp714Glu	76.5 ± 3.6	2520 ± 342	0.055 ± 0.017

*: in the presence of 800 nM palytoxin with very low K^+ efflux; n. d: not determined

3.5 Measurement of [^{3}H]ouabain binding to yeast membranes containing native or mutant Na^+/K^+-ATPase

Ouabain binds with the highest affinity to Na^+/K^+-ATPase upon formation of a phosphoenzyme intermediate (E_2-P form) to form an [E2*P·ouabain] complex [5]. Any case which reduces the stability of the E_2-P form of the enzyme can reduce the [^{3}H]ouabain affinity to the Na^+/K^+-ATPase. Mg^{2+} is necessary for activity of Na^+/K^+-ATPase as shown in its reaction cycle in Scheme 1.1 and the binding of [^{3}H]ouabain to enzyme requires Mg^{2+} ion [101, 174]. To testify whether Mg^{2+} coordination was affected by the mutant Na^+/K^+-ATPase, the ouabain binding properties were determined in the presence and absence of Mg^{2+} ion.

3.5.1 Binding of [^{3}H]ouabain to phosphoenzyme formed from P_i

In the presence of P_i and Mg^{2+} ions, the Na^+/K^+-ATPase is phosphorylated in a back-door phosphorylation fashion [15]. This ouabain binding can be inhibited by K^+ ions, causing a reduction of ouabain binding affinity [101, 173].

3.5.1.1 [^{3}H]ouabain binding in the presence of P_i

To determine whether the mutations have an effect on enzyme/phosphate interaction, the microsomal membrane containing wild-type or mutant Na^+/K^+-ATPase was incubated with various concentrations of [^{3}H]ouabain in the presence of Mg^{2+} and Pi to form a (E_2P*[^{3}H]ouabain) complex which was determined by a liquid scintillation counter.

As expected, the microsomal membrane containing wild-type Na^+/K^+-ATPase demonstrated clear [^{3}H]ouabain binding (Fig. 3.5.1) with a dissociation constant (K_D) of 20.0 ± 3.9 nM

while none of the mutant Na^+/K^+-ATPases shown a binding to [^{3}H]ouabain under these conditions. The maximal binding (B_{max}) of [^{3}H]ouabain to wild-type Na^+/K^+-ATPase was 0.809 ± 0.069 pmol (mg of protein)$^{-1}$ calculated from the Scatchard plot.

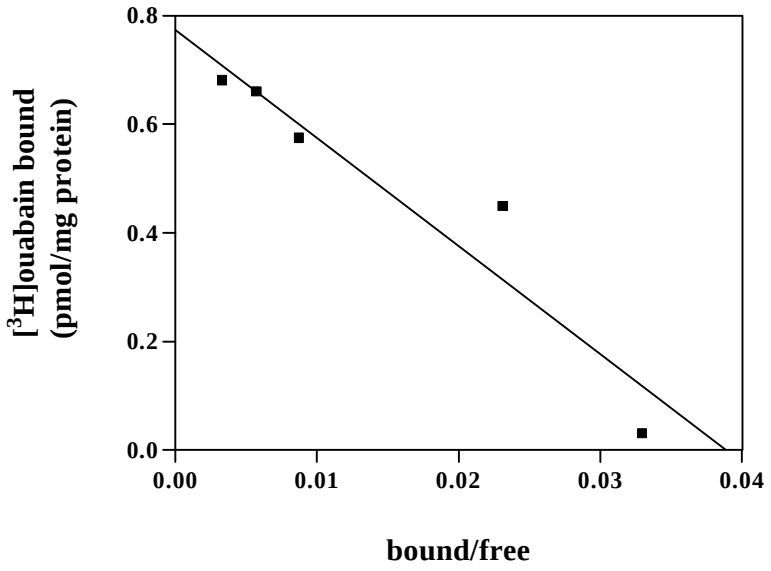

Fig. 3.5.1 Scatchard analysis of [^{3}H]ouabain binding to wild type Na^+/K^+-ATPase in the presence of Mg^{2+} ions and P_i. *250 µg membrane protein were incubated at 30°C with a reaction mixture as described in point 2.3.3.1 of Methods chapter for 30 min. The K_D value was calculated from the Scatchard plot. No ouabain binding was detected in similar experiments involving the Lys691 and Asp714.*

In the absence of Mg^{2+} ions, Lys691Arg and Asp714Glu demonstrated an ouabain binding effect at the high concentration of 100 nM [^{3}H]ouabain; the K_D values were not able to be determined under these conditions (data not shown).

3.5.1.2 Inhibition of [^{3}H]ouabain binding by K^+

Ouabain binding is at least partially competitive with K^+ [101, 173]. Alternatively, it was thought that in the presence of K^+, the enzyme is dephosphorylated, causing a conformational change from the E_2-P to the E_2 form, causing a low affinity of the enzyme for ouabain, thereby, the binding of [^{3}H]ouabain is reduced .

Fig. 3.5.2A is a representation of this experiment in the presence of Mg^{2+}. The binding of [^{3}H]ouabain to yeast membrane containing wild-type Na^+/K^+-ATPase displayed a decreased

binding to [^{3}H]ouabain with increasing K^+ concentrations. The relative affinity ($K_{0.5}$ value) of K^+ for binding to [^{3}H]ouabain was 2.43 ± 0.64 mM calculated from a Scatchard plot (inset); the relative affinity of each of the mutated Na^+/K^+-ATPases was not able to be determined.

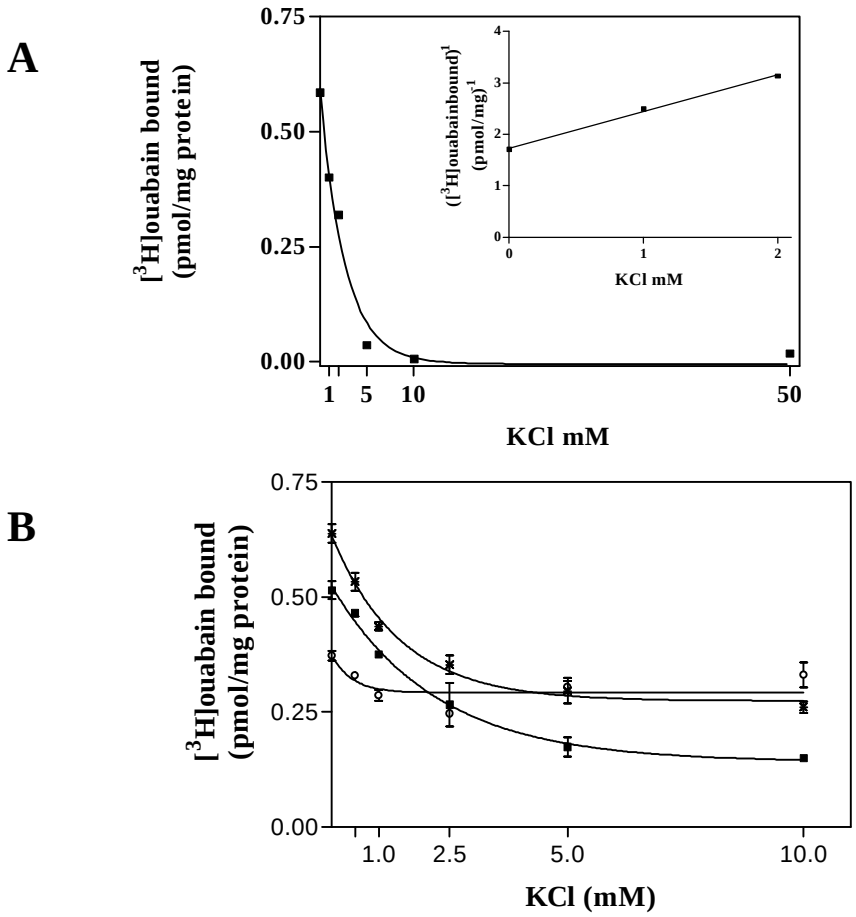

Fig. 3.5.2 Inhibition of [^{3}H]ouabain binding by K^+. *250 µg membrane protein were incubated with a reaction mixture as described in Methods.2.3.3.2 for 30 min.* ***A*** *shows the inhibitory effect of K^+ on ouabain binding to yeast membranes expressing the wild-type sodium pump in the presence of Mg^{2+} ions. The inset shows the determination of the $K_{0.5}$ for the effect of K^+ on ouabain binding. The $K_{0.5}$ value is the negative of the intercept with the abscissa.* ***B*** *is a representation of the ouabain binding as a function of K^+ concentration in the absence of Mg^{2+} ions. (■)-wild-type, (o)-Lys691Arg, (∗)-Asp714Glu*

In the absence of Mg^{2+} ions, membrane preparations expressing either the wild-type or the mutated sodium pump demonstrated a similar decreased [^{3}H]ouabain binding with an increase in K^+ concentration as shown in Fig. 3.5.2B. The $K_{0.5}$ value representing K^+ affinity for ouabain binding to the enzyme was 2.34 ± 0.71 mM obtained with the wild-type sodium pump. The values obtained for the mutant sodium pumps were similar to the wild-type

enzyme with the exception of Asp714Ala and Asp71Arg mutations with a $K_{0.5}$ value of 9. 9 ± 1.2 mM and 15.4 ± 2.0 mM, respectively (summarized in Table 3.6).

3.5.1.3 Binding of [^{3}H]ouabain as a function of Mg^{2+}

Ouabain binding to the sodium pump requires Mg^{2+} [101, 174]. In this work, choline chloride was used to equilibrate the ion strength. Yeast membranes containing either wild-type or each of the mutated sodium pumps were incubated with various concentrations of $MgCl_2$ in the presence of P_i and [^{3}H]ouabain as described in Methods point of 2.3.3.

In contrast to the wild-type Na^+/K^+-ATPase, the yeast membrane expressing either Lys691 (Lys691Ala, Lys691Arg, and Lys691Asp) or Asp714 (Asp714Ala, Asp714Arg, and Asp714Glu) mutated Na^+/K^+-ATPases showed a decreased binding of [^{3}H]ouabain as a function of an increase Mg^{2+} concentration, while the wild-type sodium pump showed an increased binding of [^{3}H]ouabain. Fig. 3.5.3 shows a representation of the results from this experiment. The $K_{0.5}$ values of Mg^{2+} for [^{3}H]ouabain binding to the various mutants of the sodium pump were 0.26 ± 0.05 mM (Lys691Ala), 0.76 ± 0.04 mM (Lys691Arg), 0.36 ± 0.05 mM (Lys196Asp), and 0.14 ± 0.03 mM (Asp714Ala), 0.12 ± 0.06 mM (Asp714Arg), 1.24 ± 0.19 mM (Asp714Glu) while that obtained for the wild-type sodium pump was 0.30 ± 0.07 mM. The $K_{0.5}$ values are summarized in Table 3.6.

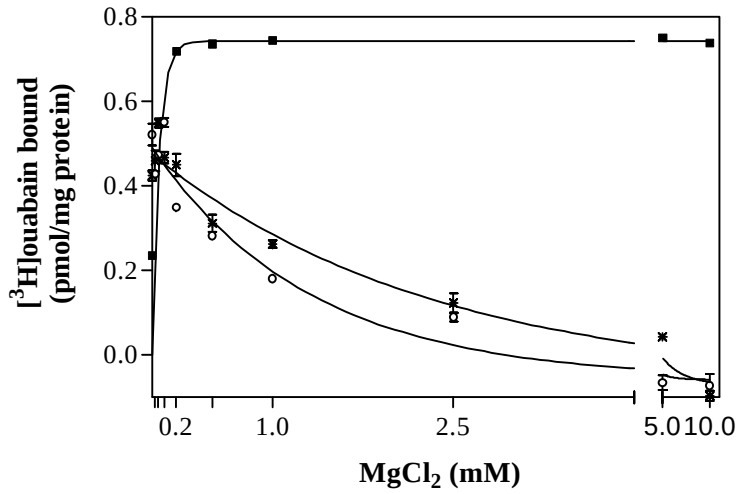

Fig. 3.5.3 Binding of [^{3}H]ouabain as a function of Mg^{2+}. *250 µg protein from a membrane preparation expressing either wild type (■), Lys691Arg (o), or Asp714Glu(*) were incubated with various concentration of Mg^{2+} in a reaction mixture as described in point 2.3.3.3 of Methods chapter at 30°C for 30 min. The amounts of [^{3}H]ouabain bound were measured as above.*

3.5.2 [^{3}H]ouabain binding to phosphoenzyme formed from ATP

In the presence of Na^+ and Mg^{2+}-ATP, the Na^+/K^+-ATPase hydrolyzes ATP and becomes phosphorylated by the γ-phosphate group of ATP at Asp369 of the α subunit [5, 76]. As shown in Scheme 1.1, the Na^+ ions are occluded within the protein at this step and subsequently released into the extracellular space. The phosphorylated enzyme is now capable of binding to ouabain with a high affinity and forms a stable complex of [E_2^*P·ouabain], which can be measured using [^{3}H]ouabain.

As expected, yeast membranes containing wild-type Na^+/K^+-ATPase demonstrated binding of [^{3}H]ouabain with a B_{max} of 0.715 ± 0.026 pmol/mg protein in the presence of 100 µM ATP. The maximal binding of [^{3}H]ouabain to each mutant of Na^+/K^+-ATPase was strongly reduced. The B_{max} of [^{3}H]ouabain binding was in the range of 0.04 to 0.07 pmol (mg of protein)$^{-1}$, as summarized in Tab 3.6 is excluded Lys691Asp mutant, which did not show an effect upon [^{3}H]ouabain binding.

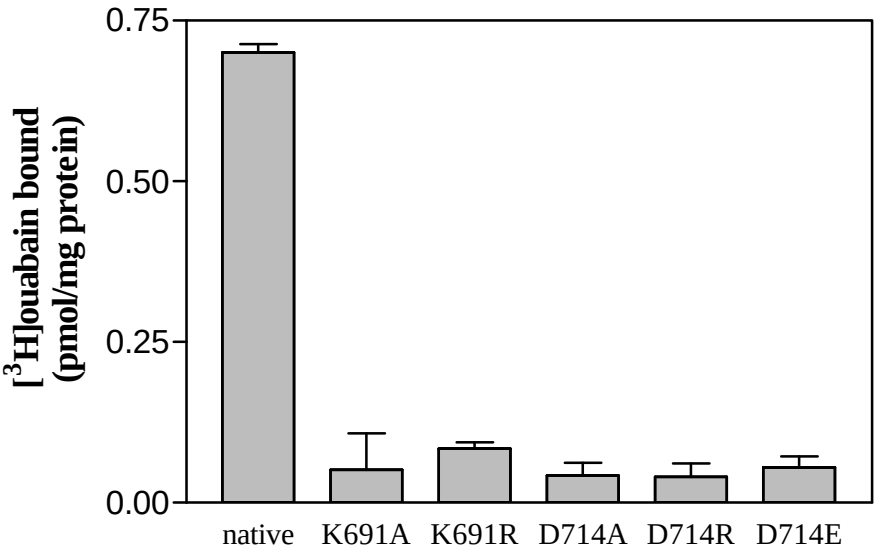

Fig. 3.5.5 [^{3}H]ouabain binding to the phosphoenzyme formed from ATP . *250 µg membrane protein were incubated with a reaction mixture containing 10 mM Tris/CL, pH 7.5, 100 mM NaCl, 100 mM ATP and 5 mM $MgCl_2$ at 30°C for 30 min. ^{3}[H]ouabain bound was calculated using a Scatchard plot analysis.*

When Mg^{2+} ion was omitted from the incubation mixture, neither the wild-type nor any of the mutant sodium pumps showed any detectable affinity for ouabain (data not shown).

Table 3.6 Measurement of the ouabain binding properties (± SD)

sodium pump	K_D value for ouabain (nM)	$K_{0.5}$ for K^+ with Mg^{2+} (mM)	$K_{0.5}$ for K^+ lack Mg^{2+} (mM)	$K_{0.5}$ for Mg^{2+} (mM)
Wild-type	20.0 ± 3.9	2.43 ± 0.64	2.34 ± 0.73	0.30 ± 0.07
Lys691Ala.	n. d.	n. d	2.56 ± 1.01	0.26 ± 0.05
Lys691Arg	n. d.	n. d	3.28 ± 0.84	0.76 ± 0.04
Lys691Asp	n. d.	n. d	2.23 ± 0.95	0.36 ± 0.05
Asp714Ala	n. d.	n. d	9.9 ± 1.2	0.14 ± 0.03
Asp714Arg	n. d.	n. d	15.4 ± 2.0	0.12 ± 0.06
Asp714Glu	n. d.	n. d	3.28 ± 0.65	1.24 ± 0.19

n. d.: not determined

3.6 Na^+/K^+-ATPase activity assay

The Na^+/K^+-ATPase couples ATP hydrolysis (ATPase activity) and cation translocation to transfer chemical energy into electrical energy as the driving force [15]. The specific ATPase activity of Na^+/K^+-ATPase was calculated as the ouabain-inhibited portion in the total ATPase activity of the sample, using SDS-extracted yeast membrane proteins containing either wild-type or the mutants.

The specific ATPase activity of the SDS-extracted membrane protein containing wild-type Na^+/K^+-ATPase was 32.2 ± 8.5 % of the total ATPase activity of 27.5 ± 9.1 mU sodium pump/(mg microsomal protein), while that obtained from the Lys691Arg mutant was 3.6 ± 1.4 %. The ATPase activity of the remaining mutations, Lys691Ala, Lys691Asp and Asp714Ala, Asp714Arg, and Asp714Glu was undetectable.

3.7 Measurement of ^{18}O exchange between P_i and water

The amount of ^{18}O exchanged between 2 mM P_i and water in the presence and absence of ouabain by yeast membranes containing wild-type and mutant Asp714Glu sodium pump are shown as a function of time in Fig. 3.6.

Yeast membranes containing Asp714Glu mutant displayed only a modest ^{18}O exchange with surrounding water when compared to the wild-type enzyme. The Lys691Arg mutant did not show any ^{18}O exchange under the same conditions. The ^{18}O exchange activity calculated from the difference between the slope of the least-square straight lines drawn through the points

obtained with or without ouabain present, are 24% for the Asp714Glu mutant and 75% of the total measured ^{18}O exchange activity for the wild-type enzyme.

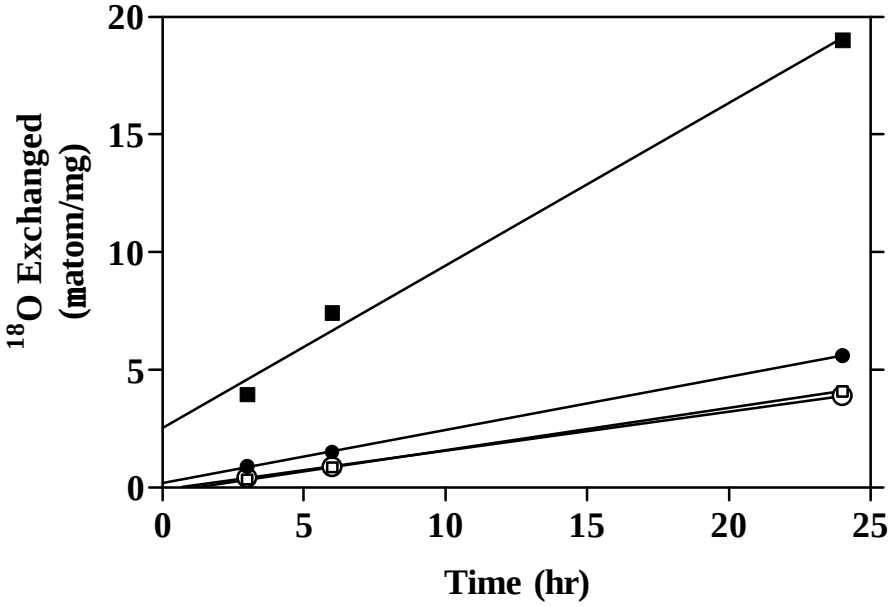

Fig. 3.6 Ouabain-sensitive ^{18}O exchange activity. *The amount of ^{18}O exchanged in microatom per milligram of protein is plotted against the time in hours. Yeast SDS-extracted membranes containing either wild-type (square) or Asp714Glu mutant (circle) were incubated at 30°C over a period of 24 h. Open symbols mean that ouabain was present and closed symbols mean that ouabain was absent. The Lys691Arg mutant did not show any ^{18}O exchange activity under these conditions (This experiment was carried out in department of Med CURE, University of California, Los Angeles, Vaglahs).*

4. Discussion

The Na^+/K^+-ATPase (sodium pump) is an active ion-motive ATPase of animal cell membranes. It converts the energy of ATP hydrolysis into an electrochemical gradient of Na^+ and K^+ ions across the membrane. Under physiological conditions, three Na^+ ions are moved out of the cell and two K^+ ions into the cytoplasm per molecule ATP hydrolyzed [21, 188]. To perform this task the enzyme goes through a cycle of conformational transitions, phosphorylation and dephosphorylation steps, and ion binding, occlusion, and release reactions [5, 25, 30]. Several functional and structural properties of the Na^+/K^+-ATPase have been revealed, such as the presence of a phosphorylation site and its location [5], the existence of occlusion states [25, 30, 34], or the finding of an extracellular access channel [29, 189, 190]. Since the phosphorylation site and cation binding sites are well separated from each other in the tertiary structure [191-194], the coupling of enzymatic and transport functions must be indirect and require conformational changes as a link between ATP hydrolysis and the translocation event. Little is known about the nature of these conformational changes during the enzymatic cycle.

A new work recently suggests that Na^+/K^+-ATPase is also a member of the hydrolase superfamily called haloacid dehalogenases (HAD) [128]. The L-2-EDX YL is a well characterized member of the HAD superfamily; it catalyses the hydrolytic dehalogenation of L-haloalkanoates to produce the corresponding D-2-haloalkanoates [195]. The catalytic reaction begins with a nucleophilic attack of Asp10 on the α-carbon of the substrate L-2-haloalkanoates and results in formation of an ester intermediate, which is subsequently hydrolyzed to release the D-2-haloalkanoate products (Scheme 1.2) [131, 133]. The crystal structure and mass spectrometric monitoring reveal the enzymatic reaction mechanism and some unique amino acid residues such as Asp10, Ser118, Lys151, and Asp180, which are crucial for forming and hydrolyzing the intermediate [132, 137]. Site-directed mutagenesis furthermore indicates such amino acid residues are essential for enzymatic activity [130]. These enzymological studies of L-2-DEX YL have provided critical information on the structure and function of Na^+/K^+-ATPase, which has a very similar reaction mechanism to L-2-DEX YL ([128]). Recent studies on the crystal structure of Ca^{2+}-ATPase from sarcoplasmic reticulum have revealed that the phosphorylation domain of this ATPase has a high three-dimensional structural similarity to that of L-2-DEX YL, and some essential amino acid residues are conserved between these two proteins [126, 136].

Using the standard gap BLAST program, the sodium pump did not show any similarity to the haloacid dehalogenase, but iterated sequence comparison and position-specific iterated BLAST (PSI-BLAST) [185, 186] starting from haloacid dehalogenase have shown that these enzymes share three statistically significant motifs with the predicted P domain of the Na^+/K^+-ATPase (Fig. 3.1). The first of these motifs contains an absolutely conserved aspartate (Asp10 in L-2-DEX YL, Asp369 in sheep Na^+/K^+-ATPase α1 subunit) which covalently binds an α-hydroxyl acid in L-2-DEX YL and phosphate in Na^+/K^+-ATPase [133, 187]. The second motif contains a strictly conserved hydroxyl residue, serine or threonine. These two motifs are separated by large inserts of variable size as shown in Fig. 3.1. The third motif contains a highly conserved lysine (Lys151 in L-2-DEX YL, Lys691 in Na^+/K^+-ATPase) residue and an absolutely conserved aspartate (Asp180 in L-2-DEX YL and Asp714 in Na^+/K^+-ATPase). These three motifs comprise a typical haloacid dehalogenase Rossmann fold (Fig. 1.5, 1.6).
In order to investigate whether Lys691 and Asp714 play the same key function for the catalytic mechanism of the sodium pump as the corresponding amino acids do for the activity of the haloacid dehalogenases, mutants of the sodium pump were produced in yeast and investigated for their properties.
Lys691, which according to Aravind's proposal [128] should be involved in the hydrolytic process of the terminal phosphate group of ATP during the self-phosphorylation process of the enzyme at Asp369, was altered to a neutral amino acid (Ala), altered in a non-conservative way (Glu), or replaced by preserving the positive charge (Arg).

Asp714 should coordinate a water molecule according to the same model, thus producing an increased nucleophilicity of the water oxygen and resulting in a nucleophilic attack of the latter on the phosphoric atom to cleave the phosphoric ester formed between Asp369 and ATP terminal phosphate. Asp714 was mutated also in a conservative (Asp714Glu), nonconservative (Asp714Arg) and neutral way (Asp714Ala).

The role of Lys691

Based on Aravind's proposal, Lys691, especially its positive charge, should be absolutely essential for the phosphorylation process of the enzyme by ATP. The positively charged ε-amino group of the lysine increases the electrophilicity of the γ-phosphoric atom, enabling it to be attacked by the carboxyl group of Asp369, a reaction leading to the phosphorylated intermediate of the sodium pump called E_1~P. Thus, the expectation, if the model is correct, was that neither the neutral nor the nonconservative mutations of Lys691 should lead to

functional enzymes. The conservative mutant Lys691Arg, on the other hand, was expected to display some of the properties of the native enzyme.

In order to ensure that changes in enzymatic properties were not due to altered protein expression, Western blots were carried out to verify the presence of the proteins in question in the membrane preparations used (Fig.3.3.3 and 3.3.4).

As expected, Lys691Ala and Lys691Asp were inactive in all respects. Not only was an ATPase activity detected in membrane preparations, but these enzyme also more or less completely failed to interact with the highly sodium pump-specific inhibitors ouabain or palytoxin.

The Na^+/K^+-ATPase is the unique receptor for ouabain [101]. Phosphate interaction at the catalytic phosphorylation site, Asp369 in the sheep $\alpha 1$ isomer, induces a conformational change in the sodium pump which increases the affinity of the enzyme for ouabain [64]. Thus, catalytic ATPase activity and ouabain binding are linked through this phosphorylation site, which supports the use of [^{3}H]ouabain binding as a method for probing the functional properties of Na^+/K^+-ATPase.

The affinity of the sodium pump for ouabain is closely linked to enzyme cycling. The effects of enzyme substrates on the protein-drug interaction has been demonstrated: Mg^{2+} and P_i stimulate ouabain binding in the absence of monovalent cations [101, 174], and Mg^{2+} and ATP stimulate ouabain binding in the presence of Na^+ [173, 175]. These ouabain binding properties can be antagonized by the addition of K^+ ion to the equilibrium medium. Presumably, K^+ induces a conformational change in the Na^+/K^+-ATPase from the E_2P to the E_2 form (Scheme 1.1); this conformational change lowers the ouabain affinity of the enzyme. Mg^{2+} is required for the maximal enzymatic activity [196].

Palytoxin is also a specific Na^+/K^+-ATPase inhibitor. This toxin is synthesized by coral (*Palythoa spp*) and is the most potent animal toxin known. Palytoxin induces a channel formation within the sodium pump, and causes K^+ efflux and Na^+ influx down their electrochemical gradients in animal cells but not in bacterial or yeast cells [91, 95]. Yeast cells become sensitive to palytoxin only when expressing with functional mammalian sodium pump [64]. This evidence supports the belief that the Na^+/K^+-ATPase is the target of palytoxin. Ouabain completely inhibits the palytoxin-induced K^+ efflux from yeast cells expressing the mammalian sodium pump [64].

Palytoxin is known to interact with the E_1 conformational state of the enzyme and its phosphorylated derivatives. This conclusion is supported by experiments on reside-reconstituted Na^+/K^+-ATPase [197]. Binding experiments with radioactively labeled palytoxin

indicating that palytoxin acts on the E_1-P conformer of the enzyme induced by cytosolic ATP and Na^+ (Scheme 1.1), and approximately 50% of the maximum palytoxin binding is obtained in the presence of ADP, which cannot be utilized by the pump to induce the E_1-P conformational state [160]. Although the phosphorylation of the Na^+/K^+-ATPase is not absolutely required for the binding of palytoxin, ATP and phosphorylation promote palytoxin binding to the Na^+/K^+-ATPase [26, 160].

In contrast to the Lys691Ala and Lys691Asp mutants, the conservative mutant Lys691Arg retained some of the partial activities of the wild-type enzyme, although it completely failed to display any ATPase activity, indicating that this mutant enzyme is not capable of undergoing all conformational transitions required for the accomplishment of the catalytic cycle.

In the presence of phosphate and Mg^{2+}, which in the wild-type enzyme induce the E_2-P conformational state and allow the binding of ouabain, the mutant was not able to bind ouabain. Thus, the [E_2-P·ouabain] complex was not formed by this enzyme.

On the other hand, yeast cells expressing this mutant become sensitive to palytoxin and lose cytosolic K^+. Their sensitivity to palytoxin was with an EC_{50} value of 118 ± 24 nM clearly reduced by almost 10-fold below the sensitivity of cells expressing the native sodium pump, where the EC_{50} value under the same conditions was 17.8 ± 2.7 nM.

In contrast to the binding experiments in the presence of Mg^{2+} and phosphate, ouabain was recognized by the mutant under these conditions and inhibited the palytoxin-induced K^+ efflux from the yeast cells. The EC_{50} for the ouabain effect, however, was about 131± 13 µM, while the corresponding value obtained with cells expressing the native sodium pump was 5.13 ± 0.71 µM.

As verified earlier with mutants of Asp369 [76], which is the phosphorylation site of the sodium pump, phosphorylation of the enzyme is not required for palytoxin-induced channel formation, although ATP promotes the reaction. Yeast cells that express this Asp369Ala mutant are sensitive to palytoxin and loose upon exposition to the toxin their intracellular K^+. The EC_{50} for palytoxin is under these conditions 6.2 ± 0.9 nM. In these experiments it also become clear that not only palytoxin but also ouabain can interact with nonphosphorylated forms of the enzyme, since the palytoxin-induced K^+ efflux from cells expressing this mutant was inhibited by ouabain with an IC_{50} of 210 ± 15 µM [76].

Thus, the fact that palytoxin induces a K^+ efflux from cells expressing the Lys691Arg mutant does not allow one to distinguish whether the enzyme retains its capability of becoming phosphorylated or not. If phosphorylation occurs, one should expect that the

dephosphorylation of this mutant enzyme should be possible, since other amino acids involved in the dephosphorylation process remained unaltered. Therefore, ^{18}O exchange experiments were carried out using ATP with ^{18}O-labeled terminal phosphate. In these experiments, one expects the phosphorylated enzyme to dephosphorylate by getting hydrolyzed [184]. Thus, depending upon the numbers of hydrolyses and back-phosphorylations, the ^{18}O-labeled phosphate will exchange several of the labeled oxygen atoms with unlabeled water oxygen, thus producing various species of labeled phosphate that can be detected in a mass spectrometer [182,183]. No ^{18}O exchange, however, was detected with membrane preparations containing the Lys691Arg mutant, allowing one to assume that phosphorylation does not take place with this mutant and that it is in unphosphorylated form that interacts with palytoxin or ouabain in the K^+ efflux experiments with whole yeast cells.

This proposal can also serve as an interpretation of the data concerning ouabain binding to membrane preparations containing the Lys691Arg mutant. There, binding was not detectable in the nM ouabain range investigated unless Mg^{2+} was omitted. Mg^{2+} (and ATP or ADP) are present in the cell, thus shifting the conformation of the mutant enzyme that is localized in the plasma membrane towards the E_1 conformational state that binds ouabain with low affinity. In the membrane preparations, however, when Mg^{2+} is omitted from the reaction mixture, an $E_1 \leftrightarrow E_2$ transition with the equilibrium towards the E_2 form [198] allows ouabain binding also at nM ouabain concentrations.

The role of Asp714

P-type ATPases such as the sodium pump appear to be members of a superfamily of hydrolases structurally typified by the L-2-haloacid dehalogenases. In the dehalogenase L-2-DEX YL, a water molecule that is directly involved in catalysis is coordinated by Asp180. Based on Aravind's proposal [128], the corresponding amino acid Asp714 of the sodium pump α subunit, especially its negative charge, should be absolutely essential for the dephosphorylation process of the enzyme. According to his proposal, the negatively charged carboxyl group of the aspartate side chain should interact with a water hydrogen, thus resulting in increased nucleophilicity of the water oxygen. This enables the oxygen to attack the phosphorus atom of the phosphoric ester formed between Asp369 and the ATP terminal phosphate and to cleave (hydrolyze) the latter.

The prediction based on this model is that neither of the Asp714Ala or As714Arg mutants should retain any ATPase activity, which was found to be the case. Other sodium pump-

associated activities were not detected with these mutants either, despite sufficient expression of the mutant proteins (Fig. 3.3.3 and 3.3.4).

In contrast, the Asp714Glu mutant retained some of the enzymatic properties, although no overall ATPase reaction was detected with SDS-extracted membrane preparations from yeast cells expressing this mutant.

Thus, cells expressing the Asp714Glu mutant were sensitive to palytoxin and released intracellular K^+ upon exposure to the toxin. The EC_{50} for palytoxin was 76.5 ± 3.6 nM for this reaction. This palytoxin-induced K^+ efflux, however, was almost completely insensitive to ouabain (Fig. 3.4.3). The EC_{50} for ouabain that was estimated from the slow inactivation of the K^+ efflux was greater than 2.5 mM, indicating either a very weak interaction of the mutant with the cardiac steroid or a very stable formation of a mutant/palytoxin complex. The relatively high EC_{50} for palytoxin and the incapacity of membrane preparations from cells expressing this mutant to bind ouabain in the presence of Mg^{2+} and inorganic phosphate indicate, however, that the Asp714Glu mutant has a rather reduced affinity for ouabain.

On the other hand, omitting Mg^{2+} and allowing ouabain to bind to the membranes are consistent with the assumption made above that Mg^{2+} shifts the enzyme conformation towards the E_1-associated conformational states. In this case, this should be the E_1-P conformational state, since ^{18}O-exchange was detectable with membranes containing this mutant. Nevertheless, the exchange rate was highly reduced in comparison to that obtained with the native enzyme, indicating — as expected — that the dephosphorylation process is substantially affected by the mutation.

Besides these conclusions, the investigation of the two conservative mutants has provided new insights into the interaction of the enzyme with its ligands Mg^{2+}, ouabain and K^+. Due to the mutations it was possible to show here, that Mg^{2+} arrests the enzyme in the E_1-conformational state and the turn to the E_2 can only proceed when phosphorylation by the terminal phosphate of ATP has taken place in the presence of Na^+. This is in good agreement with earlier results obtained from inactivation experiments of the Na^+/K^+-ATPase with Mg^{2+}-ATP analogous. In these it could be demonstrated that the Cr^{III} derivatives of 8-N_3-ATP and 3´-N_{3P} ATP inactivate the enzyme by arresting it in the E_1 conformational state and that addition of Mg^{2+} accelerates the inactivation reaction without allowing any further conformational transitions [200].

Interactions with ouabain were always thought to take place at the phosphorylated E_2 conformational state of the enzyme: A possible binding of the steroid to the E_1 conformational state was never easy to address, since addition of ATP or phosphate would both result in the

formation of the stable [E_2*P·ouabain] complex. In addition, since intermediates of ouabain with the enzyme in the E_1 state are rather difficult to isolate, the [E_2-P] conformation was always the one to investigate and possibly because of this it was established as the ouabain binding state.

With the mutants investigated here, however, it becomes apparent, that when Mg^{2+} which arrests the enzyme in the E_1 conformation is omitted, the $E_1 \leftrightarrow E_2$ transition of the enzyme allows binding of ouabain to the unphosphorylated E_2 state.

Finally, the fact that K^+ inhibiting ouabain binding to the unphosphorylated E_2 conformational state gives us the possibility to attempt an explanation of this phenomenon. With native enzyme where binding of ouabain in the presence of phosphate and Mg^{2+} has often been shown to be reduced when K^+ is included in the reaction mixture, it is always a disputable issue, whether reduced ouabain binding is due to a K^+-induced dephosphorylation or due to a direct competition between K^+ and ouabain [101, 173]. Although no competition experiments were performed here with the Lys691 and Asp714 mutants, the fact that K^+ reduces ouabain binding although no phosphorylation occurs is somehow indirectly pointing out to the possibility that K^+ and ouabain might compete for binding sites, which might overlap without being identical.

Nevertheless, the overall conclusion of the investigations described here is that Aravind's proposal is most likely correct: Lys691 is essential for the phosphorylation of the sodium pump and Asp714 for the dephosphorylation process (Fig. 4.1). Nonconservative mutants of both amino acids are completely inactive and do not display any partial reactions typical for the sodium pump. On the other hand, conservative mutant of Lys691 remains most likely unphosphorylated, while mutants of Asp714 are probably phosphorylated but remain for the most part arrested in this state by not being able to hydrolyze the phosphoric ester bond formed between Asp369 and the terminal ATP phosphate.

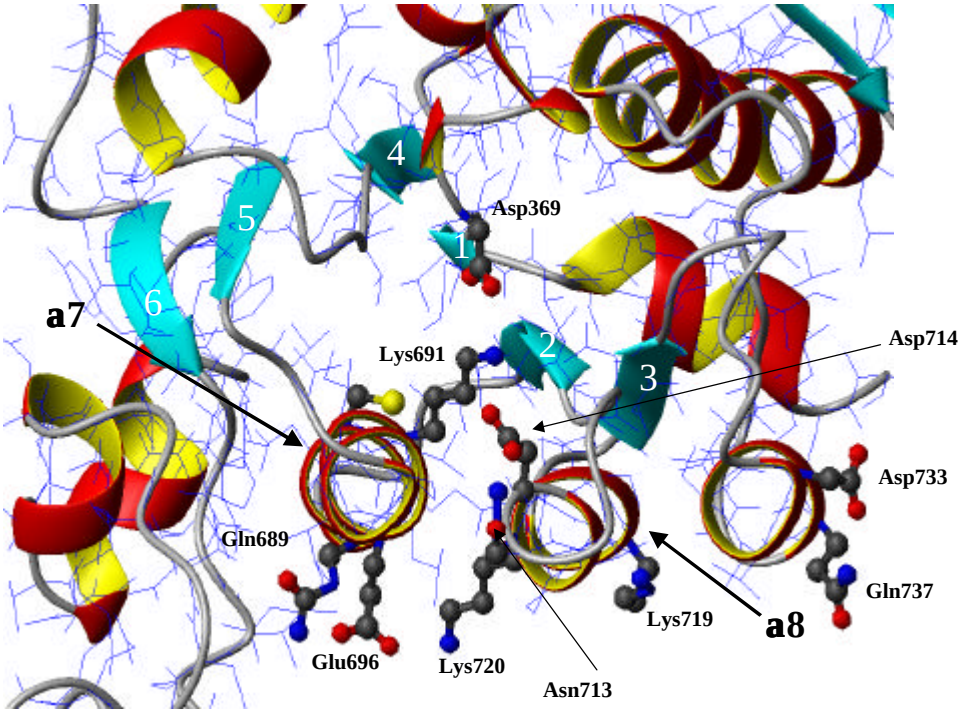

Fig. 4.1 Proposed haloacid dehalogenase fold of the sodium pump a subunit

This structural model was drown by MolMol. The arrangement of corresponding important amino acids of the sodium pump a subunit was based on the analogue of amino acids in the crystal structure of the Ca^{2+}-ATPase [126]. As the case in Ca^{2+}-ATPase, the residue Lys691 is located approximately at the beginning of the a7-helix and the Asp714 in the a8-helix in motif III, respectively, and they are arranged around the active site Asp369. The carbonyl oxygen of the phosphorylation site Asp369 is oriented toward an N atom in the side chain of the positive charged residue Lys691. The Lys691 is tightly hydrogen-bonded with the unesterified oxygen O^{d1} of Asp369 stabilizing the negative charge accumulated on the O^{d1}. The Asp714 residue probably keeps or fixes the water molecule to make a hydrogen bond with the esterified oxygen, stabilizes the transition state during the ester hydrolysis.

5. Summary

P-type ATPases such as the sodium pump appear to be the members of a superfamily of hydrolases structurally typified by the L-2-haloacid dehalogenases. In the haloacid dehalogenase L-2-DEX YL, Lys151 serves to stabilize the excess negative charge in the substrate/reaction intermediates and Asp180 coordinates a water molecule that is directly involved in ester intermediate hydrolyze. To investigate the importance of the corresponding Lys691 and Asp714 of the sodium pump α subunit, sodium pump mutants were expressed in yeast and analyzed for their properties.

The Lys691Ala, Lys691Asp, Asp714Ala, and Asp714Arg mutants were enzymatic inactive, not only with respect to ATPase activity, but also to non interaction with the highly sodium pump-specific-inhibitors ouabain or palytoxin.

In contrast, the conservative mutants Lys691Arg and Asp714Glu retained some of the partial activities of the wild-type enzyme, although they completely failed to display any ATPase activity. In the presence of P_i and Mg^{2+}, none of the mutant sodium pumps were able to bind ouabain: the [E_2*P·ouabain] complex was not able to be formed by the mutant enzymes. When Mg^{2+} was omitted, however, both Lys691Asp and Asp714Glu mutants displayed ouabain binding only at 5 mM P_i. Mg^{2+} caused a reduction in ouabain binding with an EC_{50} of 0.76 ± 0.11 mM and 1.24 ± 0.21 mM, respectively.

On the other hand, yeast cells expressing Lys691Arg and Asp714Glu mutants are sensitive to palytoxin and lose their intracellular K^+. Their sensitivity to palytoxin, with EC_{50} value of 118 ± 24 nM and 76.5 ± 3.6 nM, respectively, was clearly reduced by almost 7- or 4-fold below that of the native sodium pump (17.8 ± 2.7 nM).

In contrast to the binding experiments in the presence of Mg^{2+} and phosphate, ouabain was recognized by the mutants under these conditions and inhibited the palytoxin-induced K^+ efflux from the yeast cells. The EC_{50} for the ouabain effect was 131 ± 13 µM for Lys691Arg ,and greater than 2.5 mM for the Asp714Glu mutant, while the corresponding value obtained with cells expressing the native sodium pump was 5.13 ± 0.71 µM.

Experiments with ^{18}O-labeled Pi demonstrated that only a modest ^{18}O exchange with surrounding water occurred for Asp714 and no ^{18}O exchange was detected with the Lys691Arg mutant.

In conclusions, Lys691 and Asp714 are very important for the conformational transition of the sodium pump: Lys691 is essential for the phosphorylation process and Asp714 for the dephosphorylation process. Thus, Lys691 and Asp714 residues of the sodium pump α subunit are essential for the enzymatic activity.

6. Zusammenfassung

Die Natriumpumpe, eine P-Typ-ATPase, scheint zur Superfamilie der Hydrolysen zu gehören. Aufgrund ihrer Faltungsstruktur müßte sie als L-2-Haloazid-Dehalogenase klassifiziert werden. In der Haloazid-Dehalogenase L-2-DEX YL dient die Aminosäure Lys151 der Stabilisierung der überschüssigen negativen Ladung bei der Substratbindung bzw. der Entstehung von Reaktions-Zwischenprodukten. Asp180 koordiniert ein Wassermolekül, welches direkt bei der Hydrolyse des Ester-Intermediats beteiligt ist. Die beiden Aminosäuren könnte Lys691 und Asp714 der Natriumpumpe entsprechen. Um ihre Bedeutung für die Katalyse zu untersuchen, wurden Mutanten dieser Aminosäuren in Hefezellen exprimiert und ihre Eigenschaften untersucht.

Die Mutationen Lys691Ala, Lys691Asp, Asp714Ala, und Asp714Arg waren völlig inaktiv.

Die konservativen Mutanten Lys691Arg und Asp714Glu zeigten einige Teil-aktivitäten des Wildtyp-Enzyms, waren aber ohne ATPase-Aktivität. In Anwesenheit von P_i und Mg^{2+} zeigte keine der Mutanten eine Ouabainbindung: Der [E_2*P·ouabain] Komplex konnte bei keiner der Mutanten gebildet werden. Ohne Zugabe von Mg^{2+} zeigten die Lys691Asp- und Asp714Glu-Mutanten jedoch eine Ouabainbindung bei 5 mM P_i. Somit bewirkte Mg^{2+} eine Reduktion der Ouabainbindung.

Hefezellen, welche die Mutanten Lys691Arg oder Asp714Glu exprimierten, waren sensitiv gegenüber Palytoxin und verloren K^+. Ihre Sensitivität gegenüber Palytoxin, mit einem EC_{50} Wert von 118 ± 24 nM bzw. 76,5 ± 3,6 nM war deutlich reduziert und lag sieben- bzw. vierfach unter der Sensitivät von Hefezellen, die den Wildtyp exprimierten (17,8 ± 2,7 nM). Dieser Palytoxin-induzierter K^+-Efflux wurde durch Ouabain gehemmt. Der EC_{50} Wert für den Ouabaineffekt betrug 131 ± 13 µM bei der Lys691Arg Mutanten und war 2,5 mM oder größer bei der Asp714Glu Mutanten. Der entsprechende EC_{50} Wert nicht-mutierter Natriumpumpen lag bei 5.13 ± 0.71 µM.

Isotopenaustauschexperimente mit ^{18}O-markiertem P_i zeigten bei der Mutanten Asp714Glu nur einen geringen ^{18}O Austausch mit dem Umgebungswasser ($H_2{}^{16}O$) und keinen ^{18}O Austausch bei der Lys691Arg Mutante.

Schlussfolgernd, Lys691 und Asp714 sind sehr wichtig für die Konformationsübergänge der Natriumpumpe. Das Lys691 ist wichtig für den Phosphorylierungsprozess, Asp714 für den Dephosphorylierungsprozess. Beide Aminosäuren Lys691 und Asp714 der α Untereinheit der Natriumpumpe sind hier als essentiell für die enzymatische Aktivität nachgewiesen worden.

7. Refrences

1. Wallin, E. & von Heijne, G. (1998) Genome-wide analysis of integral membrane proteins from eubacterial, archaean, and eukaryotic organisms, *Protein Sci. 7*, 1029-38.
2. Pedersen, P. L., Williams, N. & Hullihen, J. (1987) Mitochondrial ATP synthase: dramatic Mg2+-induced alterations in the structure and function of the F1-ATPase moiety, *Biochemistry. 26*, 8631-7.
3. Axelsen, K. B. & Palmgren, M. G. (1998) Evolution of substrate specificities in the P-type ATPase superfamily, *J Mol Evol. 46*, 84-101.
4. Chow, D. C. & Forte, J. G. (1995) Functional significance of the beta-subunit for heterodimeric P-type ATPases, *J Exp Biol. 198*, 1-17.
5. Jorgensen, P. L. & Andersen, J. P. (1988) Structural basis for E1-E2 conformational transitions in Na,K-pump and Ca-pump proteins, *J Membr Biol. 103*, 95-120.
6. Kaplan, J. H., Lutsenko, S., Gatto, C., Daoud, S. & Kenney, L. J. (1997) Ligand-induced conformational changes in the Na,K-ATPase alpha subunit, *Ann N Y Acad Sci. 834*, 45-55.
7. Sachs, G. & Munson, K. (1991) Mammalian phosphorylating ion-motive ATPases, *Curr Opin Cell Biol. 3*, 685-94.
8. Green, N. M. (1992) Ion-Motive ATPases: Structure, Function, and Regulation. Proceedings of a conference. Cleveland, Ohio, June 13-17, 1992, *Ann N Y Acad Sci. 671*, 1-515.
9. Palmgren, M. G. & Axelsen, K. B. (1998) Evolution of P-type ATPases, *Biochim Biophys Acta. 1365*, 37-45.
10. Andersen, J. P. & Vilsen, B. (1995) Structure-function relationships of cation translocation by Ca(2+)- and Na+, K(+)-ATPases studied by site-directed mutagenesis, *FEBS Lett. 359*, 101-6.
11. Glynn, I. M. (1993) Annual review prize lecture. 'All hands to the sodium pump', *J Physiol. 462*, 1-30.
12. Jorgensen, P. L., Nielsen, J. M., Rasmussen, J. H. & Pedersen, P. A. (1998) Structure-function relationships of E1-E2 transitions and cation binding in Na,K-pump protein, *Biochim Biophys Acta. 1365*, 65-70.
13. MacLennan, D. H., Rice, W. J. & Green, N. M. (1997) The mechanism of Ca2+ transport by sarco(endo)plasmic reticulum Ca2+-ATPases, *J Biol Chem. 272*, 28815-8.
14. Lutsenko, S. & Kaplan, J. H. (1995) Organization of P-type ATPases: significance of structural diversity, *Biochemistry. 34*, 15607-13.
15. Skou, J. C. (1988) The Na,K-pump, *Methods Enzymol. 156*, 1-25.
16. Gabler, J., Nolte, I., Scheiner-Bobis, G., Eigenbrodt, E. & Scheiner-Bobis, K. (1993) The influence of storage time on the nucleotide concentration of canine platelets, *Zentralbl Veterinarmed A. 40*, 546-54.
17. Glynn, I. M. (1968) Membrane adenosine triphosphatase and cation transport, *Br Med Bull. 24*, 165-9.
18. Falciola, J., Volet, B., Anner, R. M., Moosmayer, M., Lacotte, D. & Anner, B. M. (1994) Role of cell membrane Na,K-ATPase for survival of human lymphocytes in vitro, *Biosci Rep. 14*, 189-204.
19. Repke, H. & Bienert, M. (1988) Structural requirements for mast cell triggering by substance P-like peptides, *Agents Actions. 23*, 207-10.
20. Moller, J. V., Juul, B. & le Maire, M. (1996) Structural organization, ion transport, and energy transduction of P-type ATPases, *Biochim Biophys Acta. 1286*, 1-51.
21. Lingrel, J. B. & Kuntzweiler, T. (1994) Na+,K(+)-ATPase, *J Biol Chem. 269*, 19659-62.
22. Lutsenko, S. & Kaplan, J. H. (1996) P-type ATPases, *Trends Biochem Sci. 21*, 467.
23. MacLennan, D. H. & Green, N. M. (2000) Structural biology. Pumping ions, *Nature. 405*, 633-4.
24. Esmann, M. & Skou, J. C. (1985) Occlusion of Na+ by the Na,K-ATPase in the presence of oligomycin, *Biochem Biophys Res Commun. 127*, 857-63.
25. Glynn, I. M. & Karlish, S. J. (1990) Occluded cations in active transport, *Annu Rev Biochem. 59*, 171-205.
26. Scheiner-Bobis, G. & Schneider, H. (1997) Palytoxin-induced channel formation within the Na+/K+-ATPase does not require a catalytically active enzyme, *Eur J Biochem. 248*, 717-23.
27. Vilsen, B. & Andersen, J. P. (1998) Mutation to the glutamate in the fourth membrane segment of Na+,K+-ATPase and Ca2+-ATPase affects cation binding from both sides of the membrane and destabilizes the occluded enzyme forms, *Biochemistry. 37*, 10961-71.
28. Hilgemann, D. W. (1997) Recent electrical snapshots of the cardiac Na,K pump, *Ann N Y Acad Sci. 834*, 260-9.
29. Wuddel, I. & Apell, H. J. (1995) Electrogenicity of the sodium transport pathway in the Na,K-ATPase probed by charge-pulse experiments, *Biophys J. 69*, 909-21.
30. Forbush, B., 3rd. (1987) Rapid release of 42K or 86Rb from two distinct transport sites on the Na,K-pump in the presence of Pi or vanadate, *J Biol Chem. 262*, 11116-27.
31. Rossi, R. C. & Norby, J. G. (1993) Kinetics of K(+)-stimulated dephosphorylation and simultaneous K+ occlusion by Na,K-ATPase, studied with the K+ congener Tl+. The possibility of differences between the first turnover and steady state, *J Biol Chem. 268*, 12579-90.

32. Karlish, S. J., Yates, D. W. & Glynn, I. M. (1978) Conformational transitions between Na+-bound and K+-bound forms of (Na+ + K+)-ATPase, studied with formycin nucleotides, *Biochim Biophys Acta. 525*, 252-64.
33. Jorgensen, P. L. (1975) Purification and characterization of (Na+, K+)-ATPase. V. Conformational changes in the enzyme Transitions between the Na-form and the K-form studied with tryptic digestion as a tool, *Biochim Biophys Acta. 401*, 399-415.
34. Post, R. L., Hegyvary, C. & Kume, S. (1972) Activation by adenosine triphosphate in the phosphorylation kinetics of sodium and potassium ion transport adenosine triphosphatase, *J Biol Chem. 247*, 6530-40.
35. Goldshleger, R. & Karlish, S. J. (1999) The energy transduction mechanism of Na,K-ATPase studied with iron-catalyzed oxidative cleavage, *J Biol Chem. 274*, 16213-21.
36. Asano, S., Kamiya, S. & Takeguchi, N. (1992) The energy transduction mechanism is different among P-type ion-transporting ATPases. Acetyl phosphate causes uncoupling between hydrolysis and ion transport in H+,K(+)-ATPase, *J Biol Chem. 267*, 6590-5.
37. Jorgensen, P. L. (1974) Isolation and characterization of the components of the sodium pump, *Q Rev Biophys. 7*, 239-74.
38. de Meis, L. & Vianna, A. L. (1979) Energy interconversion by the Ca2+-dependent ATPase of the sarcoplasmic reticulum, *Annu Rev Biochem. 48*, 275-92.
39. Brown, T. A., Horowitz, B., Miller, R. P., McDonough, A. A. & Farley, R. A. (1987) Molecular cloning and sequence analysis of the (Na+ + K+)-ATPase beta subunit from dog kidney, *Biochim Biophys Acta. 912*, 244-53.
40. Kawakami, K., Noguchi, S., Noda, M., Takahashi, H., Ohta, T., Kawamura, M., Nojima, H., Nagano, K., Hirose, T., Inayama, S. & et al. (1985) Primary structure of the alpha-subunit of Torpedo californica (Na+ + K+)ATPase deduced from cDNA sequence, *Nature. 316*, 733-6.
41. Monastyrskaia, G. S., Broude, N. E., Melkov, A. M., Smirnov, I. V. & Malyshev, I. V. (1987) [Primary structure of the alpha-subunit of Na+,K+-ATPase from the swine kidney. III. Complete nucleotide sequence corresponding to the structural region of the gene], *Bioorg Khim. 13*, 20-6.
42. Shull, G. E., Lane, L. K. & Lingrel, J. B. (1986) Amino-acid sequence of the beta-subunit of the (Na+ + K+)ATPase deduced from a cDNA, *Nature. 321*, 429-31.
43. Kyte, J. & Doolittle, R. F. (1982) A simple method for displaying the hydropathic character of a protein, *J Mol Biol. 157*, 105-32.
44. Jorgensen, P. L., Karlish, S. J. & Gitler, C. (1982) Evidence for the organization of the transmembrane segments of (Na,K)-ATPase based on labeling lipid-embedded and surface domains of the alpha-subunit, *J Biol Chem. 257*, 7435-42.
45. Mohraz, M., Arystarkhova, E. & Sweadner, K. J. (1994) Immunoelectron microscopy of epitopes on Na,K-ATPase catalytic subunit. Implications for the transmembrane organization of the C-terminal domain, *J Biol Chem. 269*, 2929-36.
46. Arystarkhova, E., Gibbons, D. L. & Sweadner, K. J. (1995) Topology of the Na,K-ATPase. Evidence for externalization of a labile transmembrane structure during heating, *J Biol Chem. 270*, 8785-96.
47. Antolovic, R., Bruller, H. J., Bunk, S., Linder, D. & Schoner, W. (1991) Epitope mapping by amino-acid-sequence-specific antibodies reveals that both ends of the alpha subunit of Na+/K(+)-ATPase are located on the cytoplasmic side of the membrane, *Eur J Biochem. 199*, 195-202.
48. Goldshleger, R., Tal, D. M. & Karlish, S. J. (1995) Topology of the alpha-subunit of Na,K-ATPase based on proteolysis. Lability of the topological organization, *Biochemistry. 34*, 8668-79.
49. Shull, G. E., Schwartz, A. & Lingrel, J. B. (1985) Amino-acid sequence of the catalytic subunit of the (Na+ + K+)ATPase deduced from a complementary DNA, *Nature. 316*, 691-5.
50. Yoon, K. L. & Guidotti, G. (1994) Studies on the membrane topology of the (Na,K)-ATPase, *J Biol Chem. 269*, 28249-58.
51. Fiedler, B. & Scheiner-Bobis, G. (1996) Transmembrane topology of alpha- and beta-subunits of Na+,K+-ATPase derived from beta-galactosidase fusion proteins expressed in yeast, *J Biol Chem. 271*, 29312-20.
52. Canfield, V. A., Norbeck, L. & Levenson, R. (1996) Localization of cytoplasmic and extracellular domains of Na,K-ATPase by epitope tag insertion, *Biochemistry. 35*, 14165-72.
53. Stokes, D. L., Taylor, W. R. & Green, N. M. (1994) Structure, transmembrane topology and helix packing of P-type ion pumps, *FEBS Lett. 346*, 32-8.
54. Hu, Y. K. & Kaplan, J. H. (2000) Site-directed chemical labeling of extracellular loops in a membrane protein. The topology of the Na,K-ATPase alpha-subunit, *J Biol Chem. 275*, 19185-91.
55. Jockel, P., Di Berardino, M. & Dimroth, P. (1999) Membrane topology of the beta-subunit of the oxaloacetate decarboxylase Na+ pump from Klebsiella pneumoniae, *Biochemistry. 38*, 13461-72.
56. Lingrel, J. B., Van Huysse, J., O'Brien, W., Jewell-Motz, E., Askew, R. & Schultheis, P. (1994) Structure-function studies of the Na,K-ATPase, *Kidney Int Suppl. 44*, S32-9.
57. Lingrel, J. B., Arguello, J. M., Van Huysse, J. & Kuntzweiler, T. A. (1997) Cation and cardiac glycoside binding sites of the Na,K-ATPase, *Ann N Y Acad Sci. 834*, 194-206.

58. Kakinuma, Y. & Igarashi, K. (1989) Sodium-translocating adenosine triphosphatase in Streptococcus faecalis, *J Bioenerg Biomembr. 21*, 679-92.
59. Kirley, T. L. (1990) Inactivation of (Na+,K+)-ATPase by beta-mercaptoethanol. Differential sensitivity to reduction of the three beta subunit disulfide bonds, *J Biol Chem. 265*, 4227-32.
60. Geering, K. (1991) The functional role of the beta-subunit in the maturation and intracellular transport of Na,K-ATPase, *FEBS Lett. 285*, 189-93.
61. Lutsenko, S. & Kaplan, J. H. (1993) An essential role for the extracellular domain of the Na,K-ATPase beta-subunit in cation occlusion, *Biochemistry. 32*, 6737-43.
62. Horowitz, B., Eakle, K. A., Scheiner-Bobis, G., Randolph, G. R., Chen, C. Y., Hitzeman, R. A. & Farley, R. A. (1990) Synthesis and assembly of functional mammalian Na,K-ATPase in yeast, *J Biol Chem. 265*, 4189-92.
63. Eakle, K. A., Kabalin, M. A., Wang, S. G. & Farley, R. A. (1994) The influence of beta subunit structure on the stability of Na+/K(+)-ATPase complexes and interaction with K+, *J Biol Chem. 269*, 6550-7.
64. Scheiner-Bobis, G., Meyer zu Heringdorf, D., Christ, M. & Habermann, E. (1994) Palytoxin induces K+ efflux from yeast cells expressing the mammalian sodium pump, *Mol Pharmacol. 45*, 1132-6.
65. Lemas, M. V., Yu, H. Y., Takeyasu, K., Kone, B. & Fambrough, D. M. (1994) Assembly of Na,K-ATPase alpha-subunit isoforms with Na,K-ATPase beta-subunit isoforms and H,K-ATPase beta-subunit, *J Biol Chem. 269*, 18651-5.
66. Ivanov, A., Zhao, H. & Modyanov, N. N. (2000) Packing of the transmembrane helices of Na,K-ATPase: direct contact between beta-subunit and H8 segment of alpha-subunit revealed by oxidative cross-linking, *Biochemistry. 39*, 9778-85.
67. Colonna, T. E., Huynh, L. & Fambrough, D. M. (1997) Subunit interactions in the Na,K-ATPase explored with the yeast two-hybrid system, *J Biol Chem. 272*, 12366-72.
68. Forbush, B., 3rd, Kaplan, J. H. & Hoffman, J. F. (1978) Characterization of a new photoaffinity derivative of ouabain: labeling of the large polypeptide and of a proteolipid component of the Na, K-ATPase, *Biochemistry. 17*, 3667-76.
69. Mercer, R. W., Biemesderfer, D., Bliss, D. P., Jr., Collins, J. H. & Forbush, B., 3rd. (1993) Molecular cloning and immunological characterization of the gamma polypeptide, a small protein associated with the Na,K-ATPase, *J Cell Biol. 121*, 579-86.
70. Kim, Y., Glatt, H., Xie, W., Sinnett, D. & Lalande, M. (1997) Human gamma-aminobutyric acid-type A receptor alpha5 subunit gene (GABRA5): characterization and structural organization of the 5' flanking region, *Genomics. 42*, 378-87.
71. Beguin, P., Wang, X., Firsov, D., Puoti, A., Claeys, D., Horisberger, J. D. & Geering, K. (1997) The gamma subunit is a specific component of the Na,K-ATPase and modulates its transport function, *Embo J. 16*, 4250-60.
72. Therien, A. G., Goldshleger, R., Karlish, S. J. & Blostein, R. (1997) Tissue-specific distribution and modulatory role of the gamma subunit of the Na,K-ATPase, *J Biol Chem. 272*, 32628-34.
73. Therien, A. G., Karlish, S. J. & Blostein, R. (1999) Expression and functional role of the gamma subunit of the Na, K-ATPase in mammalian cells, *J Biol Chem. 274*, 12252-6.
74. Collins, J. H. & Leszyk, J. (1987) The "gamma subunit" of Na,K-ATPase: a small, amphiphilic protein with a unique amino acid sequence, *Biochemistry. 26*, 8665-8.
75. Morrison, B. W., Moorman, J. R., Kowdley, G. C., Kobayashi, Y. M., Jones, L. R. & Leder, P. (1995) Mat-8, a novel phospholemman-like protein expressed in human breast tumors, induces a chloride conductance in Xenopus oocytes, *J Biol Chem. 270*, 2176-82.
76. Scheiner-Bobis, G. & Farley, R. A. (1994) Subunit requirements for expression of functional sodium pumps in yeast cells, *Biochim Biophys Acta. 1193*, 226-34.
77. Blanco, G. & Mercer, R. W. (1998) Isozymes of the Na-K-ATPase: heterogeneity in structure, diversity in function, *Am J Physiol. 275*, F633-50.
78. Shamraj, O. I. & Lingrel, J. B. (1994) A putative fourth Na+,K(+)-ATPase alpha-subunit gene is expressed in testis, *Proc Natl Acad Sci U S A. 91*, 12952-6.
79. Blanco, G., Melton, R. J., Sanchez, G. & Mercer, R. W. (1999) Functional characterization of a testes-specific alpha-subunit isoform of the sodium/potassium adenosinetriphosphatase, *Biochemistry. 38*, 13661-9.
80. Blanco, G., Sanchez, G., Melton, R. J., Tourtellotte, W. G. & Mercer, R. W. (2000) The alpha4 isoform of the Na,K-ATPase is expressed in the germ cells of the testes, *J Histochem Cytochem. 48*, 1023-32.
81. Arystarkhova, E. & Sweadner, K. J. (1997) Tissue-specific expression of the Na,K-ATPase beta3 subunit. The presence of beta3 in lung and liver addresses the problem of the missing subunit, *J Biol Chem. 272*, 22405-8.
82. Woo, A. L., James, P. F. & Lingrel, J. B. (1999) Characterization of the fourth alpha isoform of the Na,K-ATPase, *J Membr Biol. 169*, 39-44.
83. Lingrel, J. B. (1992) Na,K-ATPase: isoform structure, function, and expression, *J Bioenerg Biomembr. 24*, 263-70.

84. Besirli, C. G., Gong, T. W. & Lomax, M. I. (1997) Novel beta 3 isoform of the Na,K-ATPase beta subunit from mouse retina, *Biochim Biophys Acta. 1350*, 21-6.
85. Pestov, N. B., Korneenko, T. V., Zhao, H., Adams, G., Shakhparonov, M. I. & Modyanov, N. N. (2000) Immunochemical demonstration of a novel beta-subunit isoform of X, K-ATPase in human skeletal muscle, *Biochem Biophys Res Commun. 277*, 430-5.
86. Pestov, N. B., Adams, G., Shakhparonov, M. I. & Modyanov, N. N. (1999) Identification of a novel gene of the X,K-ATPase beta-subunit family that is predominantly expressed in skeletal and heart muscles, *FEBS Lett. 456*, 243-8.
87. Laemmli, U. K. (1970) Cleavage of structural proteins during the assembly of the head of bacteriophage T4, *Nature. 227*, 680-5.
88. Scheiner-Bobis, G. (2001) Sanguinarine induces K+ outflow from yeast cells expressing mammalian sodium pumps, *Naunyn Schmiedebergs Arch Pharmacol. 363*, 203-8.
89. Ishida, Y., Takagi, K., Takahashi, M., Satake, N. & Shibata, S. (1983) Palytoxin isolated from marine coelenterates. The inhibitory action on (Na,K)-ATPase, *J Biol Chem. 258*, 7900-2.
90. Moore, R. E. & Scheuer, P. J. (1971) Palytoxin: a new marine toxin from a coelenterate, *Science. 172*, 495-8.
91 Vick, J.A. & Wiles, J.S. (1975) The mechanism of action and treatment of palytoxin poisoning. *Toxicol. Appl Pharmacol 34*, 214-23.
92. Shimizu, Y. (1983) Complete structure of palytoxin elucidated, *Nature. 302*, 212.
93. Weidmann, S. (1977) Effects of palytoxin on the electrical activity of dog and rabbit heart, *Experientia. 33*, 1487-9.
94. Ito, K., Karaki, H. & Urakawa, N. (1979) Effects of palytoxin on mechanical and electrical activities of guinea pig papillary muscle, *Jpn J Pharmacol. 29*, 467-76.
95. Kim, S. Y., Marx, K. A. & Wu, C. H. (1995) Involvement of the Na,K-ATPase in the induction of ion channels by palytoxin, *Naunyn Schmiedebergs Arch Pharmacol. 351*, 542-54.
96. Van Renterghem, C. & Frelin, C. (1993) 3,4 dichlorobenzamil-sensitive, monovalent cation channel induced by palytoxin in cultured aortic myocytes, *Br J Pharmacol. 109*, 859-65.
97. Sauviat, M. P., Gouiffes-Barbin, D., Ecault, E. & Verbist, J. F. (1992) Blockade of sodium channels by Bistramide A in voltage-clamped frog skeletal muscle fibres, *Biochim Biophys Acta. 1103*, 109-14.
98. Guennoun, S. & Horisberger, J. D. (2000) Structure of the 5th transmembrane segment of the Na,K-ATPase alpha subunit: a cysteine-scanning mutagenesis study, *FEBS Lett. 482*, 144-8.
99. Tomas, V. (1989) [Incidence and treatment of congenital dysplasia of the hip joint in the Bardejov District over the 5-year-period 1984-1988], *Acta Chir Orthop Traumatol Cech. 56*, 502-6.
100. Ishida, H., Kohmoto, O., Bridge, J. H. & Barry, W. H. (1988) Alterations in cation homeostasis in cultured chick ventricular cells during and after recovery from adenosine triphosphate depletion, *J Clin Invest. 81*, 1173-81.
101. Hansen, O. (1984) Interaction of cardiac glycosides with (Na+ + K+)-activated ATPase. A biochemical link to digitalis-induced inotropy, *Pharmacol Rev. 36*, 143-63.
102. Kasturi, R., Yuan, J., McLean, L. R., Margolies, M. N. & Ball, W. J., Jr. (1998) Identification of a model cardiac glycoside receptor: comparisons with Na+,K+-ATPase, *Biochemistry. 37*, 6658-66.
103. Schoner, W. (2001) Endogenous cardiotonic steroids, *Cell Mol Biol (Noisy-le-grand). 47*, 273-80.
104. Price, E. M. & Lingrel, J. B. (1988) Structure-function relationships in the Na,K-ATPase alpha subunit: site-directed mutagenesis of glutamine-111 to arginine and asparagine-122 to aspartic acid generates a ouabain-resistant enzyme, *Biochemistry. 27*, 8400-8.
105. Palasis, M., Kuntzweiler, T. A., Arguello, J. M. & Lingrel, J. B. (1996) Ouabain interactions with the H5-H6 hairpin of the Na,K-ATPase reveal a possible inhibition mechanism via the cation binding domain, *J Biol Chem. 271*, 14176-82.
106. Schultheis, P. J., Wallick, E. T. & Lingrel, J. B. (1993) Kinetic analysis of ouabain binding to native and mutated forms of Na,K-ATPase and identification of a new region involved in cardiac glycoside interactions, *J Biol Chem. 268*, 22686-94.
107. Feng, J. & Lingrel, J. B. (1994) Analysis of amino acid residues in the H5-H6 transmembrane and extracellular domains of Na,K-ATPase alpha subunit identifies threonine 797 as a determinant of ouabain sensitivity, *Biochemistry. 33*, 4218-24.
108. Askew, G. R. & Lingrel, J. B. (1994) Identification of an amino acid substitution in human alpha 1 Na,K-ATPase which confers differentially reduced affinity for two related cardiac glycosides, *J Biol Chem. 269*, 24120-6.
109. Canessa, C. M., Horisberger, J. D. & Rossier, B. C. (1993) Mutation of a tyrosine in the H3-H4 ectodomain of Na,K-ATPase alpha subunit confers ouabain resistance, *J Biol Chem. 268*, 17722-6.
110. Blostein, R., Zhang, R., Gottardi, C. J. & Caplan, M. J. (1993) Functional properties of an H,K-ATPase/Na,K-ATPase chimera, *J Biol Chem. 268*, 10654-8.

111. Sumbilla, C., Lu, L., Lewis, D. E., Inesi, G., Ishii, T., Takeyasu, K., Feng, Y. & Fambrough, D. M. (1993) Ca(2+)-dependent and thapsigargin-inhibited phosphorylation of Na+,K(+)-ATPase catalytic domain following chimeric recombination with Ca(2+)-ATPase, *J Biol Chem. 268*, 21185-92.
112. Gatto, C., Wang, A. X. & Kaplan, J. H. (1998) The M4M5 cytoplasmic loop of the Na,K-ATPase, overexpressed in Escherichia coli, binds nucleoside triphosphates with the same selectivity as the intact native protein, *J Biol Chem. 273*, 10578-85.
113. Maunsbach, A. B., Skriver, E. & Hebert, H. (1991) Two-dimensional crystals and three-dimensional structure of Na,K-ATPase analyzed by electron microscopy, *Soc Gen Physiol Ser. 46*, 159-72.
114. Rice, W. J., Young, H. S., Martin, D. W., Sachs, J. R. & Stokes, D. L. (2001) Structure of Na(+),K(+)-ATPase at 11-A Resolution: Comparison with Ca(2+)-ATPase in E(1) and E(2) States, *Biophys J. 80*, 2187-2197.
115. Maruyama, K., Clarke, D. M., Fujii, J., Inesi, G., Loo, T. W. & MacLennan, D. H. (1989) Functional consequences of alterations to amino acids located in the catalytic center (isoleucine 348 to threonine 357) and nucleotide-binding domain of the Ca2+-ATPase of sarcoplasmic reticulum, *J Biol Chem. 264*, 13038-42.
116. Ohtsubo, M., Noguchi, S., Takeda, K., Morohashi, M. & Kawamura, M. (1990) Site-directed mutagenesis of Asp-376, the catalytic phosphorylation site, and Lys-507, the putative ATP-binding site, of the alpha-subunit of Torpedo californica Na+/K(+)-ATPase, *Biochim Biophys Acta. 1021*, 157-60.
117. Rao, R. & Slayman, C. W. (1993) Mutagenesis of conserved residues in the phosphorylation domain of the yeast plasma membrane H(+)-ATPase. Effects on structure and function, *J Biol Chem. 268*, 6708-13.
118. Tran, C. M. & Farley, R. A. (1999) Catalytic activity of an isolated domain of Na,K-ATPase expressed in Escherichia coli, *Biophys J. 77*, 258-66.
119. Gatto, C., Thornewell, S. J., Holden, J. P. & Kaplan, J. H. (1999) Cys(577) is a conformationally mobile residue in the ATP-binding domain of the Na,K-ATPase alpha-subunit, *J Biol Chem. 274*, 24995-5003.
120. Tsuda, T., Kaya, S., Yokoyama, T., Hayashi, Y. & Taniguchi, K. (1998) ATP and acetyl phosphate induces molecular events near the ATP binding site and the membrane domain of Na+,K+-ATPase. The tetrameric nature of the enzyme, *J Biol Chem. 273*, 24339-45.
121. Lane, L. K., Feldmann, J. M., Flarsheim, C. E. & Rybczynski, C. L. (1993) Expression of rat alpha 1 Na,K-ATPase containing substitutions of "essential" amino acids in the catalytic center, *J Biol Chem. 268*, 17930-4.
122. Scheiner-Bobis, G. & Schreiber, S. (1999) Glutamic acid 472 and lysine 480 of the sodium pump alpha 1 subunit are essential for activity. Their conservation in pyrophosphatases suggests their involvement in recognition of ATP phosphates, *Biochemistry. 38*, 9198-208.
123. Pedersen, P. A., Jorgensen, J. R. & Jorgensen, P. L. (2000) Importance of conserved alpha -subunit segment 709GDGVND for Mg2+ binding, phosphorylation, and energy transduction in Na,K-ATPase, *J Biol Chem. 275*, 37588-95.
124. Jorgensen, P. L. & Pedersen, P. A. (2001) Structure-function relationships of Na(+), K(+), ATP, or Mg(2+) binding and energy transduction in Na,K-ATPase, *Biochim Biophys Acta. 1505*, 57-74.
125. Farley, R. A., Heart, E., Kabalin, M., Putnam, D., Wang, K., Kasho, V. N. & Faller, L. D. (1997) Site-directed mutagenesis of the sodium pump: analysis of mutations to amino acids in the proposed nucleotide binding site by stable oxygen isotope exchange, *Biochemistry. 36*, 941-51.
126. Toyoshima, C., Nakasako, M., Nomura, H. & Ogawa, H. (2000) Crystal structure of the calcium pump of sarcoplasmic reticulum at 2.6 A resolution, *Nature. 405*, 647-55.
127. Zhang, Z., Lewis, D., Sumbilla, C., Inesi, G. & Toyoshima, C. (2001) The role of the m6-m7 loop (l67) in stabilization of the phosphorylation and ca2+ binding domains of the sarcoplasmic reticulum ca2+-atpase (serca), *J Biol Chem. 276*, 15232-9.
128. Aravind, L., Galperin, M. Y. & Koonin, E. V. (1998) The catalytic domain of the P-type ATPase has the haloacid dehalogenase fold, *Trends Biochem Sci. 23*, 127-9.
129. Wang, W., Kim, R., Jancarik, J., Yokota, H. & Kim, S. (2001) Crystal Structure of Phosphoserine Phosphatase from Methanococcus jannaschii, a Hyperthermophile, at 1.8 A Resolution, *Structure. 9*, 65-72.
130. Kurihara, T., Liu, J. Q., Nardi-Dei, V., Koshikawa, H., Esaki, N. & Soda, K. (1995) Comprehensive site-directed mutagenesis of L-2-halo acid dehalogenase to probe catalytic amino acid residues, *J Biochem (Tokyo). 117*, 1317-22.
131. Motosugi, K. & Soda, K. (1984) [Enzymological aspects of halo acid dehalogenation], *Tanpakushitsu Kakusan Koso. 29*, 101-10.
132. Liu, J. Q., Kurihara, T., Miyagi, M., Tsunasawa, S., Nishihara, M., Esaki, N. & Soda, K. (1997) Paracatalytic inactivation of L-2-haloacid dehalogenase from Pseudomonas sp. YL by hydroxylamine. Evidence for the formation of an ester intermediate, *J Biol Chem. 272*, 3363-8.
133. Liu, J. Q., Kurihara, T., Miyagi, M., Esaki, N. & Soda, K. (1995) Reaction mechanism of L-2-haloacid dehalogenase of Pseudomonas sp. YL. Identification of Asp10 as the active site nucleophile by 18O incorporation experiments, *J Biol Chem. 270*, 18309-12.

134. Ichiyama, S., Kurihara, T., Li, Y. F., Kogure, Y., Tsunasawa, S. & Esaki, N. (2000) Novel catalytic mechanism of nucleophilic substitution by asparagine residue involving cyanoalanine intermediate revealed by mass spectrometric monitoring of an enzyme reaction, *J Biol Chem. 275*, 40804-9.
135. Hisano, T., Hata, Y., Fujii, T., Liu, J. Q., Kurihara, T., Esaki, N. & Soda, K. (1996) Crystal structure of L-2-haloacid dehalogenase from Pseudomonas sp. YL. An alpha/beta hydrolase structure that is different from the alpha/beta hydrolase fold, *J Biol Chem. 271*, 20322-30.
136. Stokes, D. L. & Green, N. M. (2000) Modeling a dehalogenase fold into the 8-A density map for Ca(2+)-ATPase defines a new domain structure, *Biophys J. 78*, 1765-76.
137. Li, Y. F., Hata, Y., Fujii, T., Hisano, T., Nishihara, M., Kurihara, T. & Esaki, N. (1998) Crystal structures of reaction intermediates of L-2-haloacid dehalogenase and implications for the reaction mechanism, *J Biol Chem. 273*, 15035-44.
138. Collet, J. F., Stroobant, V. & Van Schaftingen, E. (1999) Mechanistic studies of phosphoserine phosphatase, an enzyme related to P-type ATPases, *J Biol Chem. 274*, 33985-90.
139. Ridder, I. S. & Dijkstra, B. W. (1999) Identification of the Mg2+-binding site in the P-type ATPase and phosphatase members of the HAD (haloacid dehalogenase) superfamily by structural similarity to the response regulator protein CheY, *Biochem J. 339*, 223-6.
140. Hisano, T., Hata, Y., Fujii, T., Liu, J. Q., Kurihara, T., Esaki, N. & Soda, K. (1996) Crystallization and preliminary x-ray crystallographic studies of L-2-haloacid dehalogenase from Pseudomonas sp. YL, *Proteins. 24*, 520-2.
141. Ridder, I. S., Rozeboom, H. J., Kalk, K. H., Janssen, D. B. & Dijkstra, B. W. (1997) Three-dimensional structure of L-2-haloacid dehalogenase from Xanthobacter autotrophicus GJ10 complexed with the substrate-analogue formate, *J Biol Chem. 272*, 33015-22.
142. Kazarian, L. S., Fishov, I. L., Rybina, V. V. & Evtodienko, I. V. (1991) [Use of the principle of reverse problems for detecting processes, occurring in cells suspended in culture. II. Distribution of glutathione, SH groups, and optical density in the E. coli cell cycle], *Biofizika. 36*, 1037-42.
143. Dower, W. J., Miller, J. F. & Ragsdale, C. W. (1988) High efficiency transformation of E. coli by high voltage electroporation, *Nucleic Acids Res. 16*, 6127-45.
144. Potter, H. (1988) Electroporation in biology: methods, applications, and instrumentation, *Anal Biochem. 174*, 361-73.
145. Szumanski, M. B., Toth, T. E. & Caceci, T. (1990) Ethanol precipitation to concentrate DNA excised from agarose gel, *Biotechniques. 9*, 708, 710.
146. Hildeman, D. A. & Muller, D. (1997) Increased yield of plasmid DNA during removal of CsCl by ethanol precipitation, *Biotechniques. 22*, 878-9.
147. Aaij, C. & Borst, P. (1972) The gel electrophoresis of DNA, *Biochim Biophys Acta. 269*, 192-200.
148. Sharp, P. A., Sugden, B. & Sambrook, J. (1973) Detection of two restriction endonuclease activities in Haemophilus parainfluenzae using analytical agarose--ethidium bromide electrophoresis, *Biochemistry. 12*, 3055-63.
149. Saiki, R. K., Gelfand, D. H., Stoffel, S., Scharf, S. J., Higuchi, R., Horn, G. T., Mullis, K. B. & Erlich, H. A. (1988) Primer-directed enzymatic amplification of DNA with a thermostable DNA polymerase, *Science. 239*, 487-91.
150. Hemsley, A., Arnheim, N., Toney, M. D., Cortopassi, G. & Galas, D. J. (1989) A simple method for site-directed mutagenesis using the polymerase chain reaction, *Nucleic Acids Res. 17*, 6545-51.
151. Rychlik, W., Spencer, W. J. & Rhoads, R. E. (1990) Optimization of the annealing temperature for DNA amplification in vitro, *Nucleic Acids Res. 18*, 6409-12.
152. Chen, H. & Zhu, G. (1997) Computer program for calculating the melting temperature of degenerate oligonucleotides used in PCR or hybridization, *Biotechniques. 22*, 1158-60.
153. Hitti, Y. S. & Bertino, A. M. (1994) Proteinase K and T4 DNA polymerase facilitate the blunt-end subcloning of PCR products, *Biotechniques. 16*, 802-5.
154. Khare, V. & Eckert, K. A. (2001) The 3' to 5' exonuclease of T4 DNA polymerase removes premutagenic alkyl mispairs and contributes to futile cycling at O{super6}-methylguanine lesions, *J Biol Chem. 4*, 4.
155. Lillehaug, J. R., Kleppe, R. K. & Kleppe, K. (1976) Phosphorylation of double-stranded DNAs by T4 polynucleotide kinase, *Biochemistry. 15*, 1858-65.
156. Topcu, Z. (2000) An optimized recipe for cloning of the polymerase chain reaction-amplified DNA inserts into plasmid vectors, *Acta Biochim Pol. 47*, 841-6.
157. Cotrutz, C., Ionescu, C. R., Cotrutz, C. E. & Kocsis, M. M. (1995) DNA sequencing. Methods and computer analysis of sequence data. Part II, *Rev Med Chir Soc Med Nat Iasi. 99*, 17-21.
158. Gietz, R. D. & Schiestl, R. H. (1991) Applications of high efficiency lithium acetate transformation of intact yeast cells using single-stranded nucleic acids as carrier, *Yeast. 7*, 253-63.
159. Gietz, R. D., Schiestl, R. H., Willems, A. R. & Woods, R. A. (1995) Studies on the transformation of intact yeast cells by the LiAc/SS-DNA/PEG procedure, *Yeast. 11*, 355-60.
160. Bottinger, H. & Habermann, E. (1984) Palytoxin binds to and inhibits kidney and erythrocyte Na+, K+-ATPase, *Naunyn Schmiedebergs Arch Pharmacol. 325*, 85-7.

161. Frelin, C., Vigne, P. & Breittmayer, J. P. (1990) Mechanism of the cardiotoxic action of palytoxin, *Mol Pharmacol. 38*, 904-9.
162. Redondo, J., Fiedler, B. & Scheiner-Bobis, G. (1996) Palytoxin-induced Na+ influx into yeast cells expressing the mammalian sodium pump is due to the formation of a channel within the enzyme, *Mol Pharmacol. 49*, 49-57.
163. Scheiner-Bobis, G. (1998) Ion-transporting ATPases as ion channels, *Naunyn Schmiedebergs Arch Pharmacol. 357*, 477-82.
164. Scheiner-Bobis, G., Zimmermann, M., Kirch, U. & Schoner, W. (1987) Ouabain-binding site of (Na+ + K+)-ATPase in right-side-out vesicles has not an externally accessible SH group, *Eur J Biochem. 165*, 653-6.
165. Ozaki, H., Nagase, H. & Urakawa, N. (1985) Interaction of palytoxin and cardiac glycosides on erythrocyte membrane and (Na+ + K+) ATPase, *Eur J Biochem. 152*, 475-80.
166. Wallick, E. T. & Schwartz, A. (1988) Interaction of cardiac glycosides with Na+,K+-ATPase, *Methods Enzymol. 156*, 201-13.
167. Fryer, H. J., Davis, G. E., Manthorpe, M. & Varon, S. (1986) Lowry protein assay using an automatic microtiter plate spectrophotometer, *Anal Biochem. 153*, 262-6.
168. Peterson, G. L. (1977) A simplification of the protein assay method of Lowry et al. which is more generally applicable, *Anal Biochem. 83*, 346-56.
169. Tobin, T. & Sen, A. K. (1970) Stability and ligand sensitivity of (3H)ouabain binding to (Na+ + K+)ATPase, *Biochim Biophys Acta. 198*, 120-31.
170. Scheiner-Bobis, G., Fahlbusch, K. & Schoner, W. (1987) Demonstration of cooperating alpha subunits in working (Na+ + K+)-ATPase by the use of the MgATP complex analogue cobalt tetrammine ATP, *Eur J Biochem. 168*, 123-31.
171. Henis, Y. I. & Levitzki, A. (1976) An analysis on the slope of Scatchard plots, *Eur J Biochem. 71*, 529-32.
172. Parsons, D. L. & Vallner, J. J. (1978) Scatchard plot analysis of ligand--erythrocyte interactions, *J Pharm Sci. 67*, 1344-5.
173. Askari, A., Kakar, S. S. & Huang, W. H. (1988) Ligand binding sites of the ouabain-complexed (Na+ + K+)-ATPase, *J Biol Chem. 263*, 235-42.
174. Erdmann, E. & Schoner, W. (1973) Ouabain-receptor interactions in (Na + +K +)-ATPase preparations from different tissues and species. Determination of kinetic constants and dissociation constants, *Biochim Biophys Acta. 307*, 386-98.
175. Hansen, O. & Skou, J. C. (1973) A study on the influence of the concentration of Mg 2+ , P i , K + , Na + , and Tris on (Mg 2+ + P i)-supported g-strophanthin binding to (Na + = K +)activated ATPase from ox brain, *Biochim Biophys Acta. 311*, 51-66.
176. Scheiner-Bobis, G. & Schoner, W. (1985) Demonstration of an Mg2+-induced conformational change by photoaffinity labelling of the high-affinity ATP-binding site of (Na+ + K+)-ATPase with 8-azido-ATP, *Eur J Biochem. 152*, 739-46.
177. Weber, K. & Osborn, M. (1969) The reliability of molecular weight determinations by dodecyl sulfate-polyacrylamide gel electrophoresis, *J Biol Chem. 244*, 4406-12.
178. Gershoni, J. M. & Palade, G. E. (1982) Electrophoretic transfer of proteins from sodium dodecyl sulfate-polyacrylamide gels to a positively charged membrane filter, *Anal Biochem. 124*, 396-405.
179. Renart, J. & Sandoval, I. V. (1984) Western blots, *Methods Enzymol. 104*, 455-60.
180. Koroleva, I. V., Sjoholm, A. G. & Schalen, C. (1998) Binding of complement subcomponent C1q to Streptococcus pyogenes: evidence for interactions with the M5 and FcRA76 proteins, *FEMS Immunol Med Microbiol. 20*, 11-20.
181. Barnes, C. S., Upadrashta, B., Pacheco, F. & Portnoy, J. (1993) Enhanced sensitivity of immunoblotting with peroxidase-conjugated antibodies using an adsorbed substrate method, *J Chromatogr. 613*, 281-8.
182. Hackney, D. D., Stempel, K. E. & Boyer, P. D. (1980) Oxygen-18 probes of enzymic reactions of phosphate compounds, *Methods Enzymol. 64*, 60-83.
183. Stempel, K. E. & Boyer, P. D. (1986) Refinements in oxygen-18 methodology for the study of phosphorylation mechanisms, *Methods Enzymol. 126*, 618-39.
184. Hackney, D. D. (1980) Theoretical analysis of distribution of [18O]Pi species during exchange with water. Application to exchanges catalyzed by yeast inorganic pyrophosphatase, *J Biol Chem. 255*, 5320-8.
185. Altschul, S. F., Madden, T. L., Schaffer, A. A., Zhang, J., Zhang, Z., Miller, W. & Lipman, D. J. (1997) Gapped BLAST and PSI-BLAST: a new generation of protein database search programs, *Nucleic Acids Res. 25*, 3389-402.
186. Altschul, S. F. & Koonin, E. V. (1998) Iterated profile searches with PSI-BLAST--a tool for discovery in protein databases, *Trends Biochem Sci. 23*, 444-7.
187. Kuntzweiler, T. A., Wallick, E. T., Johnson, C. L. & Lingrel, J. B. (1995) Amino acid replacement of Asp369 in the sheep alpha 1 isoform eliminates ATP and phosphate stimulation of [3H]ouabain binding to the Na+, K(+)-ATPase without altering the cation binding properties of the enzyme, *J Biol Chem. 270*, 16206-12.

188. Glynn, I. M. (1984) The electrogenic sodium pump, *Soc Gen Physiol Ser. 38*, 33-48.
189. Gadsby, D. C., Rakowski, R. F. & De Weer, P. (1993) Extracellular access to the Na,K pump: pathway similar to ion channel, *Science. 260*, 100-3.
190. Sturmer, W., Buhler, R., Apell, H. J. & Lauger, P. (1991) Charge translocation by the Na,K-pump: II. Ion binding and release at the extracellular face, *J Membr Biol. 121*, 163-76.
191. Amler, E., Abbott, A. & Ball, W. J., Jr. (1992) Structural dynamics and oligomeric interactions of Na+,K(+)-ATPase as monitored using fluorescence energy transfer, *Biophys J. 61*, 553-68.
192. Capasso, J. M., Hoving, S., Tal, D. M., Goldshleger, R. & Karlish, S. J. (1992) Extensive digestion of Na+,K(+)-ATPase by specific and nonspecific proteases with preservation of cation occlusion sites, *J Biol Chem. 267*, 1150-8.
193. Fortes, P. A. & Aguilar, R. (1988) Distances between 5-iodoacetamidofluorescein and the ATP and ouabain sites of (Na,K)-ATPase determined by fluorescence energy transfer, *Prog Clin Biol Res*, 197-204.
194. Vilsen, B., Ramlov, D. & Andersen, J. P. (1997) Functional consequences of mutations in the transmembrane core region for cation translocation and energy transduction in the Na+,K(+)-ATPase and the SR Ca(2+)-ATPase, *Ann N Y Acad Sci. 834*, 297-309.
195. Liu, J. Q., Kurihara, T., Hasan, A. K., Nardi-Dei, V., Koshikawa, H., Esaki, N. & Soda, K. (1994) Purification and characterization of thermostable and nonthermostable 2-haloacid dehalogenases with different stereospecificities from Pseudomonas sp. strain YL, *Appl Environ Microbiol. 60*, 2389-93.
196. Skou, J. C. (1989) The influence of some cations on an adenosine triphosphatase from peripheral nerves. 1957, *Biochim Biophys Acta*, 439-46.
197. Anner, B. M., Moosmayer, M. & Imesch, E. (1994) Na,K-ATPase characterized in artificial membranes. 1. Predominant conformations and ion-fluxes associated with active and inhibited states, *Mol Membr Biol. 11*, 237-45.
198. Skou, J. C. & Esmann, M. (1983) Effect of magnesium ions on the high-affinity binding of eosin to the (Na+ + K+)-ATPase, *Biochim Biophys Acta. 727*, 101-7.
199. Sambrook, J., Fritsch, E. F. & Maniatis, T. (1989) *Moleculare Cloning*
200. W. Schoner & G. Scheiner-Bobis (1988) Photoaffinity labeling with ATP analogs, *Methods Enzymol. 156, 312-22*
201. Koonin, E. V. & Tatusov, R. L. (1994) Computer analysis od bacterial haloacid dehalogenases defines a
202. large superfamily of hydrolases with divers application of an iterative approach to database search. *J. Mol Biol. 244*, 125-32
203. Faller, L. D. & Elgavish, G. A. (1984) Catalysis of oxygen-18 exchange between inorganic phosphate and water by the gastric H.K-ATPase. *Biochemistry. 23*, 6584-90

8. Acknowledgements

I would like to express my thanks to:

Professor Dr. G. Scheiner-Bobis for support and insightful comments throughout this work, for many helpful suggestions in the preparation of the manuscript and careful reviewing of the thesis, and also for his encouragement and financial support;

Professor Dr. F. Dreyer for his kindly guidance as my second supervise so that I can try for a Dr. med. at School of Medicine, Justus-Liebig-University Gießen, and also for reviewing and supporting the thesis;

Professor Dr. W. Schoner for helpful suggestions and reading of the manuscript, for the gift of the sodium pump protein preparations from pig kidney;

Professor Dr. Larry D. Faller (University of California, Los Angeles, Vaglahs) and Dr. David J. Kane (University of Southern California School of Medicine, Los Angeles, California) for the help in ^{18}O exchange experiments;

Professor Dr. R. A. Farley for providing yeast cell strain 30-4;

Dr. E. A. Martinson and Prof. Dr. Kuanyu Li for reading of the manuscript and critical comments;

My thanks go also to M. Bartz, S. E. Becker, R. Saunders, A. Eva and other colleges in the institute for much advice and encouragement in my work and life during my stay in Germany;

I am also grateful to everybody in my family and my chines friends here for their support and encouragement, enabling me to complete my doctoral work here in Germany.

9. Lebenslauf

Allgemeine Angaben:

Name	Su
Vorname	Ping
Geschlecht	weiblich
Geburtsort	Wuhan, V. R. China
Geburtsdatum	24. Dec. 1964
Staatsangehörigkeit	chinesisch
Familienzustand	verheiratet (ein Sohn)
Ehemann	Shao, Jingfan

Schulausbildung:

1972– 1977	Grundschule, Wuhan
1977- 1982	Mittelschule und Gymnasium, Wuhan
Juli. 1982	Abitur

Berufsausbildung:

1982 – 1988	Studium der Humanmedizin an der Tongji Medizinischen Universität Wuhan, China Abschluß: Bachelor der Humanmedizin
1988-1991 1988-1992	Studium zum Magister der Humanmedizin im Institut für Familienplanung der Tongji Medizinischen Universität Wuhan, China Abschluß: Magister der Medizin
Oct. 1999- Oct. 2001	Wissenschaftliche Mitarbeiterin (Doktorandin) im Institut für Biochemie und Endokrinologie des Fachbereichs Veterinärmedizin, Justus-Liebig-Universität Gießen, Gießen, Deutschland

Berufstätigkeit:

1991-1994	wiss. Assistentin. Institut für Familienplanung der Tongji Medizinischen Universität Wuhan, China
1994-1998	Dozentin. Institut für Familienplanung der Tongji Medizinischen Universität Wuhan, China
1998-1999	Fortbildung im Forschunszentrum der Fertilisationskontrolle der Firma Schering AG in Berlin, Deutschland